National Aeronautics and
Space Administration

CxP 70142

BASELINE

RELEASE DATE: MAY 19, 2008

CONSTELLATION PROGRAM
NAVIGATION STANDARDS

The electronic version is the official approved document.
Verify this is the correct version before use.

REVISION AND HISTORY PAGE

Status	Revision No.	Change No.	Description	Release Date
Baseline			Baseline (Reference CxCBD 000221R1/1-1, dated 04/08/08 and CAR 000221, dated 05/02/08)	05/19/08

NOTE: Updates to this document, as released by numbered changes (Change XXX), are identified by a black bar on the right margin.

TABLE OF CONTENTS

PARAGRAPH **PAGE**

1.0 INTRODUCTION 8
1.1 PURPOSE 8
1.2 SCOPE 8
1.3 CHANGE AUTHORITY/RESPONSIBILITY 9
1.4 ACKNOWLEDGEMENTS 9
2.0 DOCUMENTS 9
2.1 APPLICABLE DOCUMENTS 9
2.2 REFERENCE DOCUMENTS 10
3.0 EARTH DATA 10
3.1 EARTH GRAVITY FIELD 10
3.2 EARTH POLE AND PRIME MERIDIAN 12
3.3 EARTH SHAPE PARAMETERS 13
3.4 ATMOSPHERIC ENTRY INTERFACE RADIUS FOR SAMPLE RETURN TRAJECTORIES 13
3.5 TRACKING STATION LOCATIONS 14
4.0 MOON DATA 14
4.1 LUNAR GRAVITY FIELD 14
4.2 MOON POLE AND PRIME MERIDIAN 18
4.3 MOON SHAPE PARAMETERS 20
4.4 LUNAR ORBIT 21
4.4.1 Lagrange Points 28
4.4.2 Lunar Eclipses 29
4.5 LUNAR LIBRATIONS 32
4.5.1 Geometric (or Optical) Librations 32
4.5.2 Physical Librations 35

TABLE OF CONTENTS

PARAGRAPH **PAGE**

4.6 PHYSICAL PROPERTIES 35
4.6.1 Topography 35
4.6.2 Lunar Control Network 38
4.6.3 Atmosphere 39
4.6.4 Temperature 39
4.6.5 Albedo 41
5.0 MARS DATA 41
5.1 MARS GRAVITY FIELD 41
5.2 MARS POLE AND PRIME MERIDIAN 42
5.3 MARS SHAPE PARAMETERS 42
5.4 MARS SATELLITES 43
5.5 MARS SEASONS 43
6.0 UNITS AND TIME SYSTEMS 44
6.1 UNITS 44
6.2 TYPES OF TIME SYSTEMS 45
6.2.1 Dynamical Time (or “Ephemeris Time”) 46
6.2.2 International Atomic Time 47
6.2.3 Universal Time 47
6.2.4 Coordinated Universal Time 48
6.2.5 Difference between ET and UTC 48
6.2.6 <TBR 6-1> 48
6.3 REPRESENTATION OF TIME 48
6.4 LUNAR TIME SYSTEMS 48
6.4.1 Local True Solar Time 49
6.4.2 Orbit Local Solar Time System 50
6.4.3 Surface Local Solar Time System 51

TABLE OF CONTENTS

PARAGRAPH **PAGE**

6.5 MARS TIME SYSTEMS 51
6.5.1 Martian Solar Day 51
6.5.2 Local True Solar Time/Local Mean Solar Time 52
6.5.3 Equation of Time 54
7.0 FUNDAMENTAL CONSTANTS AND PLANETARY/SATELLITE EPHEMERIDES 55
7.1 PLANETARY EPHEMERIS 55
7.2 SATELLITE EPHEMERIDES 57
7.3 SOLAR CONSTANT 57
8.0 COORDINATE SYSTEMS 58
9.0 MEAN ORBIT ELEMENTS 58

APPENDIX **PAGE**

A ACRONYMS AND ABBREVIATIONS AND GLOSSARY OF TERMS 59
B OPEN WORK 65
C LUNAR MAPS 67
D LUNAR EXPLORATION 73
E GRAVITY FIELD INFORMATION 85
F BIBLIOGRAPHY 92

TABLE

3.1-1 EARTH GRAVITY FIELD PARAMETERS 11
3.2-1 EARTH POLE AND PRIME MERIDIAN PARAMETERS 12
3.3-1 EARTH SHAPE PARAMETERS 13
3.4-1 ATMOSPHERIC ENTRY INTERFACE RADIUS 14
3.5-1 <TBR3-1> 14
4.1-1 LUNAR GRAVITY FIELD PARAMETERS 15
4.3-1 MOON SHAPE PARAMETERS 21
4.4-1 TYPES AND DURATIONS OF LUNAR MONTHS 23
4.4-2 SYNODIC MONTH VARIATION FROM 2009–2012 27
4.4.2-1 LUNAR ECLIPSES FROM 2009–2012 30

TABLE

4.6.4-1 ESTIMATED LUNAR SURFACE TEMPERATURES 40
5.1-1 MARS GRAVITY FIELD PARAMETERS 42
5.2-1 MARS POLE AND PRIME MERIDIAN PARAMETERS 42
5.3-1 MARS SHAPE PARAMETERS 43
5.4-1 MARS SATELLITE PARAMETERS 43
5.5-1 SUN LONGITUDES FOR MARS SEASONS 43
6.4-1 DURATION OF MEAN LUNAR DAY 49
6.5.1-1 DURATION OF A MARTIAN SOL 52
6.5.2-1 OFFSET BETWEEN MARS IAU VECTOR AND MARS VERNAL EQUINOX DIRECTIONS 53
7.1-1 PLANETARY GM VALUES 57
7.1-2 CONSTANTS FROM DE421 57
7.3-1 SOLAR CONSTANT 58
B1-1 TO BE DETERMINED ITEMS 65
B2-1 TO BE RESOLVED ISSUES 66
D2-1 IMPACT/LANDING SITES FOR LUNAR MISSIONS (AND MISSION ELEMENTS). 79
D2-2 SITE COORDINATES OF APOLLO SURFACE MISSION ELEMENTS AND LUNOKHOD 2 ROVER 81
D2-3 IMPACT SITE COORDINATES OF APOLLO ORBITAL MISSION ELEMENTS 83
D3-1 SPACECRAFT/MISSION ELEMENTS THAT PROBABLY HAVE IMPACTED THE MOON 84

FIGURE

4.1-1 LUNAR GEOID, LP150Q (METERS) 17
4.1-2 LUNAR GEOID UNCERTAINTIES, LP150Q (METERS, N=90) 18
4.4-1 ORIENTATION OF LUNAR ORBIT POLE 22
4.4-2 LUNAR ORBIT EVOLUTION - 1980–2020 24
4.4-3 LUNAR ORBIT EVOLUTION - 2009–2012 25
4.4-4 DIAGRAM OF EARTH/MOON SYSTEM (TO SCALE) 26
4.4.1-1 LAGRANGE POINTS IN THE VICINITY OF THE EARTH-MOON SYSTEM 28
4.4.2-1 DIAGRAM OF A LUNAR ECLIPSE 31
4.4.2-2 EXAMPLE OF LUNAR ECLIPSE DATA AVAILABLE AT NASA WEBSITE 31

FIGURE

4.6.1-1 COLOR-CODED TOPOGRAPHY AND SHADED RELIEF OF NEAR SIDE HEMISPHERE 37

4.6.1-2 COLOR-CODED TOPOGRAPHY AND SHADED RELIEF OF FAR SIDE HEMISPHERE 38

4.6.4-1 PLANETARY SURFACE TEMPERATURES 40

4.6.5-1 LUNAR ALBEDO MAP 41

5.5-1 LONGITUDE OF THE SUN FOR DETERMINING THE SEASONS OF MARS (APPENDIX F, REFERENCE 52) 44

6.4.1-1 DEFINITION OF LTST 50

6.5.2-1 DEFINITION OF LTST AND LMST 53

6.5.3-1 EQUATION OF TIME IN SOLAR MINUTES AND AREOCENTRIC LONGITUDE IN DEGREES FOR TEN JULIAN YEARS AFTER THE J2000 EPOCH 55

C1.1-1 SHADED RELIEF MAP OF THE LUNAR NEAR SIDE 68

C1.2-1 SHADED RELIEF MAP OF THE LUNAR FAR SIDE 69

C1.3-1 SHADED RELIEF MAP OF THE LUNAR POLAR REGIONS 70

C1.5-1 SAMPLE FROM THE NATIONAL GEOGRAPHIC SOCIETY WEBSITE 72

1.0 INTRODUCTION

This document sets out the assumptions (including definitions and data values) needed for inter-element information exchange about navigation processes across the Constellation Program (CxP).

At a very high level the navigation process can be described as follows: construct a model of a spacecraft trajectory, from that model generate predictions of measurements, and then use a filter to adjust the parameters of the model to minimize the residuals (i.e., the differences between actual and predicted measurements).

A trajectory model necessarily includes models of the environment of the trajectory. Some of those models are described in this document; for example, one model is of the major bodies of the solar system. (See the Section 7.1 discussion of ephemerides.) Other models (e.g., atmospheres) are defined in CxP 70044, Constellation Program Natural Environment Definition for Design (NEDD) and CxP 70023 Constellation Program Design Specification for Natural Environments (DSNE). Typically, measurements involve cooperation between different elements of Constellation; radiometric data, for example, depend on signals being transmitted between the ground and spacecraft, between two or more spacecraft, between lunar surface elements, etc.

The location of the navigation process (e.g., ground or on a spacecraft), the depth of the trajectory model used, and the accuracy required for the results all depend on the particular application. These criteria will be determined by the requirements on specific elements of Constellation and by relevant interface documents between elements. Elements of the Constellation Navigation Architecture are described in CxP 70077 Constellation Program Architecture Description Document (ADD).

The coordinate systems in this document are configuration-controlled at Level 2 by the Constellation Analysis Working Group and are defined in CxP 70138, Constellation Program Level 2 Coordinate Systems.

1.1 PURPOSE

The purpose of this document is to ensure consistency and compatibility in inter-element and inter-Systems Integration Group (SIG) analyses and communication of navigation data and results.

1.2 SCOPE

This document is intended to be descriptive and to serve as a high-level reference for the navigation process in Constellation. This document does not set requirements; requirements are carried in CxP 70000, Constellation Architecture Requirements Document (CARD) and in relevant interface documents, although those may refer back to this document.

Data from this document should be used when modeling trajectories unless there is a compelling reason to change a value, in which case the change should be clearly and frequently called out.

1.3 CHANGE AUTHORITY/RESPONSIBILITY

Proposed changes to this document shall be submitted by a Constellation Program Change Request (CR) to the appropriate Constellation Control Board for consideration and disposition.

All such requests will adhere to the Constellation Program Configuration Management Change Process.

The appropriate NASA Office of Primary Responsibility (OPR) identified for this document is the Level 2 System Engineering and Integration Office in the Constellation Program Office.

1.4 ACKNOWLEDGEMENTS

The bulk of this document was taken from JPL D-32296, Lunar Constants and Models Document by R. Roncoli available at http://ssd.jpl.nasa.gov/?lunar_doc. (See Appendix F, reference 50.) Section 5.0, Mars Data was taken from JPL D-27212, Mars Science Laboratory Planetary Constants and Models Document by J. Kangas. (See Appendix F, reference 51.)

2.0 DOCUMENTS

2.1 APPLICABLE DOCUMENTS

The following documents include specifications, models, standards, guidelines, handbooks, and other special publications. The documents listed in this paragraph are applicable to the extent specified herein.

CxP 70000	Constellation Architecture Requirements Document (CARD)
CxP 70022-01	Constellation Program Command, Control, Communication, and Information (C3I) Interoperability Standards Book, Volume 1: Interoperability Specification
CxP 70022-04	Constellation Program Command, Control, Communication, and Information (C3I) Interoperability Standards Book, Volume 4: Information Representation Specification
CxP 70023	Constellation Program Design Specification for Natural Environments

CxP 70044	Constellation Program Natural Environment Definition for Design
CxP 70077	Constellation Program Architecture Description Document (ADD)
CxP 70138	Constellation Program Level 2 Coordinate Systems
Fed-Std-376B	Preferred Metric Units for General Use by the Federal Government
NPD 8010.2E	Use of the SI (Metric) System of Measurement in NASA Programs

2.2 REFERENCE DOCUMENTS

The documents listed in Appendix F, Bibliography, contain supplemental information to guide the user in the application of this document.

3.0 EARTH DATA

3.1 EARTH GRAVITY FIELD

The Earth gravity field currently recommended is the Gravity Recovery and Climate Experiment (GRACE) gravity model GGM02C. This is a 200th spherical harmonic degree and order model that combines nearly a year of GRACE K-band range-rate, attitude, and accelerometer data with surface gravity and mean sea surface information. (See Appendix F, reference 20.)

NOTE: The GGM02C Earth gravity model was released October 29, 2004 and supersedes the three different Earth gravity models recommended in Appendix F, reference 3.

For the majority of lunar missions, particularly those that do not spend too much time in Low Earth Orbit (LEO), use of an 8th degree and order subset of the GGM02C gravity field is sufficient. Appendix E lists the normalized coefficients for an 8x8 subset of the GGM02C gravity field, including the zonals from J2 through J8. In addition, Appendix E indicates where the full GGM02C field can be found.

TABLE 3.1-1 EARTH GRAVITY FIELD PARAMETERS

$R_{Earth\text{-}Ref}$	= 6378.1363 km	(Dynamical reference radius, GGM02C)
GM_{Earth}	= 398600.4356 km^3/s^2	(Gravitational parameter, GGM02C, GGM02C value transformed to a solar system barycentric reference frame. See 'Note' below)
$\bar{J}_{2\ Earth}$	= $4.841652160548 \times 10^{-4}$	(Earth 2nd degree zonal, Normalized, GGM02C)
		(Epoch J2000, no permanent tide)
$J_{2\ Earth}$	= $1.082626335439 \times 10^{-3}$	(Earth 2nd degree zonal, Un-normalized, GGM02C)
		(Epoch J2000, no permanent tide)
$\dot{J}_{2\ Earth}$	= -2.6×10^{-11} /year	(Earth 2nd degree zonal rate, Un-normalized, GGM02C)
$D_{SOI\ Earth}$	= 9.25×10^5 km	(Earth Sphere of Influence, calculated at 1 AU)
g_{Earth}	= 9.80665 m/s^2	(Earth standard acceleration of gravity (See Appendix F, reference 21; see also Section 6.1.)

NOTE: The gravitational parameter (GM) of Earth (GM_{Earth}) value specified in the GGM02C Earth gravity field is 398600.4415 km^3/s^2. This value differs slightly from the GM_{Earth} value quoted above. The two different values are actually both "equally correct", but they represent the GM_{Earth} in two different reference frames.

The GGM02C model was developed assuming a geocentric reference frame. The time system used in the geocentric reference frame, as discussed in Section 6.2.1, is Terrestrial Time (TT), also known as Terrestrial Dynamical Time (TDT). The Jet Propulsion Laboratory (JPL) planetary and satellite ephemerides (including the GMs of the other solar system bodies), on the other hand, were developed using a solar system barycentric based time scale called T_{eph}. (See Section 6.2.1.) The time scale T_{eph} differs slightly from TT due to relativistic effects. Since the units of GM involve time (km^3/s^2), the value of GM_{Earth} is slightly different in the geocentric reference frame versus the solar system barycentric reference frame. Since the DE421 ephemeris and the lunar gravity field presented in this document were developed using the solar system barycentric reference frame, the solar system barycentric value for GM_{Earth} must be used for everything to be consistent. Furthermore, precision navigation is normally performed using a solar system barycentric reference frame with relativistic corrections (even in cases when propagation is being numerically calculated geocentrically); the major portion of the relativistic corrections can be approximated by using the geocentric reference frame value for GM_{Earth}. However, one must be careful not to doubly correct for relativity—it is safer to use the solar system barycentric reference frame value given in the table.

Note also that the GM of the Earth used in the development of DE421 (see Section 7.1) is slightly different from the solar system barycentric value quoted above, which is kept for consistence with GGM02C. For more information on the transformation between the geocentric and solar system barycentric

reference frames and how the selection of those frames affect the value of GM_{Earth}. (See Appendix F, Bibliography, references 3 and 22.)

3.2 EARTH POLE AND PRIME MERIDIAN

The direction of the Earth's north pole and prime meridian can be approximated by the equations in Table 3.2-1 below, taken from the International Astronomical Union/International Association of Geodesy (IAU/IAG) 2000 Report. (See Appendix F, reference 6.) This report gives the Earth Mean Equator and Prime Meridian (EMEPM) coordinate system defined in CxP 70138. These simple approximations from the IAU/IAG 2000 Report are adequate for concept development and initial mission design, but are insufficient for precision orbit determination: they are most divergent in prime meridian location, which is modeled as moving uniformly.

TABLE 3.2-1 EARTH POLE AND PRIME MERIDIAN PARAMETERS

$\alpha_{Earth\text{-}IAU}$	= 0.00 – 0.641 * T deg	(Right ascension of Earth pole in EME2000)
$\delta_{Earth\text{-}IAU}$	= 90.00 – 0.557 * T deg	(Declination of Earth pole in EME2000)
$W_{Earth\text{-}IAU}$	= 190.147+ $\dot{W}_{Earth}$ * D deg	(Prime meridian with respect to Earth IAU-Node vector, Earth equinox of J2000+90 deg = IAU-Node)
$\dot{W}_{Earth}$	= 360.9856235 deg/day	(Rotational rate of Earth)
T	$= \frac{D}{36525}$	(Julian centuries past epoch of J2000)
D	= (Julian Day – J2000)	(Days past epoch of J2000)
J2000	= 2451545.0	(Reference epoch of J2000 in Julian days)
	= Jan. 1, 2000 12:00:00 TDB	(Calendar date of J2000 reference epoch. See Section 6.2.1 for a description of TDB)

NOTE: The equations above were taken from Appendix F, reference 6, Table I, which incorrectly indicates that these equations were developed using the Barycentric Coordinate Time (TCB) system. The correct time system reference for Table I (as well as the other tables in Appendix F, reference 6) should be Barycentric Dynamical Time (TDB). See Section 6.2.1 for a brief discussion of dynamical time systems, including TCB and TDB.

For precise navigation calculations, the issue is the orientation of the International Terrestrial Reference Frame (ITRF), which defines the true Earth equator, in the International Celestial Reference Frame (ICRF). These coordinate systems are defined in CxP 70138. NASA's deep space navigation system applies to the ITRF93 frame the precession theory of Lieske et al (see Appendix F, references 41 and 42 and the 1980 IAU nutation theory in reference 43), combined with nutation corrections and precise measurements of polar motion and the prime meridian, which are published internally in a Deep Space Network (DSN) Earth Orientation Parameter (EOP) file. Software implementations of this coordinate transformation, with documentation and files kept up-to-date with the current DSN EOP file data, are available from the Navigation

Ancillary Information Facility (NAIF) node of NASA's Planetary Data System (PDS), which can be linked to from http://pds.nasa.gov. In particular, the file, ftp://naif.jpl.nasa.gov/pub/naif/generic_kernels/pck/earth_070425_370426_predict.bpc, predicts the orientation of ITRF93 in the ICRF up to 2037. While this prediction does not include time and polar motion data, the file is in the same format as the files which do include those data, so this file can be used for testing (including regression testing) of navigation software as well as for mission design. (Note that in future this file may be moved to an archive at ftp://naif.jpl.nasa.gov/pub/naif/generic_kernels/pck/old_versions.) The prediction of Earth's future orientation is based on the precession and nutation models mentioned above. A slightly less accurate coordinate transformation for the ITRF2000 frame is given in the International Earth Rotation and Reference Systems Service (IERS) standards. (See Appendix F, reference 3.) In June of 2007 the IERS published a coordinate transformation, comparable in accuracy to that maintained by NASA's deep space navigation system, for the ITRF2005 frame.

The locations of DSN stations are also provided by the NAIF node of NASA's PDS at ftp://naif.jpl.nasa.gov/pub/naif/generic_kernels/fk/stations/earth_topo_050714.tf. Again, this file may be moved to an "old_versions" folder in the future.

3.3 EARTH SHAPE PARAMETERS

The Earth radii that should be used for determining Sun and spacecraft visibility are taken from the IAU/IAG 2000 Report. (See Appendix F, reference 6.) These radii are shown in Table 3.3-1 below.

TABLE 3.3-1 EARTH SHAPE PARAMETERS

$R_{Earth\text{-}Equator}$	= 6378.14 km	(Radius of Earth equator from IAU/IAG)
$R_{Earth\text{-}Pole}$	= 6356.75 km	(Radius of Earth pole from IAU/IAG)
f_{Earth}	= 0.00335364228	(Earth flattening factor, derived from IAU/IAG values ($(R_{Earth\text{-}Equator} - R_{Earth\text{-}Pole})/ R_{Earth\text{-}Equator}$))

NOTE: The radii given in Table 3.3-1 are for Earth's physical shape. Equations for spherical harmonics which describe Earth's gravity field include reference to a dynamical radius for Earth (Section 3.1), which is slightly different from the equatorial radius given here for the shape.

3.4 ATMOSPHERIC ENTRY INTERFACE RADIUS FOR SAMPLE RETURN TRAJECTORIES

The radius that defines the atmospheric boundary at the Earth for sample return missions is given in Table 3.4-1 below. This radius is used for targeting the entry aimpoint.

NOTE: The value indicated below is the same value used for the Genesis and Stardust sample return missions. It was originally defined as 125 km above an Earth equatorial radius of 6378.14 km.

TABLE 3.4-1 ATMOSPHERIC ENTRY INTERFACE RADIUS

$R_{Atmos\text{-}Interface}$ = 6503.14 km (Radius at atmospheric entry interface)

NOTE: The Apollo and Shuttle programs used a radius of 6500.1 km, which was derived from a round number in English units, 400000 ft altitude. Care should be taken using heritage analysis or systems from those programs.

The atmospheric entry interface is defined in terms of a radius instead of an altitude because radius is less ambiguous. Orbits are often described by giving reference altitudes, which are defined to be altitudes of the mean orbit above a spherical Earth whose radius is the equatorial radius of 6378.14 km. Thus a “500 km orbit” would refer to a circular or near-circular orbit with a mean semi-major axis of 6878.14 km, and a “600 km by 480 km orbit” would have a mean orbit apoapse radius of 6978.14 km and a mean orbit periapse radius of 6858.14 km (though it would be more correct not to include so many digits in the radii).

Although the atmospheric entry interface is defined to correspond to a reference altitude, actual entry altitudes within the atmosphere should be given as geodetic altitudes to allow them to be related directly to the topography.

3.5 TRACKING STATION LOCATIONS

<TBR3-1>

TABLE 3.5-1 <TBR3-1>

4.0 MOON DATA

4.1 LUNAR GRAVITY FIELD

The latest lunar gravity field, LP150Q, is a 150th spherical harmonic degree and order model. (See Appendix F, reference 1.) This gravity field was developed using all available data from past U.S. missions to the Moon including the Lunar Orbiter missions, the Apollo 15 and Apollo 16 sub-satellites, the Clementine mission, and all of the Lunar Prospector mission Doppler and range data. The Lunar Prospector data includes all of the 100 km altitude data from the primary mission (which lasted approximately one year) and all of the extended mission data consisting of one month at an average altitude 40 km and six months at an altitude of 30 km. Appendix E lists the normalized coefficients for an 8x8 subset of the LP150Q gravity field (including zonals

up to degree 50). In addition, Appendix E indicates where the full LP150Q field can be found.

TABLE 4.1-1 LUNAR GRAVITY FIELD PARAMETERS

$R_{Moon\text{-}Ref}$	= 1738.0 km	(Mean dynamical radius of Moon from LP150Q)
GM_{Moon}	= 4902.801076 km^3/s^2	(Gravitational parameter from LP150Q)

NOTE: While the LP150Q gravity field represents the current best (complete) lunar gravity field, the GM_{Moon} value from LP150Q does not represent the single best estimate of the GM of the Moon. Appendix F, reference 2 provides a more precise estimate, at 4902.8000 ± 0.0003 km^3/s^2, of the lunar GM. For calculations that require a lunar GM value (as opposed to a complete gravity field), the value from Appendix F, reference 2 should be used.

The second degree terms of LP150Q do not include permanent tide effects.

NOTE: The corrections to the standard spherical harmonic coefficients (C_{nm} and S_{nm}) of a gravitational potential due to solid body tides include both a constant (time independent) correction and a periodic (time dependent) correction. The term “permanent tide”, as used in this document, refers to the constant part of the tide correction calculation. See Appendix F, reference 3 for more information on the treatment of permanent tide corrections.

Given the following Love Numbers for the Moon

k_{20} ($J_{2\ \text{Love Number}}$)	= 0.0248	(Moon Love Number for 2nd degree zonal, J_2)
k_{22} ($C_{22\ \text{Love Number}}$)	= 0.0248	(Moon Love Number for 2nd degree sectorial, C_{22})

the corrected, un-normalized J2 and C22 values are given below.

$J_{2\ \text{Moon-Tide}}$	= $2.033542482111609 \times 10^{-4}$	(Zonal value adjusted for permanent tide - Rigid J_2)
$C_{22\ \text{Moon-Tide}}$	= $2.240509900845084 \times 10^{-5}$	(Sectorial value adjusted for permanent tide - Rigid C_{22})

The permanent tide corrections for other 2nd degree terms are small (i.e., smaller than the uncertainties in the coefficients themselves) and can be ignored. The normalized J_2 and C_{22} values are:

$\bar{J}_{2\ \text{Moon-Tide}}$	= $9.094278450270 \times 10^{-5}$	(Zonal value adjusted for permanent tide - Rigid J_2)
$\bar{C}_{22\ \text{Moon-Tide}}$	= $3.470983013194 \times 10^{-5}$	(Sectorial value adjusted for permanent tide - Rigid C_{22})

NOTE: If an analysis is performed using only J_2, the user should make sure that the permanent tide effects are included. In other words, either the program being used should automatically adjust the input (uncorrected) J_2 value to include permanent tide effects or the user should directly input the J_2 value adjusted for permanent tide. The Orbit Determination Program/Double Precision Trajectory Program (ODP/DPTRAJ) (i.e., the legacy navigation software used at the JPL) and the Goddard Trajectory Determination System (GTDS) software used at Goddard Space Flight Center can include permanent tide effects.

NOTE: Three different Love Numbers are used to characterize the internal elastic parameters of the Moon. Tidal variations that influence the Moon's gravity and rotation are a function of the Love Number k_2, vertical displacements are a function of the Love Number h_2, and horizontal displacements are dependent on the Love Number l_2. For example, the ODP software takes into account the effects of gravitational tides (from k_2), but does not account for the effects of surface deformation tides (from h_2 and l_2). Tidal influences on the lunar rotation rate are part of the model used to generate the physical librations of the Moon. (See Section 4.5.) Analysis of lunar laser ranging data has shown that, depending on the location, the position of a point on the surface of the Moon can change by up to 0.1 m about the mean over a period of one month as a result of surface deformation from lunar tides.

$D_{SOI\ \text{Moon}}$	= 6.6×10^4 km	(Moon Sphere of Influence, calculated at 384400 km, the mean semi-major axis of the Moon's orbit)
$g_{\text{Moon-Mean}}$	= 1.62422 m/s^2	(Mean lunar gravitation at the surface, calculated using the GM_{Moon} given above in this Section from Appendix F, reference 2 and the lunar radius from Section 4.3)

Figure 4.1-1 (provided by Alex Konopliv) shows the lunar geoid relative to the reference sphere as given by the LP150Q gravity field. The geoid clearly shows the long

wavelength features of the gravity field. Some large features in the geoid are visible on both the near side (left side of figure) and far side (right side of figure) of the Moon. There are, however, large uncertainties in the lunar far-side gravity for harmonic series representations greater than approximately degree and order 20. These uncertainties can be seen in the lunar geoid uncertainty map illustrated in Figure 4.1-2 (provided by Alex Konopliv). The geoid uncertainties are from the first 90th degree and order terms of the LP150Q gravity field and represent similar errors to the full degree and order of 150.

NOTE: For general mission design studies involving lunar orbiters with altitudes as low as 100 km, the analysis in Appendix F, reference 4 suggests that a 40x40 field is sufficient to represent the lunar gravity field. For orbits with altitudes in the range of 30–100 km, a minimum 50x50 degree and order field should be used. The degree and order of the gravity field model needed for more detailed mission design and navigation analyses will depend on the specific problem. For any particular degree and order, the "best fit" model is a simple truncation of the full model.

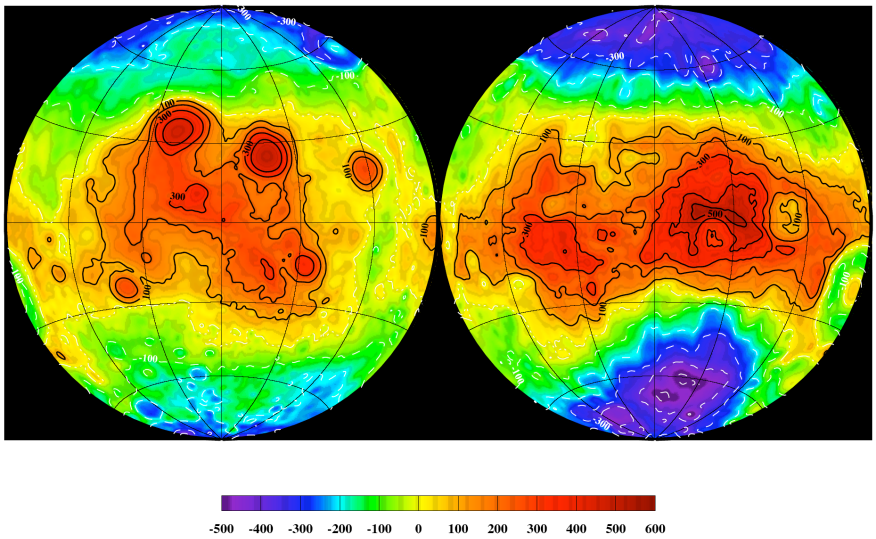

FIGURE 4.1-1 LUNAR GEOID, LP150Q (METERS)

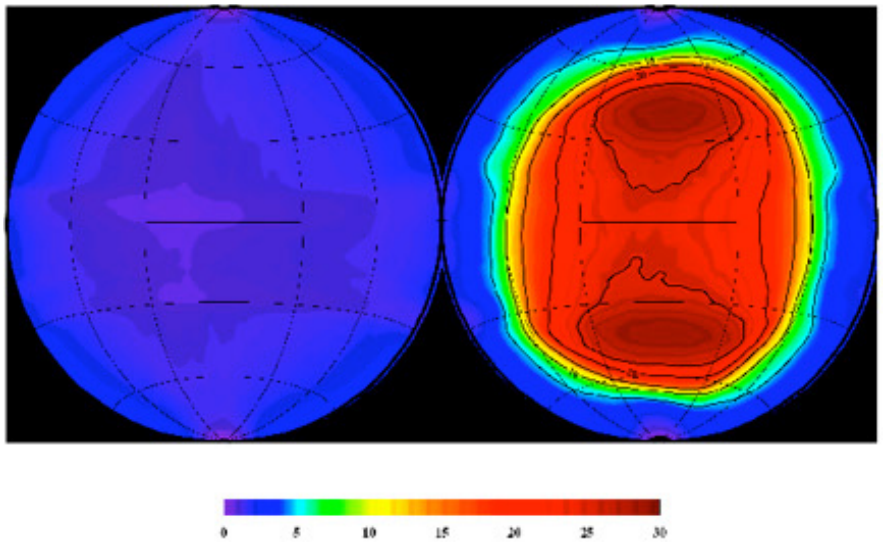

FIGURE 4.1-2 LUNAR GEOID UNCERTAINTIES, LP150Q (METERS, N=90)

4.2 MOON POLE AND PRIME MERIDIAN

Two slightly different systems are commonly used to define a lunar body-fixed coordinate system: a mean Earth/rotation system and a principal axis system. The mean Earth/rotation system (sometimes called the mean Earth/polar axis system) is a lunar body-fixed coordinate system based upon a mean direction to the Earth and a mean axis of rotation of the Moon. The principal axis system is a lunar body-fixed coordinate system aligned with the principal axes of the Moon. Because the Moon is synchronously rotating but is not as symmetric as a triaxial ellipsoid, the principal axes and the mean Earth/rotation axes of the Moon do not coincide. Appendix F, references 1 and 5 describe and compare the two different coordinate systems and indicate that at the lunar surface, the axes of the two systems differ by just under 1 km. In other words, the locations of surface features will differ by about 1 km in the two coordinate frames.

The equations included in this section are taken from the IAU/IAG 2000 Report. (See Appendix F, reference 6.) The IAU/IAG Report estimates the direction of the Moon's north pole and prime meridian using a mean Earth/rotation axis convention. As a result, these equations only approximate the physical librations (i.e., lunar pole and prime meridian directions) which can be obtained directly as a constant rotation from the DE421 ephemeris file (see Section 7.1 for more information about the DE421 ephemeris and CxP 70138 for further discussion of the coordinate systems). The numerically integrated librations in DE421 are expressed for a principal axis-based, lunar coordinate system.

NOTE: The LP150Q gravity field was developed using a principal axis-based coordinate system.

NOTE: The equations on the next page were taken from Table II in Appendix F, reference 6, which incorrectly indicates that these equations were developed using the TCB time system. The correct time system reference for Table II (as well as the other tables in reference 6) should be TDB. See Section 6.2.1 for a brief discussion of dynamical time systems, including TCB and TDB.

Table 4.2-1 Lunar Pole and Prime Meridian Parameters

(Right ascension of Moon rotation pole in EME2000, deg)

$\alpha_{Moon\text{-}IAU}$ = 269.9949+0.0031*T – 3.8787*sinE1 – 0.1204*sinE2 + 0.0700*sinE3
– 0.0172*sinE4 + 0.0072*sinE6 – 0.0052*sinE10
+ 0.0043*sinE13

(Declination of Moon rotation pole in EME2000, deg)

$\delta_{Moon\text{-}IAU}$ = 66.5392+0.0130*T + 1.5419*cosE1 + 0.0239*cosE2 – 0.0278*cosE3
+ 0.0068*cosE4 – 0.0029*cosE6 + 0.0009*cosE7
+ 0.0008*cosE10 – 0.0009*cosE13

(Prime meridian (mean Earth direction) with respect to Moon IAU-Node vector, deg, which is the ascending node of the Lunar Mean-Earth Equator on the ICRF. (See CxP 70138.)

$W_{Moon\text{-}IAU}$ = W_P + 3.5610*sinE1 + 0.1208*sinE2 – 0.0642*sinE3
+ 0.0158*sinE4 + 0.0252*sinE5 – 0.0066*sinE6
– 0.0047*sinE7 – 0.0046*sinE8 + 0.0028*sinE9
+ 0.0052*sinE10 + 0.0040*sinE11 + 0.0019*sinE12
– 0.0044*sinE13

where W_P = 38.3213 + $\dot{W}_{Moon}$ * D -1.4x10^{-12} * D^2

E1	=	125.045	–	0.0529921*D	E8	=	276.617	+	0.3287146*D
E2	=	250.089	–	0.1059842*D	E9	=	34.226	+	1.7484877*D
E3	=	260.008	+	13.0120009*D	E10	=	15.134	–	0.1589763*D
E4	=	176.625	+	13.3407154*D	E11	=	119.743	+	0.0036096*D
E5	=	357.529	+	0.9856003*D	E12	=	239.961	+	0.1643573*D
E6	=	311.589	+	26.4057084*D	E13	=	25.053	+	12.9590088*D
E7	=	134.963	+	13.0649930*D					

$\dot{W}_{Moon}$	=	13.17635815 deg/day	(1st order rotational rate of Moon)
T	=	$\frac{D}{36525}$	(Julian centuries past epoch of J2000)
D	=	(Julian Day – J2000)	(Days past epoch of J2000)
J2000	=	2451545.0	(Reference epoch of J2000 in Julian days)
	=	Jan. 1, 2000 12:00:00 TDB	(Calendar date of J2000 reference epoch. See Section 6.2.1 for a description of TDB)

NOTE: Appendix F, reference 1 indicates the relationship between the lunar body-fixed DE421 principal axis system and the IAU/IAG mean Earth/rotation system. The two systems are related (approximately) by three small rotation angles. The conversion from the mean Earth/rotation system (M) to the principal axis system (P) is given by

$$P = R_Z(63.8986'') \, R_Y(79.0768'') \, R_X(0.1462'') \, M \, .$$

Using spherical trigonometry relationships, these three small rotation angles can be included in the IAU/IAG right ascension, declination, and prime meridian equations indicated above, by adding additional terms, in order to produce directions that approximate the principal axis system. The modified equations from reference 1 are

$$\alpha_{Moon\text{-}PA\text{-}Approximate} = \alpha_{Moon\text{-}IAU} + 0.0553 * \cos W_P + 0.0034 \cos(W_P + E1)$$

$$\delta_{Moon\text{-}PA\text{-}Approximate} = \delta_{Moon\text{-}IAU} + 0.0220 * \sin W_P + 0.0007 \sin(W_P + E1)$$

$$W_{Moon\text{-}PA\text{-}Approximate} = W_{Moon\text{-}IAU} + 0.01775 - 0.0507 \cos W_P - 0.0034 \cos(W_P + E1)$$

It should be noted, however, that a slightly different relationship between Lunar Principal Axis Body-Fixed (LPABF) and Lunar Mean Earth Body-Fixed (LMEBF) has been determined by J. G. Williams, and this revised rotation is in CxP 70138.

4.3 MOON SHAPE PARAMETERS

The general shape of the Moon is very nearly a perfect sphere, excluding local topographic variations. In fact, the magnitude of the local topographic variations are much larger than the overall flattening of the lunar poles or any ellipticity of the lunar equator. Based upon the data presented in Appendix F, reference 7, the magnitude of the lunar flattening relative to the equatorial radius is about 2 km. This memo, however, recommends representing the overall shape of the Moon for any mission design and navigation analyses as a perfect sphere for the following reasons.

First, the IAU/IAG 2000 Report recommends using the same radius value for both the lunar equator and the lunar pole (i.e., a sphere). Second the lunar topographic data, discussed in Section 4.6.1, are expressed relative to a sphere with the same radius as that recommended by the IAU/IAG 2000 Report. The values in the IAU/IAG 2000 Report are listed in Table 4.3-1 below.

NOTE: The radius recommended here is different than the dynamical reference radius for the LP150Q gravity field.

TABLE 4.3-1 MOON SHAPE PARAMETERS

$R_{Moon\text{-}Equator}$	= 1737.4 km	(Radius of Moon equator from IAU/IAG)
$R_{Moon\text{-}Pole}$	= 1737.4 km	(Radius of Moon pole from IAU/IAG)
f_{Moon}	= 0.0	(Moon flattening factor, derived from IAU/IAG values ($(R_{Moon\text{-}Equator} - R_{Moon\text{-}Pole})/ R_{Moon\text{-}Equator}$))

Since the reference surface for the Moon is a sphere, reference altitudes (for orbits) and geodetic altitudes coincide.

4.4 LUNAR ORBIT

Unlike the orbits of most artificial satellites about the Earth, the principal perturbation on the Moon's orbit is due to the third-body, gravitational attraction of the Sun as opposed to the non-spherical nature of the Earth's gravity field. In fact, even the periodic perturbations (on the radial distance of the Moon) caused by Jupiter and Venus are both slightly larger than the perturbation caused by the Earth's J_2. (See Appendix F, reference 8.) As a result, the orbit of the Moon is very complex and cannot be described using the simple "precessing, inclined ellipse" model so often used to describe the orbits of low-altitude Earth satellites.

In simple terms, the lunar orbit is slightly elliptical (mean eccentricity = 0.05490) with a mean semi-major axis of about 384,400 km. Its inclination is nearly constant with respect to the ecliptic (mean inclination = 5.15 deg), but its inclination with respect to the Earth's equator varies from approximately 18–29 degrees. (See Appendix F, references 8 and 9.) All three of these orbital elements (a, e, and i) are subject to periodic variations due to solar perturbations.

The remaining orbital elements describing the orientation of the lunar orbit with respect to a particular coordinate system (i.e., longitude of the ascending node and argument of periapsis) both undergo secular and periodic changes. The durations of those periodic variations are indicated below.

With respect to an ecliptic and equinox referenced coordinate system (e.g., EMO2000):

The period of regression of the longitude of the ascending node (Ω) = 18.6 years

The period of precession of the argument of periapsis (ω) = 6.0 years

NOTE: The period of precession of the longitude of periapsis ($\Omega+\omega$) = 8.85 years

With respect to an Earth equator and equinox referenced coordinate system (e.g., EME2000):

The period of precession of the argument of periapsis (ω) = 8.85 years

NOTE: With respect to an Earth equator and equinox referenced coordinate system, the longitude of the ascending node does not regress through 360 degrees. It oscillates about a right ascension of 0 degrees with a period of 18.6 years (see Figure 4.4-2H). Thus, there is no secular rate for the longitude of the ascending node. As a result, the period of precession of the argument of periapsis (ω), when measured relative to an Earth equator and equinox referenced coordinate system, is equal to the period of precession of the longitude of periapsis ($\Omega+\omega$), when measured relative to the ecliptic and equinox referenced coordinate system.

Figure 4.4-1 illustrates the relationship between the ecliptic north pole, the Earth north pole, and the lunar orbit pole.

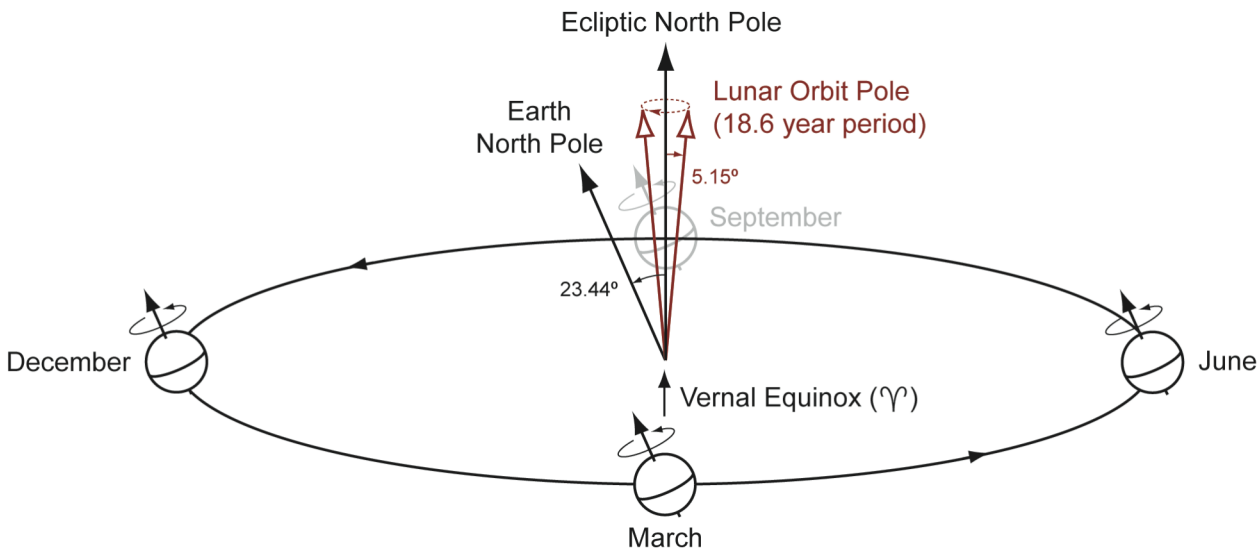

FIGURE 4.4-1 ORIENTATION OF LUNAR ORBIT POLE

Figure 4.4-2 illustrates the evolution of the lunar orbit over a 40-year time span from 1980–2020 – long enough to see the characteristics of the long period changes in the orbital elements. A few of the parameter time histories are provided relative to both the ecliptic plane (EMO2000) and the Earth equator plane (EME2000). The same data are presented in Figure 4.4-3, but the time scale of the plots is only 3 years, from 2009–2012.

NOTE: The data presented in Figures 4.4-2 and 4.4-3 were generated using the DE403/LE403 ephemeris. (See Section 7.1.)

There are a number of different ways to define the period of one revolution of the Moon in its orbit. The following table, taken from Appendix F, reference 9, indicates several of the more common types of lunar “months” (mean values are shown).

TABLE 4.4-1 TYPES AND DURATIONS OF LUNAR MONTHS

Month	Duration (Earth days)	Duration days	hrs	min	sec
Synodic Month (new Moon to new Moon)	29.53059	29	12	44	03
Anomalistic Month (perigee to perigee)	27.55455	27	13	18	33
Sidereal Month (fixed star to fixed star)	27.32166	27	07	43	12
Tropical Month (Equinox to Equinox)	27.32158	27	07	43	05
Nodical (Draconic) Month (node to node)	27.21222	27	05	05	36

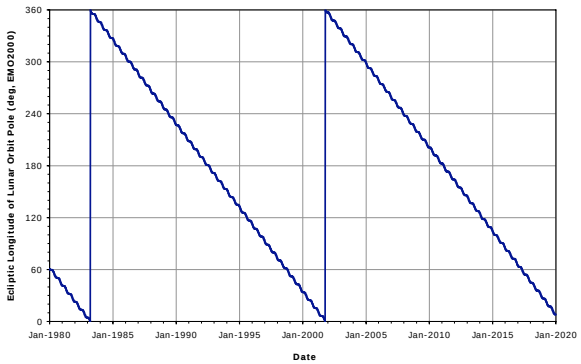

(A: Ecliptic Long of Lunar Orbit Pole)

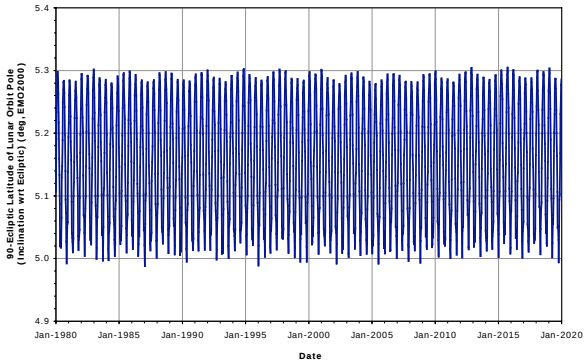

(B: Inclination wrt Ecliptic)

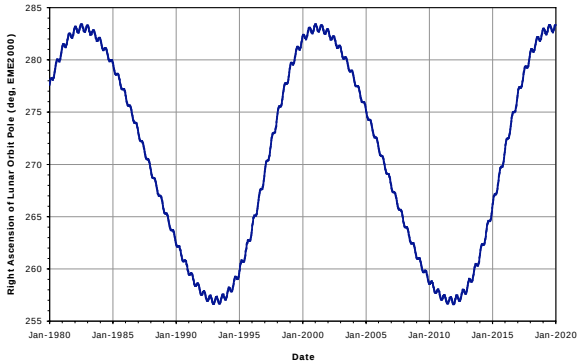

(C: Right Asc of Lunar Orbit Pole)

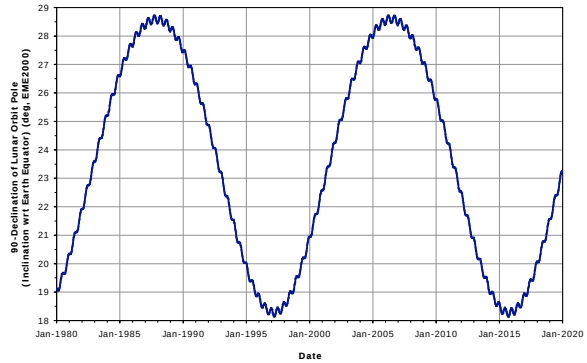

(D: Inclination wrt Earth Equator)

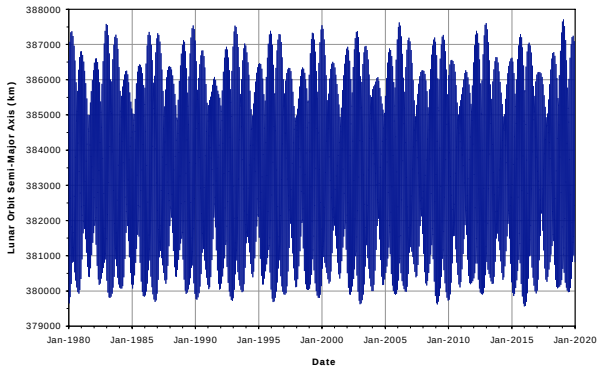

(E: Semi-Major Axis)

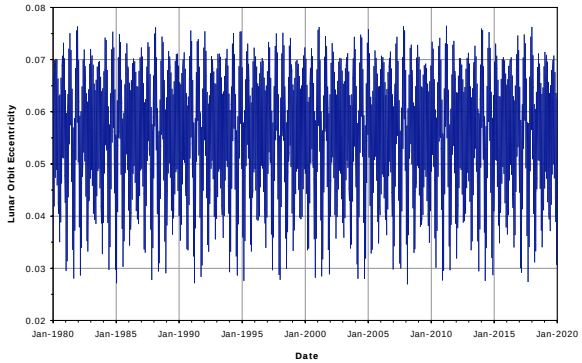

(F: Eccentricity)

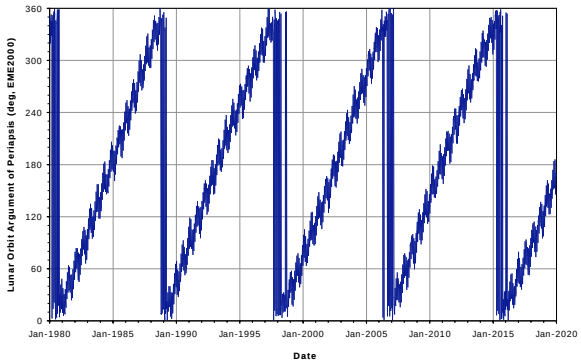

(G: Argument of Periapsis, EME2000)

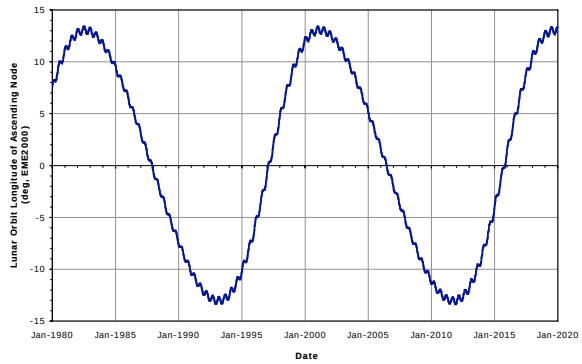

(H: Longitude of Asc Node, EME2000)

FIGURE 4.4-2 LUNAR ORBIT EVOLUTION - 1980–2020

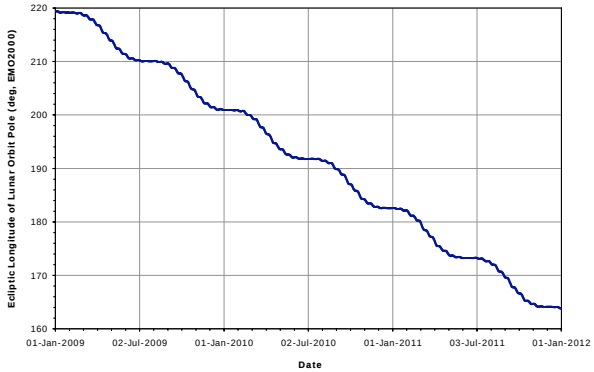

(A: Ecliptic Long of Lunar Orbit Pole)

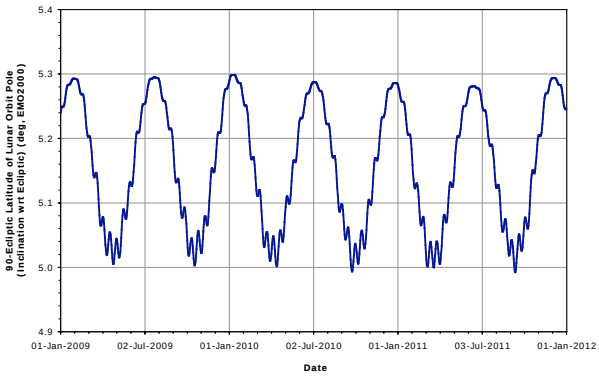

(B: Inclination wrt Ecliptic)

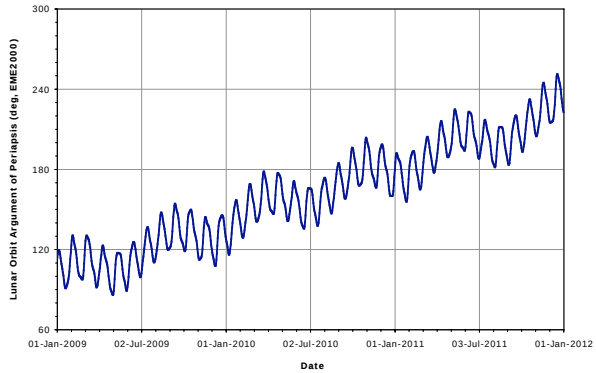

(C: Right Asc of Lunar Orbit Pole)

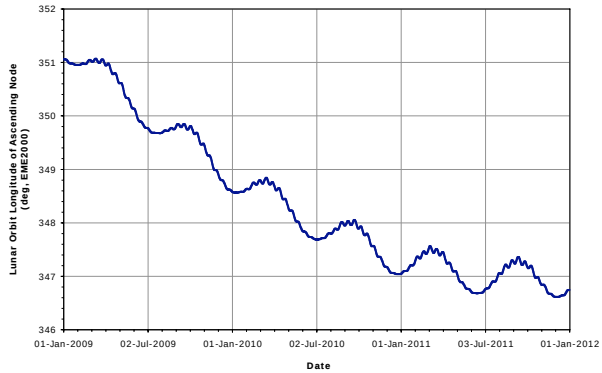

(D: Inclination wrt Earth Equator)

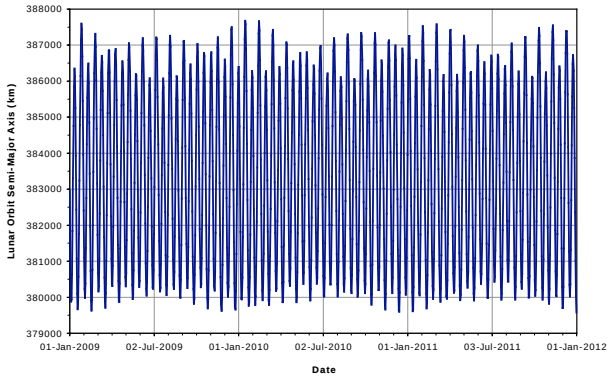

(E: Semi-Major Axis)

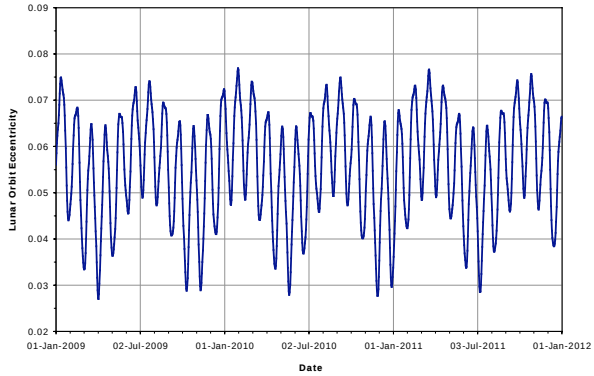

(F: Eccentricity)

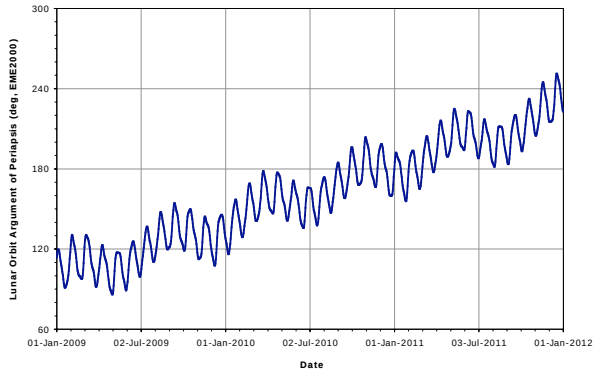

(G: Argument of Periapsis, EME2000)

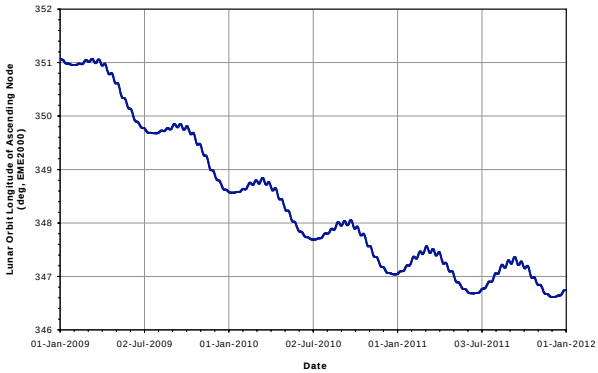

(H: Longitude of Asc Node, EME2000)

FIGURE 4.4-3 LUNAR ORBIT EVOLUTION - 2009–2012

For reference, Table 4.4-2 indicates the times of the new Moon for every month during the years 2009–2012.

NOTE: The strict definition of a new Moon is when the apparent ecliptic longitude of the Moon and the Sun as viewed from the center of the Earth are equal. Apparent ecliptic longitudes are measured eastward in the ecliptic plane from the vernal equinox of epoch (the epoch, or date, of the observation) taking into account the light-times from the Moon and the Sun to get their apparent positions. (See Appendix F, reference 9.)

The new Moon times were generated using the DE403/LE403 ephemeris. (See Section 7.1.)

The table also indicates the variation in the duration of time between new Moons during the three-year period. The duration can vary by as much as approximately 3 hours from one month to the next. In addition, the duration of an actual synodic month can be as much as approximately 7 hours longer or 6 hours shorter than the duration of the mean synodic month.

The simple diagram below illustrates, to scale, the sizes of the Earth, the Moon, and the distance between them. The Earth/Moon barycenter lies within the Earth at a distance of approximately 4670 km from the Earth's center toward the Moon. The current best estimate of the Earth-Moon mass ratio is 81.300570±0.000005. (See Appendix F, reference 2.)

FIGURE 4.4-4 DIAGRAM OF EARTH/MOON SYSTEM (TO SCALE)

TABLE 4.4-2 SYNODIC MONTH VARIATION FROM 2009–2012

New Moon Time (UTC) *	Time to Next New Moon (Earth days)	Synodic Month Variation (hours)	Difference from Mean Synodic Month (hours)
26-Jan-2009 07:55:19			
	29.73596		4.929
25-Feb-2009 01:35:06		-3.149	
	29.60476		1.780
26-Mar-2009 16:05:57		-3.237	
	29.46988		-1.457
25-Apr-2009 03:22:35		-2.470	
	29.36698		-3.927
24-May-2009 12:11:02		-1.408	
	29.30831		-5.335
22-Jun-2009 19:35:00		-0.406	
	29.29141		-5.740
22-Jul-2009 02:34:38		0.456	
	29.31041		-5.284
20-Aug-2009 10:01:37		1.263	
	29.36301		-4.022
18-Sep-2009 18:44:21		2.101	
	29.45053		-1.921
18-Oct-2009 05:33:07		2.865	
	29.56990		0.943
16-Nov-2009 19:13:46		3.129	
	29.70025		4.072
16-Dec-2009 12:02:08		2.348	
	29.79810		6.420
15-Jan-2010 07:11:24		0.511	
	29.81941		6.932
14-Feb-2010 02:51:21		-1.503	
	29.75678		5.429
15-Mar-2010 21:01:07		-2.699	
	29.64433		2.730
14-Apr-2010 12:28:57		-2.873	
	29.52463		-0.143
14-May-2010 01:04:25		-2.421	
	29.42375		-2.564
12-Jun-2010 11:14:37		-1.739	
	29.35130		-4.303
11-Jul-2010 19:40:29		-0.969	
	29.31090		-5.272
10-Aug-2010 03:08:11		-0.101	
	29.30671		-5.373
08-Sep-2010 10:29:51		0.883	
	29.34352		-4.490
07-Oct-2010 18:44:31		1.877	
	29.42174		-2.612
06-Nov-2010 04:51:49		2.610	
	29.53050		-0.002
05-Dec-2010 17:35:44		2.717	
	29.64369		2.714
04-Jan-2011 09:02:39		2.019	
	29.72780		4.733
03-Feb-2011 02:30:41		0.786	
	29.76057		5.519
04-Mar-2011 20:45:54		-0.479	
	29.74059		5.040
03-Apr-2011 14:32:21		-1.468	
	29.67943		3.572
03-May-2011 06:50:44		-2.108	
	29.59161		1.464
01-Jun-2011 21:02:39		-2.344	
	29.49396		-0.879
01-Jul-2011 08:53:57		-2.090	
	29.40686		-2.969
30-Jul-2011 18:39:50		-1.360	
	29.35021		-4.329
29-Aug-2011 03:04:08		-0.329	
	29.33652		-4.658
27-Sep-2011 11:08:43		0.709	
	29.36605		-3.949
26-Oct-2011 19:55:50		1.446	
	29.42631		-2.503
25-Nov-2011 06:09:43		1.714	
	29.49772		-0.789
24-Dec-2011 18:06:26			

* Assumes ET-UTC = 64.184 s

4.4.1 Lagrange Points

In the study of the circular, restricted three-body problem, much has been written about the existence of five special equilibrium points in which a small body (e.g., a spacecraft) can essentially maintain a fixed distance from two larger orbiting bodies. These points are called Lagrange points or sometimes Libration points. There are three collinear Lagrange points with the two primary bodies and two points that form equilateral triangles with the two primary bodies. For a more detailed description about the characteristics of these points, particularly regarding the stability of a body placed at these points, the reader can refer to any of a number of celestial mechanics or orbital dynamics references, including Appendix F, references 10 and 11.

For missions that operate in the vicinity of the Earth-Moon system, there are often two different three-body systems that need to be taken into account: the Sun-Earth-spacecraft system and the Earth-Moon-spacecraft system. A four-body system best represents such missions, but much of the terminology used is derived from studying the two different three-body systems.

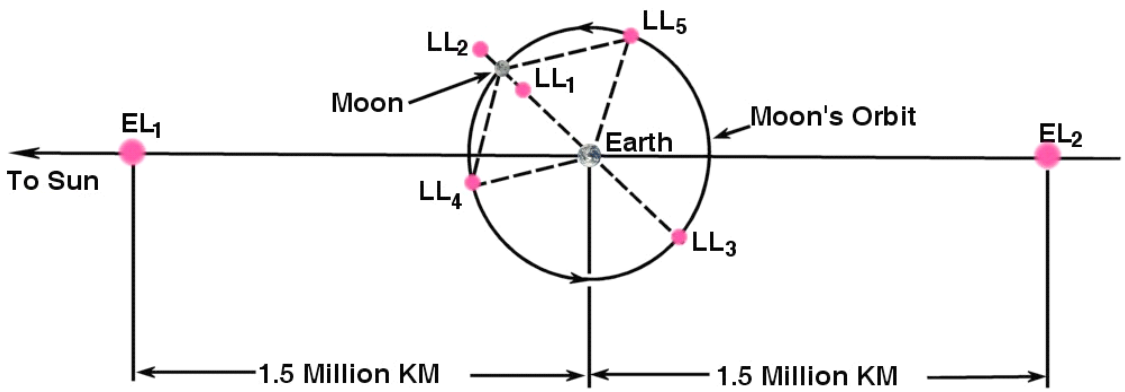

FIGURE 4.4.1-1 LAGRANGE POINTS IN THE VICINITY OF THE EARTH-MOON SYSTEM

Figure 4.4.1-1 [courtesy of Martin Lo] illustrates the two collinear Lagrange points in the Sun-Earth system near the Earth, labeled EL1 and EL2, as well as all five Lagrange points in the Earth-Moon system. The EL1 and EL2 points are approximately 1.5 million kilometers away from the Earth or about 1% of the distance from the Earth to the Sun. Low-energy transfers from the Earth to the Moon or from the Moon to the Earth often involve trajectories that pass near or around the EL1 and/or EL2 points. The collinear Lagrange points in the Earth-Moon system near the Moon, labeled LL1 and LL2 in Figure 4.4.1-1, are approximately 60000 km from the center of the Moon or about 16% of the distance from the Moon to the Earth.

4.4.2 Lunar Eclipses

A specific geometry must exist between the Sun, the Earth, and the Moon for a lunar eclipse to occur. (See Figure 4.4.2-1.) The Moon must lie in the ecliptic plane (or be very near it – within a couple of lunar diameters of the ecliptic) and the line of nodes of the Moon's orbit with respect to the ecliptic plane must lie along the Sun-Earth line. Since the Earth revolves about the Sun (in 1 year) much faster than the lunar orbit pole revolves about the ecliptic north pole (in 18.6 years), the Earth crosses the line of nodes of the Moon's orbit approximately every six months. Thus, approximately every six months there is an opportunity for a lunar eclipse.

Table 4.4.2-1 shows all lunar eclipses that will occur from 2009–2012. The table was constructed from data available at the following NASA website http://sunearth.gsfc.nasa.gov/eclipse/lunar.html. The website includes a wealth of data for each lunar eclipse – including figures such as Figure 4.4.2-2. The reader should consult the website if more information or explanation is desired regarding lunar eclipses.

NOTE: Because of the collection date of the data found at http://sunearth.gsfc.nasa.gov/eclipse/lunar.html, the times given there may be several minutes off.

TABLE 4.4.2-1 LUNAR ECLIPSES FROM 2009–2012

Date	Eclipse Type	Saros [1]	Umbral Magnitude [2]	Eclipse Duration [3]	Geographic Region of Eclipse Visibility [4]
2009 Feb 09	Penumbral	143	-0.083	-	e Europe, Asia, Aus., Pacific, w N.A.
2009 Jul 07	Penumbral	110	-0.909	-	Aus., Pacific, Americas
2009 Aug 06	Penumbral	148	-0.661	-	Americas, Europe, Africa, w Asia
2009 Dec 31	Partial	115	0.082	01h02m	Europe, Africa, Asia, Aus.
2010 Jun 26	Partial	120	0.542	02h44m	e Asia, Aus., Pacific, w Americas
2010 Dec 21	Total	125	1.262	03h29m **01h13m**	e Asia, Aus., Pacific, Americas, Europe
2011 Jun 15	Total	130	1.705	03h40m **01h41m**	S.America, Europe, Africa, Asia, Aus.
2011 Dec 10	Total	135	1.110	03h33m **00h52m**	Europe, e Africa, Asia, Aus., Pacific, N.A.
2012 Jun 04	Partial	140	0.376	02h08m	Asia, Aus., Pacific, Americas
2012 Nov 28	Penumbral	145	-0.184	-	Europe, e Africa, Asia, Aus., Pacific, N.A.

NOTES:

1 The Saros cycle is the periodic recurrence of solar and lunar eclipses with a period of approximately 6,585.3 days (18 years 11 days 8 hours). When two eclipses are separated by a period of one Saros, they share a very similar geometry. The eclipses occur at the same node with the Moon at nearly the same distance from Earth and at the same time of year. Thus, the Saros is useful for organizing eclipses into families or series. Each series typically lasts 12 to 13 centuries and contains 70 or more eclipses.

2 Umbral Magnitude is the fraction of the Moon's diameter obscured by Earth's umbra. For penumbral eclipses, the umbral magnitude is always less than 0. For partial eclipses, the umbral magnitude is always greater than 0 and less than 1. For total eclipses, the umbral magnitude is always greater than or equal to 1.

3 Eclipse Duration is the duration of a partial eclipse. If the eclipse is total, the duration of totality is given in bold.

4 Geographic Region of Eclipse Visibility is the portion of Earth's surface where a lunar eclipse can be seen. Geographic abbreviations (used above): n = north, s = south, e = east, w = west, c = central.

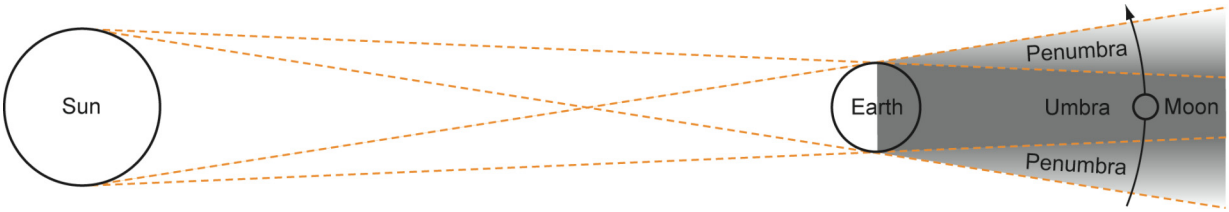

FIGURE 4.4.2-1 DIAGRAM OF A LUNAR ECLIPSE

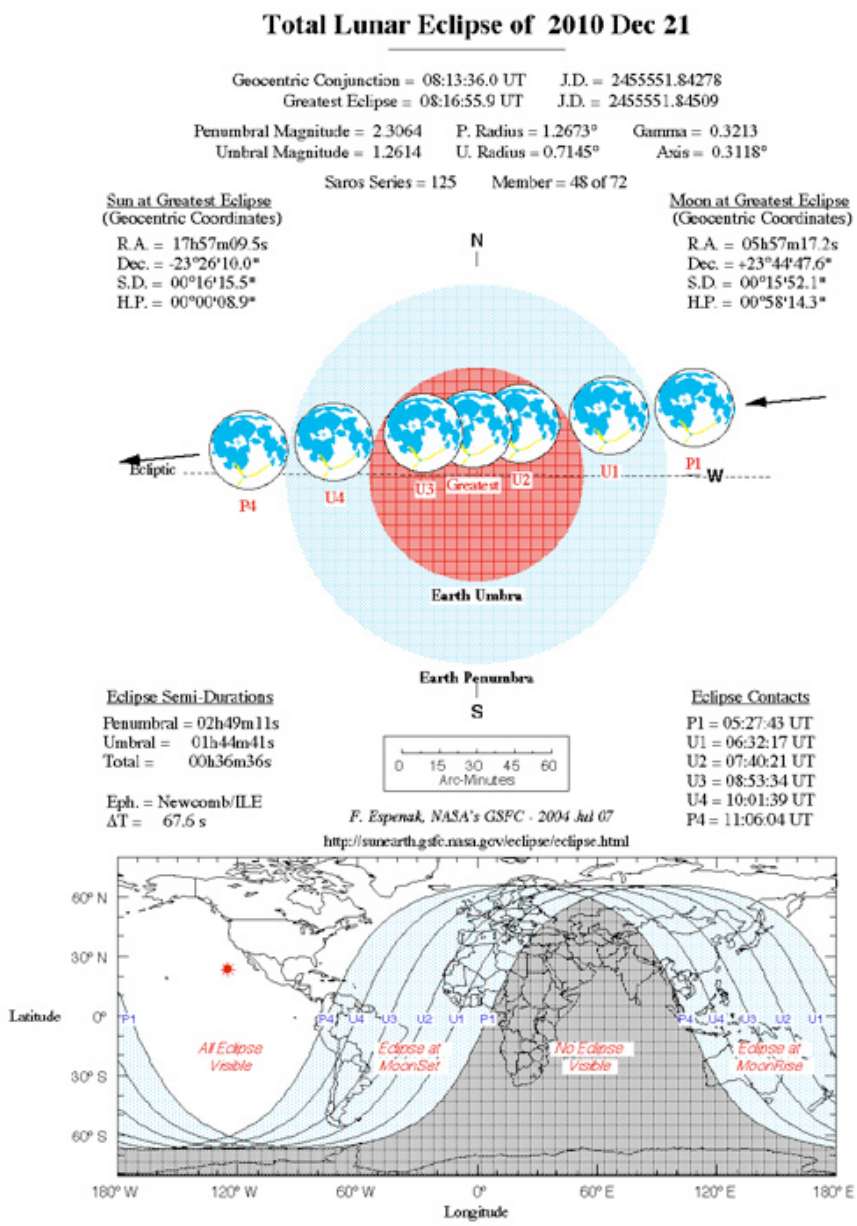

FIGURE 4.4.2-2 EXAMPLE OF LUNAR ECLIPSE DATA AVAILABLE AT NASA WEBSITE

Eclipse map/predictions courtesy of Fred Espenak, NASA/Goddard Space Flight Center. For more information on solar and lunar eclipses, see Fred Espenak's Eclipse Web Site: http://sunearth.gsfc.nasa.gov/eclipse/lunar.html.

4.5 LUNAR LIBRATIONS

The Moon only presents one face towards the Earth. This is because the Moon rotates at a rate equal to the sidereal rate of the Moon in its orbit about the Earth. For a variety of reasons, however – some geometric and some physical – more than 50% of the Moon is visible from Earth over time. The motions of the Moon and the Earth that allow observers on Earth to see slightly different parts of the Moon's surface at different times are called librations.

4.5.1 Geometric (or Optical) Librations

There are three different types of librations that are based solely on the geometry between the Earth (or an observer on the Earth) and the Moon. They are librations in longitude, librations in latitude, and diurnal librations. See Appendix F, reference 12 for more information. All three librations are illustrated in Figure 4.5.1-1.

Figure 4.5.1-1A illustrates librations in longitude. The figure shows that while the Moon rotates at a constant rate, its velocity about the Earth is not constant because the Moon's orbit is elliptical. For example, in the time it takes for the Moon to rotate 90 degrees, the Moon has traveled less than 90 degrees in its orbit (from position j to k in the figure). This discrepancy leads to an apparent east-west "rocking" motion of the Moon over one complete orbit as viewed from Earth allowing an observer on the Earth to see a little bit around to the "back side" or far side of the Moon.

NOTE: The maximum longitudinal libration of 8.16 degrees depicted in Figure 4.5.1-1A is considerably larger than the value that appears in most textbooks (usually quoted as 6.28 degrees). The maximum angle is produced as a result of multiple, periodic perturbations on the Moon's orbit, primarily due to the Sun. (See Appendix F, reference 3.) Considering the Moon's orbit as a simple,two-body elliptical orbit produces the more commonly referenced 6.28 degree value.

Figure 4.5.1-1B illustrates librations in latitude. This libration results from the fact that the Moon's equator is inclined to the plane of its orbit by 6.69 degrees. (The total angle can be represented by the sum of the inclination of the Moon's orbit to the ecliptic plane and the inclination of the Moon's equator to the ecliptic plane). Over the course of one month, the total inclination produces an apparent north-south "nodding" motion of the Moon allowing an observer on the Earth to see a little bit beyond the north and south poles of the Moon.

NOTE: The maximum latitudinal libration of 6.87 degrees depicted in Figure 4.5.1-1B is slightly larger than the value that appears in most textbooks (usually quoted as 6.69 degrees) for the same reason discussed in the previous paragraph – perturbations on the Moon's orbit due to the Sun. (See Appendix F, reference 13.)

Figure 4.5.1-1C illustrates diurnal librations (sometimes also called topocentric librations). This libration is caused by the fact that an observer on the earth sees the moon from different angles due to the rotation of the Earth. For example, over a 12-hour period, an observer at the Earth's equator can see a total of almost 2 degrees more of the Moon in longitude than at any instant in time during the day.

The geometric librations allow 59% of the Moon's surface to be visible from Earth; 41% of the surface is always visible, 41% is never visible, and 18% is alternately visible and not visible.

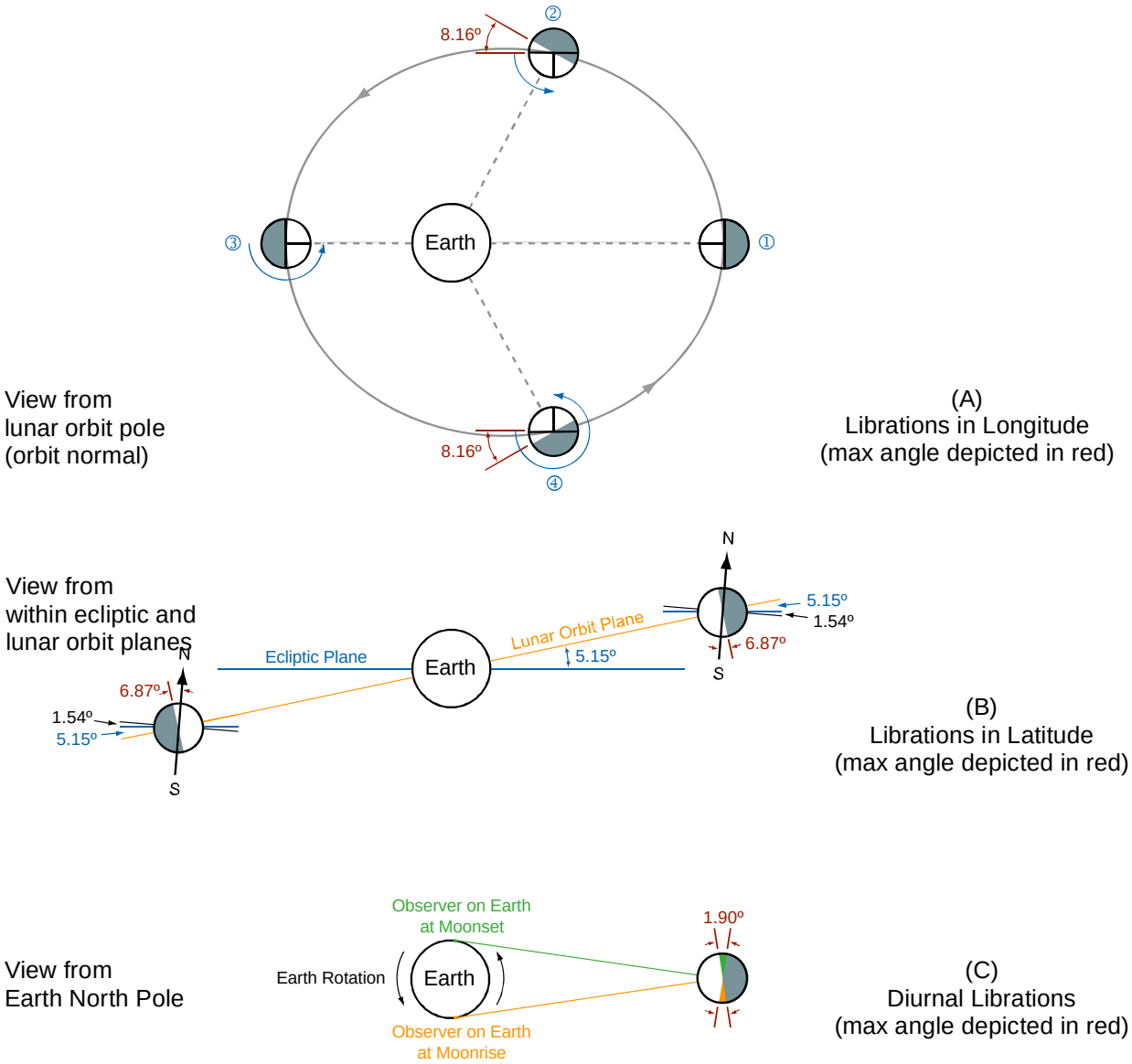

FIGURE 4.5.1-1 GEOMETRIC LUNAR LIBRATIONS

4.5.2 Physical Librations

As stated in Section 4.3, the Moon's shape is very nearly spherical. Nevertheless, it is not a perfect sphere. As a result, the Earth's gravitational attraction on the slight "bulges" on the Moon produce small irregularities in the rotation rate of the Moon. These irregularities produce very small physical librations – occasionally displacing surface positions by just over a kilometer. The libration periods range from a month to many years. (See Appendix F, reference 8.) In contrast to the magnitude of the geometric librations, the maximum amplitude of the physical librations is less than approximately 125 arcseconds or less than about 0.035 degrees.

The libration discussion included here is largely for background information. Since the DE421 ephemeris file includes all of the physical lunar librations, the mission analyst does not need to explicitly keep track of these effects. In fact, physical lunar librations could be ignored for all mission design studies and all but the most precise navigation analyses.

4.6 PHYSICAL PROPERTIES

This section describes the physical properties of the Moon, particularly those properties or characteristics that can influence the trajectory design and/or navigation development of a lunar mission. Some of the physical properties, however, have little influence on mission design and are provided for informational purposes only.

NOTE: The data presented here are not intended to replace or serve as a substitute for the production of a detailed Environmental Requirements Document necessary for flight system design and test.

4.6.1 Topography

The deviations from the overall spherical shape of the Moon due to local topography can be substantial. The maximum and minimum variations are approximately +8 km/-9 km with both extremes occurring on the far side of the Moon (relative to a sphere with a radius of 1737.4 km). (See Appendix F, references 14 and 7 for more information.) The maximum surface elevations occur in the region surrounding the Korolev crater while the minimum elevations occur in the geographically nearby South Pole-Aitken basin.

The topography of the Moon is illustrated in Figures 4.6.1-1 and 4.6.1-2 (taken from Appendix F, reference 14). Color-coded topographic information is overlaid onto shaded relief maps of the near side and far side hemispheres of the Moon. The topographic data depicted in the maps are based primarily upon range measurements taken by a Light Detection and Ranging (LIDAR) laser altimeter on board the 1994 Clementine mission between approximately 70º N and 70º S latitudes. Since there were comparatively few LIDAR measurements taken near the poles, and none taken

over the poles, topographic data in the polar regions were collected photogrammatically using nadir and oblique Clementine images. (See Appendix F, reference 14).

The following United States Geological Survey (USGS) website, ftp://ftpflag.wr.usgs.gov/dist/pigpen/moon/usgs/topo/, provides digital elevation data for the lunar surface. ASCII files containing lunar topographic data are located in the folder 'global_ASCII'. The files are listed below:

a. lunarDEM_ASCII_dd_geocentric_v2.asc.gz
(includes areas with no elevation data)

b. lunarDEM_ASCII_interp_dd_geocentric.asc.gz
(includes interpolated/extrapolated data)

The first file is a compressed file that spans the entire lunar surface. That file does include some areas where no topographic data exist. (The elevation data are assigned a value of -9999 in these areas). The second file is similar to the first, except that the areas with no elevation data have been filled in with interpolated or extrapolated data values.

The elevation data in the files are expressed in meters and are referenced to a sphere with radius 1737.4 km (the same value quoted in Section 4.3). The data are provided at a resolution of 0.0625º (which is equivalent to 1895.209 m along a great circle of the Moon). The data are stored in a simple cylindrical map projection starting at the North pole. The simple graphic below illustrates the data-file format of the two files.

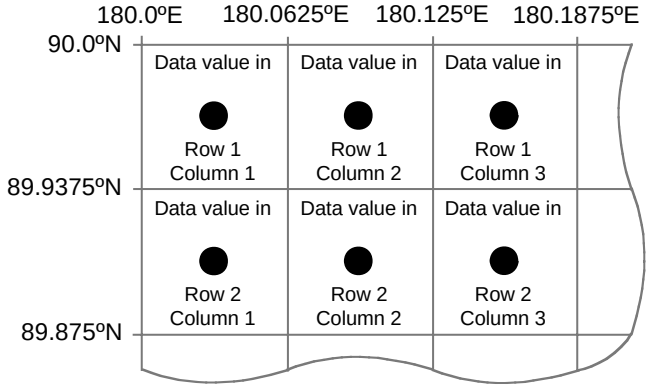

Each file contains a matrix of data, where an element (or grid cell) within the matrix is an interpolated elevation value for the center (latitude/longitude) of the cell (represented by the black dots in the illustration above).

While the elevation data in the files is provided down to the meter level, the uncertainty in the elevation data is considerably larger. The relative uncertainty in the elevation data from point to point (or grid cell to grid cell) is probably on the order of 200–500 m. The absolute uncertainty in the elevation data is probably on the order of 1.0–1.5 km.

For more information, see the '.txt' files (or ReadMe files) in the 'global_ASCII' topography folder. Those files, along with the text in Appendix F, reference 14, provide a detailed description of the format, limitations, and uncertainty of the topographic data.

NOTE: The topographic data in these files are the same data that are depicted in Figures 4.6.1-1 and 4.6.1-2. The interpolated values are based on Clementine LIDAR elevation data and point elevations collected in the polar areas that were sampled to form a regular spaced grid of points.

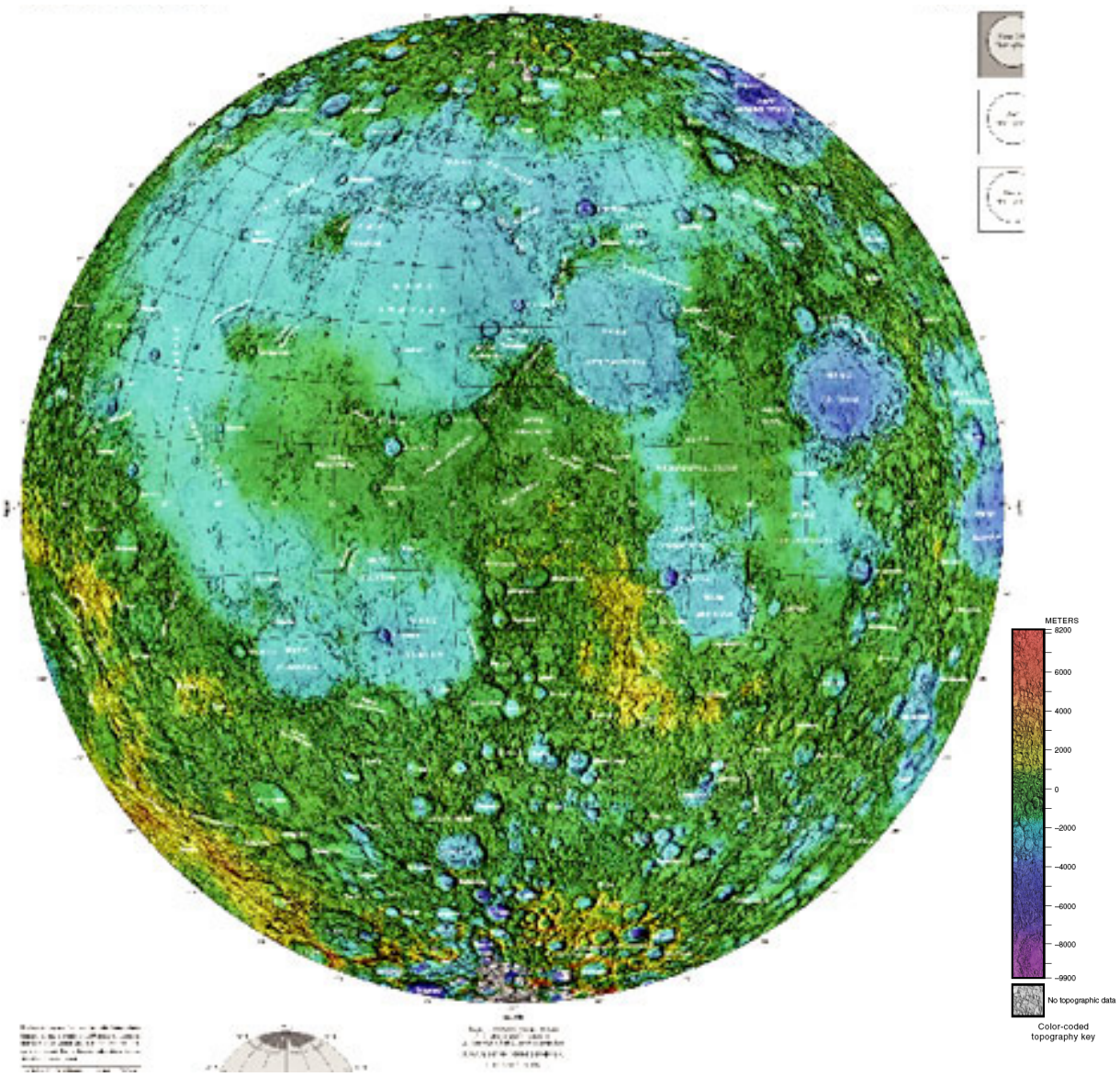

FIGURE 4.6.1-1 COLOR-CODED TOPOGRAPHY AND SHADED RELIEF OF NEAR SIDE HEMISPHERE

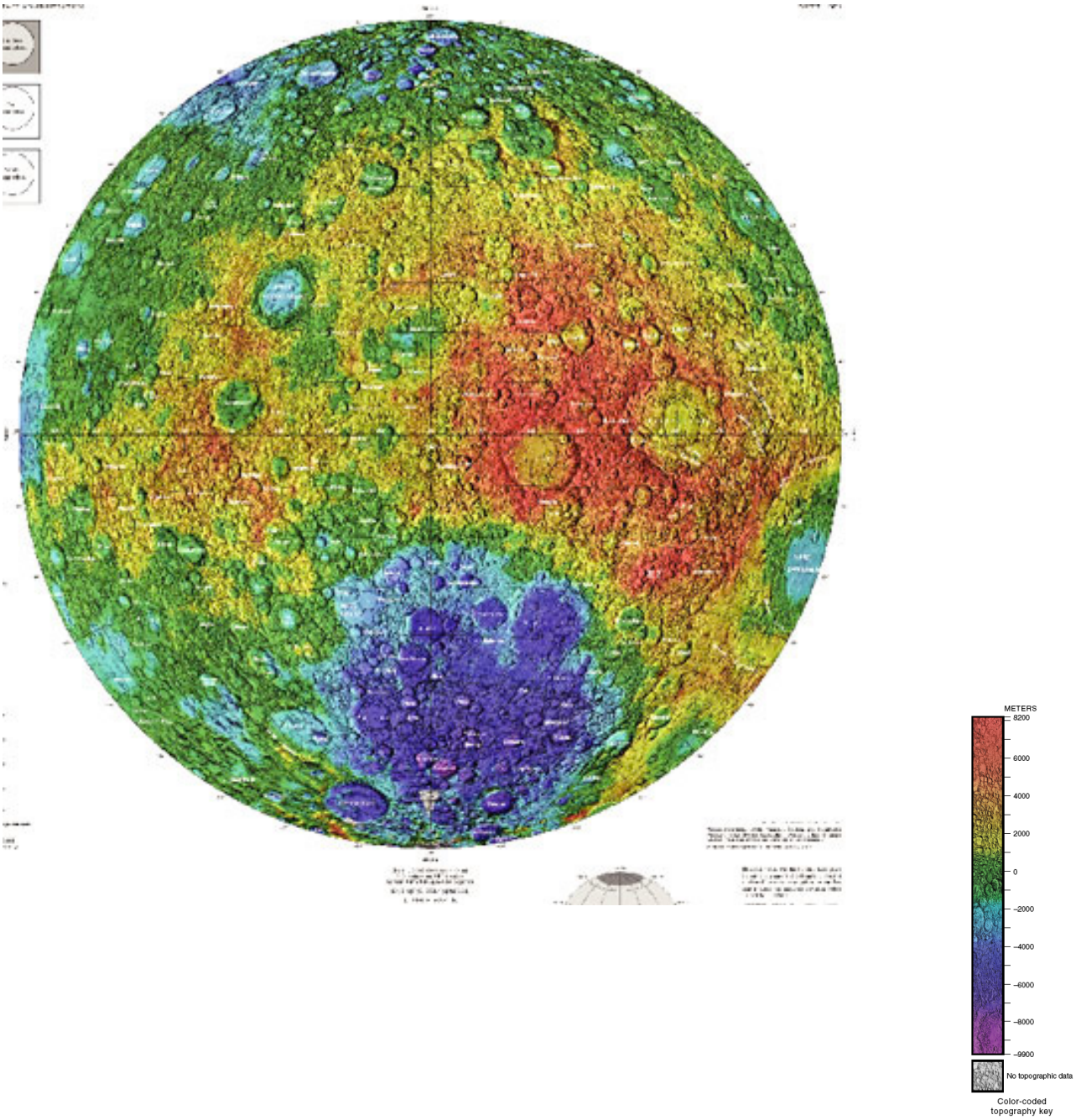

FIGURE 4.6.1-2 COLOR-CODED TOPOGRAPHY AND SHADED RELIEF OF FAR SIDE HEMISPHERE

4.6.2 Lunar Control Network

The previous section described the current state of knowledge regarding the “vertical accuracy” of the lunar topographic data. While this section does not strictly discuss a

physical property of the Moon, this section does provide the current state of knowledge regarding the "horizontal accuracy" of the placement of lunar images (i.e., surface features) onto a well-defined lunar coordinate system. This process is known as establishing a "lunar control network" and usually involves taking image data from a variety of sources, selecting "control points" (e.g., craters or imaged spacecraft hardware) for which good position estimates are known, and transforming the control point coordinates into a common coordinate system (usually the mean Earth/rotation system described in CxP 70138). The uncertainty or error in the placement of these images onto the lunar body-fixed coordinate system is often called the "map-tie error". This uncertainty must be accounted for when attempting to land on the Moon or to precisely image a particular spot or feature from lunar orbit.

Appendix F, reference 15 describes an analysis that produced a Unified Lunar Control Network (ULCN) using images from Apollo, Mariner 10, Galileo, and Earth-based telescopes. The estimated horizontal accuracies of the ULCN range from 100 m–3 km – with the smaller numbers near the Apollo sites and the larger numbers on the lunar far side and near the poles. Appendix F, reference 16 describes an activity in progress (in 2005) to update the ULCN by merging the existing ULCN (developed in 1994) with a control network based on the image data set collected by the Clementine mission.

4.6.3 Atmosphere

For nearly all intents and purposes, the Moon can be considered to have no atmosphere. Certainly from a mission design or navigation perspective no atmospheric drag or heating effects need to be considered when analyzing the trajectory of a spacecraft near the surface of the Moon.

In reality, however, the Moon has a very tenuous atmosphere with gases that are easily lost to space. The atmospheric density on the Moon is about 14 orders of magnitude less dense than the Earth's atmosphere. (See Appendix F, reference 17.) Although difficult to detect, the primary constituents of the ambient lunar atmosphere are: neon (^{20}Ne), helium (He), hydrogen (H_2), and argon (^{40}Ar), listed *roughly* in order of their abundance. Trace amounts of other gases were also detected. The lunar atmosphere is believed to be largely composed of particles from the solar wind and atoms from the surface rocks and soil released by the impacts of comets and meteorites. Argon, by contrast, is produced by the radioactive decay of potassium (^{40}K) in the lunar interior. (See also *http://www.lpi.usra.edu/expmoon/Apollo17/A17_Experiments_LACE.html*). Appendix F, reference 17 indicates the interesting trivial fact that the "six Apollo landings delivered six times as much gas to the lunar surface as there is in the ambient atmosphere".

4.6.4 Temperature

The temperatures on the lunar surface vary widely from location to location and are greatly influenced by the diurnal cycle. Near the equator the surface temperatures

increase about 280º C from just before lunar dawn to lunar noon. Table 4.6.4-1 taken from Appendix F, reference 17 indicates the estimated average surface temperatures and the temperature extremes at various locations on the Moon. Average surface temperature at local noon on the Moon changes by about 6º C between Earth perihelion and aphelion.

TABLE 4.6.4-1 ESTIMATED LUNAR SURFACE TEMPERATURES

	Shadowed Polar Craters	Other Polar Areas	Near Side Equatorial	Far Side Equatorial	Limb Equatorial	Typical Mid Latitudes
Average Temp.	-233º C (?)	-53º C	-19º C	-17º C *	-18º C	-53º C < T < -18º C
Monthly Range	None	±10º C †	±140º C	±140º C	±140º C	±110º C

NOTES:

* The far side of the Moon is closer to the Sun at noon than the near side is, so it gets ≈1% more solar energy.

† Average temperature has a yearly variation that makes it very cold (T < -73º C) for several weeks.

Figure 4.6.4-1, taken from Appendix F, reference 18 provides an interesting graphical comparison of surface temperatures on the Earth, the Moon, and Mars.

The minimum and maximum lunar surface temperatures are average mid-latitude daytime and nighttime temperatures — not the extremes that can be experienced at, for example, the polar regions on the Moon.

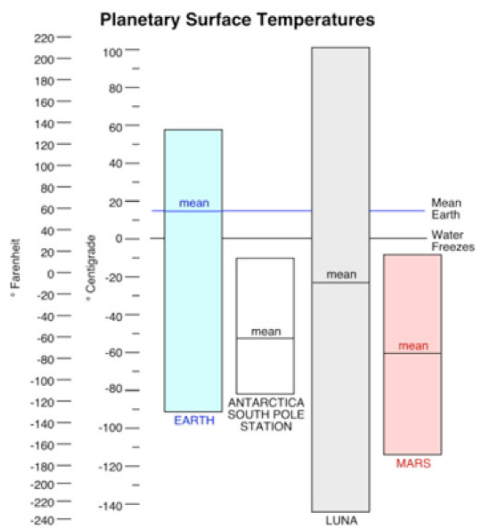

FIGURE 4.6.4-1 PLANETARY SURFACE TEMPERATURES

The general temperature information given in Figure 4.6.4-2 and the albedo information in Section 4.6.5 are included for general information purposes only and should not be considered binding as navigation standards. Other temperature and albedo data, including more detailed maps, may be appropriate in some orbit determination contexts.

4.6.5 Albedo

Despite appearing from Earth as the brightest object in the sky next to the Sun, the Moon is actually a very dark object. The Moon only reflects about 7–24% of the visible light that reaches its surface. The light-colored rocks of the lunar highlands have generally higher albedos ranging from 11–18%, while the lunar maria have low albedos in the range of 7–10%. (See Appendix F, reference 17.)

NOTE: Earth-based albedo measurements are made during the full moon.

The images in Figure 4.6.5-1 represent an albedo map of the Moon indicating the relative brightness of lunar surface features. (See Appendix F, reference 19). The Moon is rotated 60 degrees east in longitude between each view.

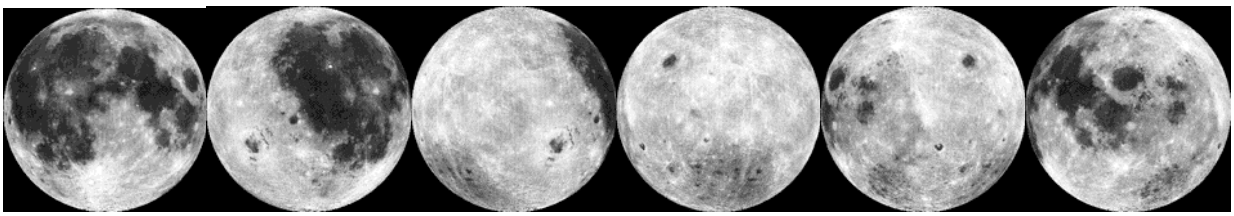

FIGURE 4.6.5-1 LUNAR ALBEDO MAP

5.0 MARS DATA

5.1 MARS GRAVITY FIELD

The latest Mars gravity field is MGS95J, which is a 95 degree and order model. (See Appendix F, reference 5.) It was developed using data collected from the Mars Global Surveyor (MGS) and Odyssey through Dec. 6, 2004, and includes a seasonal variation to J_3. The Mars orientation is constrained by the inclusion of surface tracking data from Mars Pathfinder and the Viking 1 and 2 Landers. This orientation model is the same as that used by Pathfinder, with the constants re-estimated in the gravity solution. For the Mars Science Laboratory (MSL) project, an 8 degree and order model is currently being used for interplanetary navigation within the Mars Sphere of Influence (SOI), and a model including J_2 and J_3 is currently being used for atmospheric entry targeting and Entry Descent and Landing (EDL) analysis. The 8 degree and order normalized gravity field coefficients for MGS95J are listed in the Appendix E.

TABLE 5.1-1 MARS GRAVITY FIELD PARAMETERS

R_{ref}	= 3396.0 km	(Reference Radius)
GM_{Mars}	= 42828.375214 km^3/s^2	(Gravitational Parameter)
D_{SOI}	= 5.8×10^5 km	(Mars Sphere of Influence)
$\bar{J}_{2\,Mars}$	= $0.875021446929 \times 10^{-3}$	(Mars 2nd Degree Zonal, Normalized)
$J_{2\,Mars}$	= $0.195660743710347 \times 10^{-2}$	(Mars 2nd Degree Zonal, Un-normalized)
$\bar{J}_{3\,Mars}$	= $.1189646066880 \times 10^{-4}$	(Mars 3nd Degree Zonal, Normalized)
$J_{3\,Mars}$	= $0.314750764115059 \times 10^{-4}$	(Mars 3rd Degree Zonal, Un-normalized)

5.2 MARS POLE AND PRIME MERIDIAN

The Mars pole and prime meridian values are based upon the definitions in the IAU/IAG 2000 Report. (See Appendix F, reference 6.)

TABLE 5.2-1 MARS POLE AND PRIME MERIDIAN PARAMETERS

α_{Mars}	= 317.68143-0.1061*T deg	(Right Ascension of Mars Pole in EME2000)
δ_{Mars}	= 52.8865-0.0609*T deg	(Declination of Mars Pole in EME2000)
W_{Mars}	= $176.630 + \dot{W}_{Mars} * D$ deg	(Prime Meridian with respect to Mars IAU Vector)
$\dot{W}_{Mars}$	= 350.89198226 deg/day	(Rotational Rate of Mars)
T	$= \frac{D}{36525}$	(Centuries Past Epoch of J2000)
D	= (Julian Date – J2000)	(Days Past Epoch of J2000)
J2000	= 2451545.0	(Reference Epoch of J2000 in Julian Days) = Jan. 1, 2000 12:00:00 TDB (Calendar date of J2000 reference epoch. See Time Systems Section 5.2.1 for a description of TDB.)

5.3 MARS SHAPE PARAMETERS

The Mars radii that should be used for determining Earth, Sun, and spacecraft visibility are taken from the IAU/IAG 2000 Report. The values for radii were computed using an ellipsoidal surface fit to the Mars Orbiter Laser Altimiter (MOLA) data at a uniform angular spacing of 0.5 degrees in latitude and longitude. (See Appendix F, references 3 and 4).

TABLE 5.3-1 MARS SHAPE PARAMETERS

$R_{Mars\text{-}Equator}$	= 3396.19 km	(Mean Radius of Mars Equator)
$R_{Mars\text{-}Pole}$	= 3376.20 km	(Mean Radius of Mars Poles)
f	= 0.00588600756	(Mars Flattening Factor)

MOLA topographic data for Mars are presently (2007) given in terms of altitude above the areoid, where the areoid itself is specified using high-order spherical harmonics.

5.4 MARS SATELLITES

TABLE 5.4-1 MARS SATELLITE PARAMETERS

Phobos

GM_{Phobos}	= 7.158×10^{-4} km^3/s^2	(Gravitational Parameter from MGS95J)
$R_{Phobos\text{-}mean}$	= 11.1 km	(Mean radius of Phobos from IAU/IAG)
$R_{Phobos\text{-}equatx}$	= 13.4 km	(Subplanet equatorial radius of Phobos (IAU/IAG))
$R_{Phobos\text{-}equaty}$	= 11.2 km	(Along orbit equatorial radius of Phobos (IAU/IAG))
$R_{Phobos\text{-}polar}$	= 9.2 km	(Polar radius of Phobos from IAU/IAG)

Deimos

GM_{Deimos}	= 0.983×10^{-4} km^3/s^2	(Gravitational Parameter from MGS95J)
$R_{Deimos\text{-}mean}$	= 6.2 km	(Mean radius of Deimos from IAU/IAG)
$R_{Deimos\text{-}equatx}$	= 7.5 km	(Subplanet equatorial radius of Deimos (IAU/IAG))
$R_{Deimos\text{-}equaty}$	= 6.1 km	(Along orbit equatorial radius of Deimos (IAU/IAG))
$R_{Deimos\text{-}polar}$	= 5.2 km	(Polar radius of Deimos from IAU/IAG)

5.5 MARS SEASONS

Mars seasons are determined by the longitude of the Sun as viewed from Mars relative to the vernal equinox of Mars. Sun longitude, typically referred to as "Ls" (read as "L sub s"), is effectively a measure of the position of Mars in its orbit. Ls is measured eastward from the vernal equinox in the orbital plane of Mars as shown in Figure 5.5-1. Table 5.5-1 below indicates the relationship between Ls and the seasons on Mars.

TABLE 5.5-1 SUN LONGITUDES FOR MARS SEASONS

Ls	Event	Season
0°	Vernal equinox	Start of northern spring/southern fall
90°	Summer solstice	Start of northern summer/southern winter
180°	Autumnal equinox	Start of northern fall/southern spring
270°	Winter solstice	Start of northern winter/southern summer

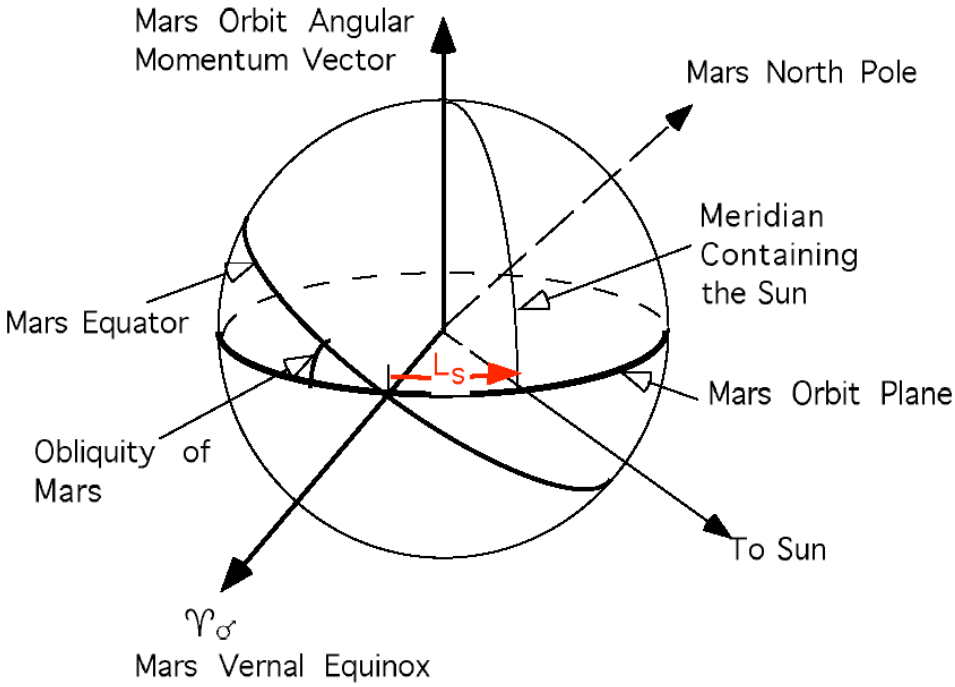

FIGURE 5.5-1 LONGITUDE OF THE SUN FOR DETERMINING THE SEASONS OF MARS (APPENDIX F, REFERENCE 52)

6.0 UNITS AND TIME SYSTEMS

6.1 UNITS

The Constellation Program will use the International System of Units (SI) as its primary system of units per CxP 70000 and NASA Policy Directive NPD 8010.2E, Use of the SI (Metric) System of Measurement in NASA Programs. For historical reasons inch-pound units are still used in some circumstances; conversion of these units to SI is defined by the National Institute of Standards and Technology (NIST). (See Appendix F, reference 38.) The definitions and conversions given there are consistent with the ANSI SI 10 standard adopted in 2002 and with Federal Standard 376B 1993. (See Appendix F, reference 39.) A comprehensive guide to the use of SI is given in NIST SP811. (See Appendix F, reference 49.)

A few points are worth a mention here:

a. Because of a definition change in 1959, there are actually two different definitions for “foot” in use in the United States. The standard foot is now defined to be 0.3048 m (so that 1 inch=2.54 cm exactly), in accordance with international usage. The previous definition of 1200/3937 m, now called a U.S. survey foot, is still used for maps and area calculations in the U.S.

The U.S. survey foot differs from a standard foot by about 2 parts per million.

b. A nautical mile is 1.852 km exactly, by definition. Early definitions, expressed in terms of feet, varied (for example, 6080.27 feet in the U.S., 6080 feet in Britain, with the added problem of the definition of “feet” not necessarily matching) and were more than a meter longer than the current value.

c. The standard acceleration due to Earth gravity is defined to be 9.80665 m/s^2 exactly. This value should be used to associate weight to mass and in the rocket equation with the weight-flow definition of specific impulse. Specific impulse then has units of seconds and is the same in both metric and English units, for which reason the weight-flow definition is much to be preferred to the mass-flow definition of specific impulse. Note that this acceleration value reflects a technical distinction that is made between gravity and gravitation by physical geodesists. Physical geodesists consider that gravity is what you measure when you weigh something on the surface of the Earth and thus includes the centrifugal force of Earth’s rotation along with the force of gravitation. Navigators, however, in general ignore the distinction between the terms and speak indistinguishably of gravity fields around planets and point gravity models for perturbing bodies.

d. A pound is defined to be the standard weight of 0.453 592 37 kg exactly (i.e., under the standard acceleration for Earth). Thus a pound is approximately 4.448222 N.

One subtlety in the use of SI units which is not discussed in any of the standards is that, as explained by relativity theory, measurements of time and length depend on the coordinate frame and on gravitational potential. The next section goes into further detail about this dependence with respect to time. The way the SI is constructed, length depends on time, i.e., the meter depends on the second, and in space navigation, meters are consistent with TDB.

6.2 TYPES OF TIME SYSTEMS

Appendix F, reference 9 provides the following broad definitions of the four types of time systems in common use in physics and astronomy. To varying degrees, each of these types of time systems (and the relationships between them) is important to the mission analyst.

a. Atomic time, in which the unit of duration corresponds to a defined number of wavelengths of radiation of a specified atomic transition of a chosen isotope.

b. Universal time, in which the unit of duration represents the solar day, defined to be as uniform as possible, despite variations in the rotation of the Earth.

c. Sidereal time, in which the unit of duration is the period of the Earth's rotation with respect to a point nearly fixed with respect to the stars.

d. Dynamical time, in which the unit of duration is based on the orbital motion of the Earth, Moon, and planets.

NOTE: It is very difficult to be both succinct and technically correct when defining the different types of time systems that exist. The definitions provided above, taken from Appendix F, reference 9, generally convey the proper intent, but not all of them are strictly correct. No attempt, however, has been made to modify them since they were intended to simply introduce the subject. In light of the complexity of this topic, in particular for precision navigation applications, this section only summarizes basic definitions.

6.2.1 Dynamical Time (or "Ephemeris Time")

Despite being somewhat misleading (and in a strict sense, incorrect), Ephemeris Time (ET), as used by the present-day mission analyst, generally is the independent variable in the equations of motion governing the major bodies of the solar system. This time scale, referred to as T_{eph} in Appendix F, reference 23, represents a smooth-flowing coordinate time that is used in the development of the numerically integrated solar system ephemerides produced at JPL and distributed worldwide.

Over the years, a number of different types of dynamical times have been incorrectly assumed to be equivalent to T_{eph}. Reference 23 describes a few of the more common misconceptions and illustrates the differences between T_{eph} and these other time systems. For example,

a. As initially defined in the 1960s, ET was the independent variable of the (then) existing *analytic* planetary and lunar theories. As a result, ET is subject to the inadequacies of those analytical theories and is not exactly equivalent to T_{eph}.

b. Later in the 1970s, another pair of dynamical time systems was defined: a geocentric based time scale initially called TDT, but later renamed TT, and a solar system barycentric based time scale called TDB. TDB was initially defined to differ from TT by only periodic terms, but this difference yields a time scale which is physically impossible. (See Appendix F, reference 23.) In a resolution adopted by the IAU in 2006, the time scale TDB was defined to be consistent with the JPL ephemeris time, T_{eph} [private communication from Bill Folkner].

c. Meanwhile, in 1991, in an attempt to clarify relationships between space-time coordinates, the IAU defined another solar system barycentric based time scale called TCB for Barycentric Coordinate Time. IERS 2003 (reference 3) recommends the use of the TCB time scale.

In addition, Appendix F, reference 23 states that "T_{eph} is mathematically and physically equivalent to the newly-defined TCB, differing from it by only an offset and a constant rate". The TCB time scale, however, is not used at JPL – nor is it used by most astronomers. At least for the present, it should be ignored.

This document uses the label ET instead of the label T_{eph} in some places despite the fact that ET is not technically correct. Ironically, ET was sometimes chosen to avoid further confusion that would be introduced by changing the name in those particular instances. ET is also the label commonly used in many of NASA's navigation communities for the internal time scale used in ephemeris products, both planetary and other astronomical body ephemerides and spacecraft ephemerides. Ephemeris Time is also the time scale used internally in the orbit determination software systems used at NASA's JPL.

6.2.2 International Atomic Time

Temps Atomique International (or International Atomic Time) (TAI) is defined as a continuous time scale resulting from a statistical analysis by the Bureau International des Poids et Mesures (or International Bureau of Weights and Measures; France) (BIPM). The BIPM performs this analysis using a large number of atomic clocks operating around the world. An atomic clock uses the oscillations of an undisturbed cesium atom to measure the passage of time. A specific number of oscillations is used to define the fundamental unit of time (the second) in the SI. The value of TT–TAI was set to a fixed value of 32.184 seconds on January 1, 1958.

NOTE: TT–TAI = 32.184 seconds; T_{eph} (often called "ET") = TT + relativistic terms; thus, ET–TAI = 32.184 + relativistic terms, where | relativistic terms | < 2 ms.

6.2.3 Universal Time

Universal Time (UT) is the name for a family of time scales that are based upon the mean solar day.

UT1 represents the daily rotation of the Earth, independent of the observing location (i.e., including corrections for polar motion on the longitude of the observing site). It might be considered as an angle rather than a time, since it uses seconds to label the instants when the Earth has rotated 1/86400 of the way from one midnight position to the next. Thus by specifying a UT1 time, one is really specifying a particular orientation of the Earth. Since the Earth's rotation rate is somewhat irregular and unpredictable, UT1 is deduced from the combination of a variety of different types of observations

including Very Long Baseline Interferometry (VLBI) measurements of extragalactic radio sources (quasars), Lunar Laser Ranging (LLR), Satellite Laser Ranging (SLR), and Global Positioning System (GPS) measurements to name a few.

6.2.4 Coordinated Universal Time

Coordinated Universal Time (UTC) is the basis for the worldwide system of civil timekeeping and is available from radio broadcast signals. It is the time system used by flight operations teams and tracking stations (so that radiometric data used by NASA's orbit determination software systems is time-tagged in UTC). UTC was set equal to TAI in 1958 and is adjusted with leap seconds so that it remains within 0.9 seconds of UT1.

6.2.5 Difference between ET and UTC

"ET", as referred to in Sections 6.2.1 and 6.2.2, is currently (in 2007) 65.184 seconds (excluding periodic relativistic terms) ahead of UTC, as it has been since January 1, 2006. From the previous definitions, this difference consists of two parts. ET–TAI =32.184 seconds (excluding relativistic terms) and currently (in 2007) TAI–UTC=33.0 (leap) seconds. According to the IERS Bulletin C (current Leap Seconds Announcement), the most recent leap second was introduced at the end of December 2005. Bulletin C is available at the U.S. Naval Observatory (USNO) internet website (*http://maia.usno.navy.mil/*). The bulletin is updated approximately six months in advance of leap second opportunities that occur at the end of June and December.

6.2.6 <TBR 6-1>

6.3 REPRESENTATION OF TIME

In accordance with Constellation Program requirement CA5618, a continuous reference time and standard representations for that time have been adopted for use by all elements in defining and exchanging time information. Requirements for this time system, Constellation Reference Time, are given in CxP 70022-01, Constellation Program Command, Control, Communication, and Information (C3I) Interoperability Standards Book Volume 1: Interoperability Specification. The actual definition of, and the requirement for the representation of, Constellation Reference Time is given in CxP 70022-04, Constellation Program Command, Control, Communication, and Information (C3I) Interoperability Standards Book Volume 4: Information Representation Specification.

6.4 LUNAR TIME SYSTEMS

For a spacecraft in orbit about the Moon or on the surface of the Moon, it is often more convenient to keep track of events using a time system associated with the time of day on the Moon rather than the time of day on Earth. Since the word "day" is usually associated with a mean solar day, a day on the Moon – or a mean lunar day – is

defined to be the mean interval of time between successive crossings of the Sun on a particular lunar longitude (e.g., the lunar prime meridian). As a result, the period of one mean lunar day is equal to the period of a mean synodic lunar month.

TABLE 6.4-1 DURATION OF MEAN LUNAR DAY

	Duration (Earth days)	Duration days	hrs	min	sec
Mean Lunar Day (mean synodic lunar month)	29.53059	29	12	44	03

NOTE: Due to the eccentricity of the Earth's orbit and small periodic variations in the Moon's rotation rate, the duration of an actual lunar day (associated with a given location on the Moon) can vary, over the course of a year, by nearly ±2 hours from the mean value quoted above.

6.4.1 Local True Solar Time

Local True Solar Time (LTST) on the Moon is defined as follows:

$$LTST = \left(\lambda_P - \lambda_{TS}\ deg\right)\frac{24\ hr}{360\ deg} + 12\ hr$$

where, in the simplest case, l_P is the East longitude of a point P on the surface of the Moon and l_{TS} is the East longitude of the true Sun (see Figure 6.4.1-1). The equation above converts the difference in angles from degrees to true solar hours, with 12 hours representing the time that the true Sun crosses the meridian containing the point P (local noon). The conventional method for computing LTST is to determine l_{TS} from the planetary ephemeris file.

NOTE: The choice of the reference vector within the lunar equatorial plane from which l_P and l_{TS} are measured is somewhat arbitrary, since only the angular difference between the point P and the true Sun is important. Thus, while the lunar prime meridian is an obvious (and perhaps the simplest) choice for the reference vector, it is not the only choice. For example, the X-axis in a Moon-centered, IAU-defined coordinate system (i.e., the Moon IAU-Node of Epoch) works equally well. See Appendix F, reference 6 for a definition of the IAU-defined coordinate system.

NOTE: LTST is not a uniform time system. Since LTST is based upon the true motions of the Earth and the Moon, LTST does not progress at a constant rate.

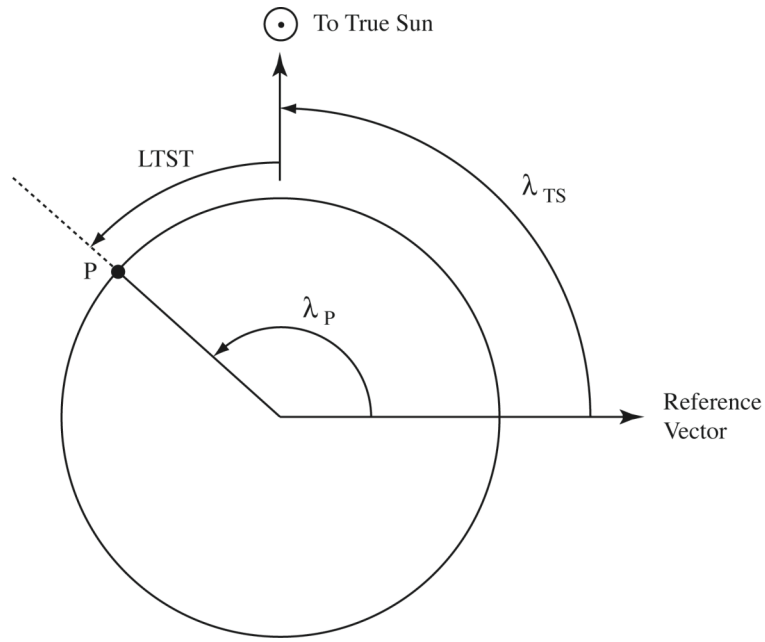

FIGURE 6.4.1-1 DEFINITION OF LTST

6.4.2 Orbit Local Solar Time System

During the development and operations of nearly all planetary and satellite orbiting missions, understanding how the geometry of the orbit plane changes relative to the Sun over time is extremely important – from both an engineering and science perspective. A useful way to characterize the orbit geometry, particularly for high-inclination orbiters, is to report the local solar time of the ascending or descending node. The convention generally adopted is to report the local time of the orbit node relative to the mean Sun.

For an orbit about the Moon that remains essentially inertially fixed in space, the following partial derivative for the change in Orbit Local Solar Time (OLST) per unit time can be derived from the mean synodic and sidereal periods of the Moon's orbit.

$$\text{OLST}_{\text{in LTST}} \text{ changes by } -3.94 \frac{\text{minutes}}{\text{Earth day}} = -27.60 \frac{\text{minutes}}{\text{week}} = -1.94 \frac{\text{hours}}{\text{mean lunar day}}$$

NOTE: Despite being associated with an orbit about the Moon, the partial quoted above is primarily a function of the rate at which the Earth moves about the Sun. Thus, the partial will change slightly as a function of time due to the eccentricity of the Earth's orbit. For example, each year during the three-year period from 2009–2012, the partial will vary roughly within the following range:

$$\text{OLST}_{\text{in LTST}} \text{ changes by } -4.1 \frac{\text{minutes}}{\text{Earth day}} \text{ to } -3.8 \frac{\text{minutes}}{\text{Earth day}} \text{ within 2009-2012.}$$

6.4.3 Surface Local Solar Time System

Due to the basic diurnal nature of mission operations for a surface mission, a landing site or surface local solar time system has to be defined. For lunar surface missions, an appropriate local solar time system to use is LTST.

For an object on the surface of the Moon, the following partial for the change in Surface Local Solar Time (SLST) per unit time can be derived from the mean synodic period of the Moon's orbit.

$$\text{SLST}_{\text{in LTST}} \text{ changes by } +48.76\ \frac{\text{minutes}}{\text{Earth day}} = +5.69\ \frac{\text{hours}}{\text{week}}$$

NOTE: The partial quoted above will change slightly as a function of time due to the eccentricity of the Earth's orbit and small periodic variations in the Moon's rotation rate. For example, during the three-year period from 2009–2012, the partial will vary roughly within the following range:

$$\text{SLST}_{\text{in LTST}} \text{ changes by } +48.6\ \frac{\text{minutes}}{\text{Earth day}} \text{ to } +48.9\ \frac{\text{minutes}}{\text{Earth day}} \text{ within 2009–2012}$$

Note that for a given site on the Moon, the time from local noon (i.e., SLST = 12:00:00) to local noon is not exactly equal to the time from new Moon to new Moon. In other words, at each of the new Moon times listed in Table 4.4-2, a slightly different lunar longitude is experiencing local noon.

6.5 MARS TIME SYSTEMS

6.5.1 Martian Solar Day

The Martian solar day is called a sol, and it is approximately 40 minutes longer than an Earth day. The mean sol is computed from the rotation rate of Mars and the rate of the Fictitious Mean Sun (FMS), described in the next section. In one mean sol, Mars rotates through 360 degrees plus the amount that the mean sun moved during that time:

$$1 \text{ deg/Sol} = 360 \text{ deg} + \dot{\alpha}_{FMS} \text{ deg/day} * \kappa \text{ days/Sol} * 1 \text{ Sol}$$

where κ represents the ratio of days per sol. Dividing the relationship above by the rotation rate of Mars in deg/day produces the ratio κ days/sol. Solving for κ produces the relationship

$$\kappa \text{ days/Sol} = (360 \text{ deg}) / (\dot{W}_{Mars} - \dot{\alpha}_{FMS} \text{ deg/day})$$

where $\dot{W}_{Mars} = 350.89198521$ deg/day is the rotation rate from Folkner (see Appendix F, reference 45), and $\dot{\alpha}_{FMS} = 0.5240384$ deg/day is the FMS rate given in the next section. Note that a different value for $\dot{W}_{Mars}$ is given here than was given as the IAU 2000 value in Section 5.2. The value used here accounts for nutation, whereas the IAU 2000 value from Section 5.2 does not. See Appendix F, reference 45 for more details. The mean sol is then

TABLE 6.5.1-1 DURATION OF A MARTIAN SOL

1 Sol	= 1.02749125 days
	= 88775.244 seconds
	= 24 hours, 39 minutes, 35.244 seconds

6.5.2 Local True Solar Time/Local Mean Solar Time

From the Mars Exploration Rover (MER) Project Planetary Constants and Models document (see Appendix F, reference 46), the LTST and Local Mean Solar Time (LMST) equations are

$$LTST = \left(\alpha_P - \alpha_{TS}\ deg\right)\frac{24\ hr}{360\ deg} + 12\ hr$$

$$LMST = \left(\alpha_P - \alpha_{FMS}\ deg\right)\frac{24\ hr}{360\ deg} + 12\ hr$$

where α_P is the Areocentric Right Ascension (ARA) of a point on the surface of Mars, α_{TS} is the ARA of the true sun, and α_{FMS} is the ARA of the FMS. The ARA is an angle measured in the Mars mean equator plane eastward from the vernal equinox vector to the intersection of the meridian containing the point with the equator. (See Figure 6.5.2 1.) In practice, there is no generally accepted definition of the vernal equinox direction of Mars, so the IAU vector is used instead. The relationships above are still valid for IAUreferenced angles so long as all three right ascension values are referenced to the IAU vector at the same epoch.

These equations convert the difference in angles from degrees to true or mean solar hours, with 12 hours representing the time that the true or mean sun is at zenith (i.e., local noon). The conventional method for computing the times above are to compute α_{TS} from the planetary ephemeris file and α_{FMS} from a fit of the Mars ephemeris for the period applicable to a given mission. In a recently published paper, however, Allison and McEwen (see Appendix F, reference 47) developed a best least-squares quadratic fit for the computation of α_{FMS} over 134 Mars orbits spanning the calendar years 1874–2126. Below is the expression for α_{FMS} for the epoch of J2000, adjusted to reflect with respect to the Mars IAU vector given for the epoch of J2000.

α_{FMS}	= (270.3863 - $\Psi(t)$ deg)+(0.5240384 deg/day) (t – t_0)
t_0	= Reference epoch Jan. 1, 2000 12:00:00 TDB = Julian date 2451545.0
t	= Current Julian date
$\Psi(t)$	= Offset between Mars vernal equinox and IAU vectors (See Table 6.5.2-1 below.)

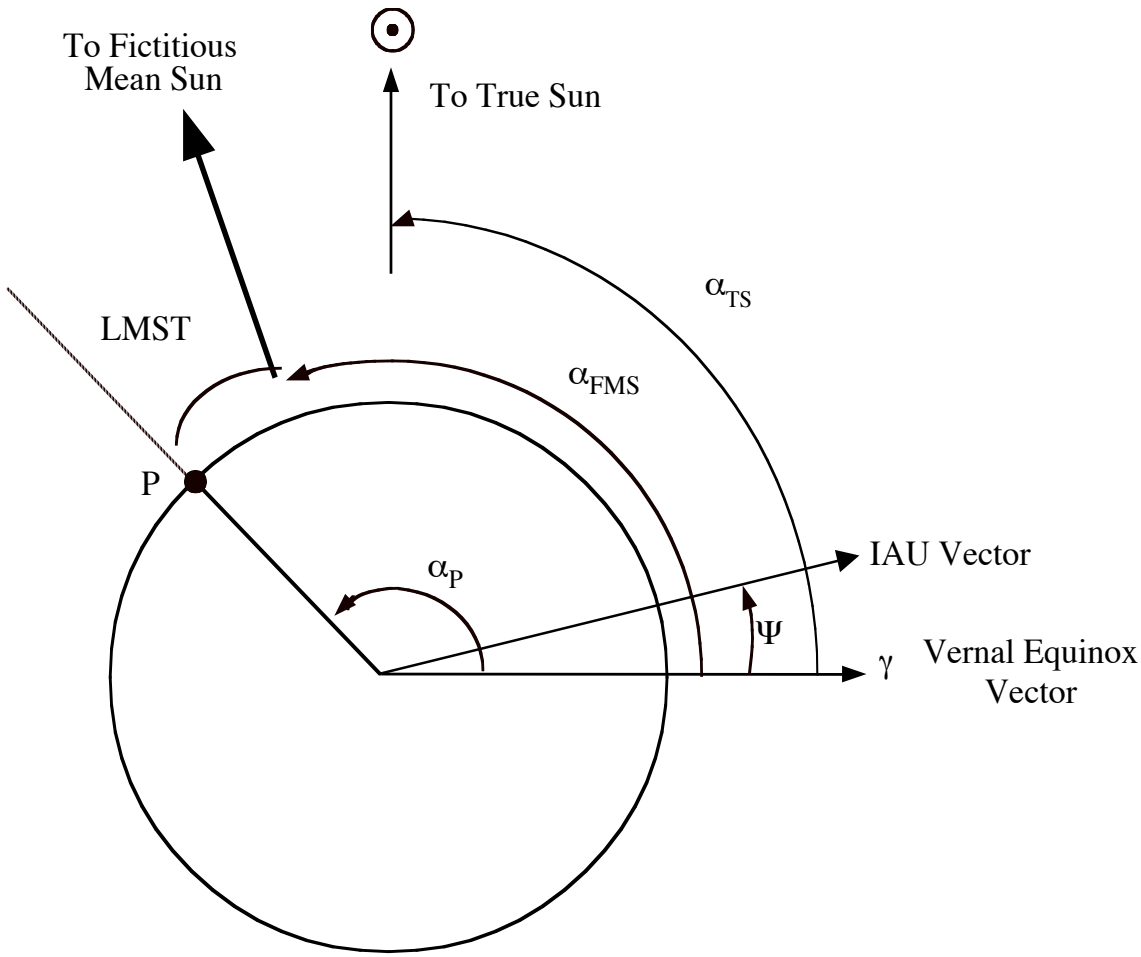

FIGURE 6.5.2-1 DEFINITION OF LTST AND LMST

TABLE 6.5.2-1 OFFSET BETWEEN MARS IAU VECTOR AND MARS VERNAL EQUINOX DIRECTIONS

Epoch	Julian Date	$\Psi(t)$ (deg)
01-JAN-06 12:00:00 ET	2453737.0	136.7582
01-JAN-07 12:00:00 ET	2454102.0	136.7595
01-JAN-08 12:00:00 ET	2454467.0	136.7606
01-JAN-09 12:00:00 ET	2454833.0	136.7614
01-JAN-10 12:00:00 ET	2455198.0	136.7622
01-JAN-11 12:00:00 ET	2455563.0	136.7631
01-JAN-12 12:00:00 ET	2455928.0	136.7643
01-JAN-13 12:00:00 ET	2456294.0	136.7655

The first term in parentheses in the above equation has a constant 270.3863 degree offset with respect to the Mars vernal equinox, as given in Appendix F, reference 47, and a time-dependent offset $\Psi(t)$ to transform it into the IAU frame for the current epoch. $\Psi(t)$ is measured positive eastward along the Mars mean equator from the vernal equinox to the IAU vector. It is computed using the algorithm given in Appendix F, reference 40, with the results for the MSL mission time frame given in Table 6.5.2-1. The table shows that the offset between the Mars IAU frame and the Mars vernal equinox increases at a rate of approximately 0.001 deg/year. Therefore, missions that are expected to last more than a year must account for this correction in computing α_{FMS}. In addition, the equation in Appendix F, reference 47 includes a quadratic term, which has been ignored here because it contributes less than 0.0001 degree over the next 40 years.

6.5.3 Equation of Time

The Equation Of Time (EOT) is the difference between the right ascension of the FMS and the right ascension of the true sun:

$$\begin{aligned} \text{EOT} &= \alpha_{FMS} - \alpha_{TS} \text{ deg} && \text{(Equation of Time in degrees)} \\ &= \text{LTST} - \text{LMST} && \text{(Equation of Time in minutes)} \end{aligned}$$

where α_{TS} can be computed from planetary ephemeris data. The EOT can be converted to minutes to determine the time difference between the LTST and the LMST. Figure 6.5.3-1 shows the EOT in minutes over a period of 10 Julian years (1 JY=365.25 days) from the reference epoch January 1, 2000 12:00:00 TDB. The figure shows that the LTST can vary from the LMST by as much as 50 minutes over the duration of the Martian year.

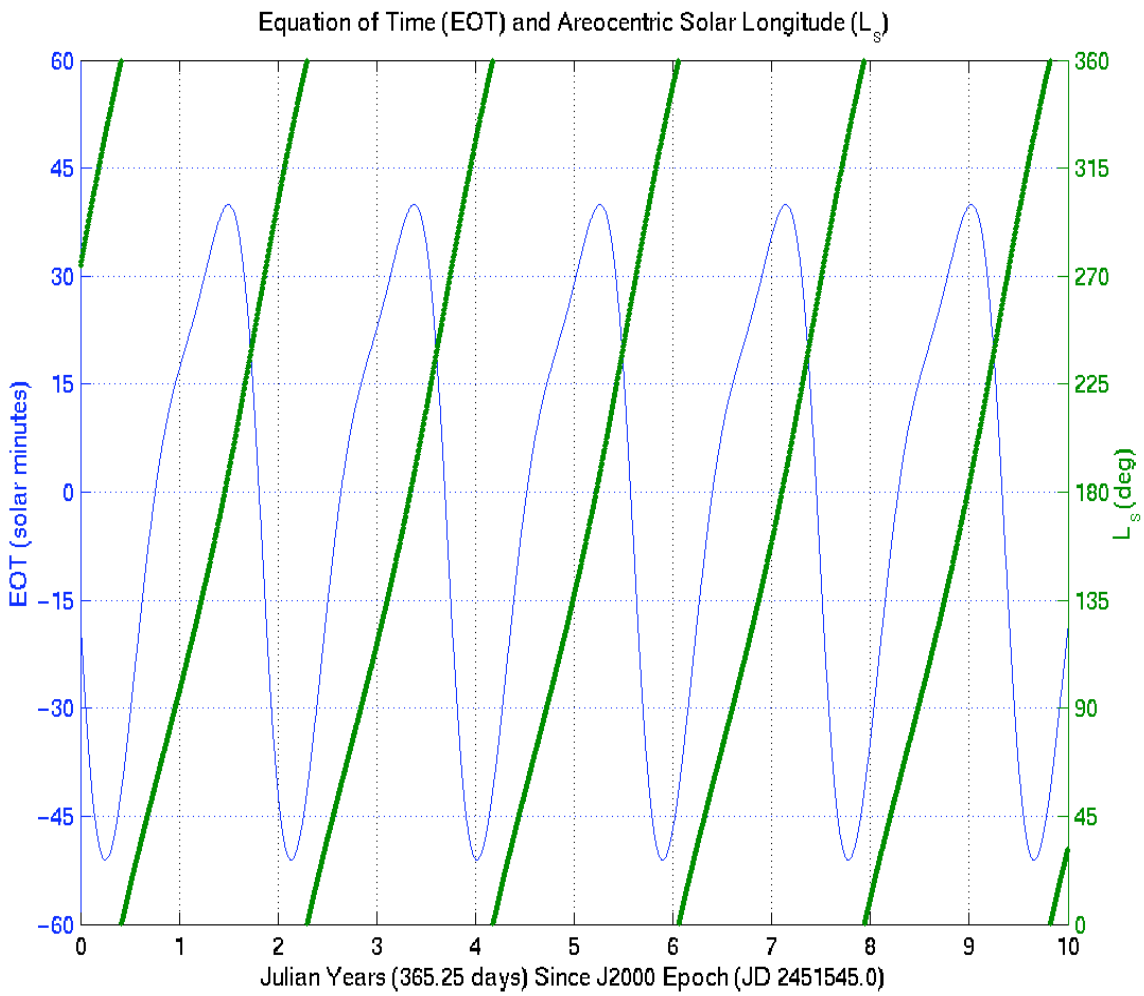

FIGURE 6.5.3-1 EQUATION OF TIME IN SOLAR MINUTES AND AREOCENTRIC LONGITUDE IN DEGREES FOR TEN JULIAN YEARS AFTER THE J2000 EPOCH

The EOT scale is shown on the left axis, and the Ls scale is shown on the right axis.

7.0 FUNDAMENTAL CONSTANTS AND PLANETARY/SATELLITE EPHEMERIDES

7.1 PLANETARY EPHEMERIS

The planetary ephemeris file that contains the current (in 2008) best lunar ephemeris for general mission and navigation analyses and external export is DE421 (Developmental Ephemeris 421 from Appendix F, reference 24), which was released in 2008.

Ephemeris versions which were released before DE421 most often have been intermediate releases to serve the needs of specific missions or programs (e.g., one

containing an improved ephemeris for Pluto). In 2007, efforts began to develop another fully integrated planetary and lunar ephemeris to include further observations made using improved lunar laser ranging measurements. These improved measurements were made post the 1995 release of DE403, the previous best combined planetary and lunar ephemeris. The first result from that effort was DE418, released in August 2007, which improved the lunar position ephemeris by a few meters at the present time (increasing to about 16 m by 2020). In addition, DE418 improved the orientation of the lunar principal axes by about 3.5 arcsec (about 30 m at the lunar surface).

The efforts to develop a new fully integrated ephemeris culminated in DE421, a major new ephemeris release in February of 2008, which refined and improved the internal consistency of the ephemeris from DE418. The Moon's principal axis orientation is given as a function of time with respect to the International Celestial Reference Frame (ICRF) in DE421 and is constant with respect to the LMEBF coordinate system, which itself has changed very little. When a future major ephemeris update is released, a CR will be submitted to update this document to include it, but such releases are expected to be rare (i.e., many years apart), if indeed any are needed at all.

NOTE: The DE421 ephemeris file is available, in its export format, via the following website: http://ssd/iau-comm4/. Once at the website, click on "Where to Obtain Ephemerides". Then read the README file in the section titled "Modern High-Accuracy Ephemerides". To construct a DE421 ephemeris file that covers the years from 1900 to 2053, download the ASCII file ascp1900.421 from the ftp site and follow the instructions.
Ephemeris files are also available from the NAIF node of NASA's PDS in the Space Planet Instrument C-matrix Events (SPICE) kernel (SPK) format at http://pds.nasa.gov.

The gravitational parameters of the Sun and planets that are used by DE421 are:

TABLE 7.1-1 PLANETARY GM VALUES

Body	GM (km^3/s^2)	- All GMs are consistent with a solar system barycentric reference frame.
Sun	132712440040.9446	
Mercury	22032.09	
Venus	324858.592	
Earth	398600.436233	Use GGM02C value (398600.4356 km^3/s^2) for mission analysis and navigation; this is discussed in Section 3.1.
Mars*	42828.375214	Set equal to the MGS95J value; this is discussed in Section 5.1.
Jupiter*	126712764.8	
Saturn*	37940585.2	
Uranus*	5794548.6	
Neptune*	6836535.0	
Pluto*	977.	
Moon	4902.800076	- Use 4902.8000 for mission analysis and navigation; see Section 4.1 for a discussion on current best estimate of the lunar GM.

* Includes the gravitational parameters of the planet's satellites.

NOTE: The JPL planetary ephemerides are developed in a solar system barycentric reference frame.

The following constants were assumed/derived in the development of DE421.

TABLE 7.1-2 CONSTANTS FROM DE421

c	= 299792.458 km/s	(Speed of light, defined quantity)
AU	= 149597870.691 km	(Astronomical Unit, solved for quantity in the development of DE421)

7.2 SATELLITE EPHEMERIDES

Since the lunar ephemeris is contained within the DE421 planetary ephemeris file, no separate satellite ephemeris file is needed for the Moon. Characteristics of the lunar ephemeris in DE421 are discussed in Appendix F, reference 48.

The most recent ephemeris for the Martian satellites is mar063.bsp (NAIF SPICE SPK file) and is available at ftp://naif.jpl.nasa.gov/pub/naif/generic_kernels/spk/satellites.

7.3 SOLAR CONSTANT

The total solar irradiance at 1 AU, which is used for computing the solar radiation force on a spacecraft, is specified in Appendix F, reference 25.

TABLE 7.3-1 SOLAR CONSTANT

$F1_{AU}$ = 1366.1 W/m^2 (Solar constant; total solar irradiance at 1 AU)

8.0 COORDINATE SYSTEMS

The coordinate systems used by Constellation to archive or exchange information between different elements are documented in CxP 70138. Many other coordinate systems are used for particular purposes within Constellation elements and are (or should be) documented by those elements.

The coordinate system generally used for navigation information and used internally in most orbit determination processes is the ICRF. The ICRF is often referred to as Earth Mean Equator and Equinox of J2000 (EME2000); it is sometimes just called J2000, although strictly speaking, the term “J2000” refers just to the IAU/IGU epoch of January 1.5, 2000 (Julian date 2451545.0). This non-rotating frame is preferred because it is the one in which basic navigation data are given, in particular, the planetary and lunar ephemerides (including coefficients defining the orientation of the LPABF frame).

Most coordinate frames are defined in reference to characteristics of the physical universe, and as such it is impossible (perhaps even in principle) to know *exactly* how these coordinate frames relate to each other (i.e., what the coordinate transformations between them are). A basic set of useful approximations to these coordinate transformations is provided by a IAU/IGU Working Group in Appendix F, reference 6. Note, however, as stated in Section 3.2, that the epoch and time scale are erroneously stated in reference 6 to be TCB, when it in fact they are given in ephemeris time, or TDB, which is implicit in the formula given for the position of the Earth’s prime meridian. The simple approximations given in reference 6 are adequate for concept development and initial mission design, but are insufficient for precision orbit determination. (The approximations are most divergent in prime meridian location, which is modeled as moving uniformly.) More accurate approximations are discussed in Section 3.2 above and in CxP 70138.

In many cases, the accuracy of coordinate system relationships is measured in milliarcseconds (mas). For reference, one degree is about 17 milliradians (mrad), one arcsecond is about 5 microradians (μrad), and one mas is about 5 nanoradians (nrad), this last corresponding as a central angle to about 30 mm on the surface of the Earth, 9 mm on the surface of the Moon, 2 m at the distance of the Moon from the Earth, and just over 1 km at 1.5 AU, a typical distance from Earth to Mars.

9.0 MEAN ORBIT ELEMENTS

<TBR

APPENDIX A
ACRONYMS AND ABBREVIATIONS AND GLOSSARY OF TERMS

A1.0 ACRONYMS AND ABBREVIATIONS

ADD	Architecture Description Document
ALSEP	Apollo Lunar Surface Experiment Package
ANSI	American National Standards Institute
ARA	Areocentric Right Ascension
AU	Astronomical Unit
BIPM	Bureau International des Poids et Mesures (or International Bureau of Weights and Measures; France)
$C_{22\ \text{Moon-Tide}}$	Sectorial value adjusted for perm. tide — Rigid C_{22}
CARD	Constellation Architecture Requirements Document
CR	Change Request
D	Days past epoch of J2000
DIS	Draft International Standard
$D_{\text{SOI Moon}}$	Moon Sphere of Influence
DSN	Deep Space Network
DSNE	Design Specification for Natural Environments
$D_{\text{SOI Earth}}$	Earth sphere of influence
$D_{\text{SOI Mars}}$	Mars Sphere of Influence
EASEP	Early Apollo Scientific Experiment Package
EDL	Entry Descent and Landing
EMEPM	Earth Mean Equator and Prime Meridian
EOP	Earth Orientation Parameter
EOT	Equation of Time
ET	Ephemeris Time
f	Flattening Factor
F_{Earth}	Earth flattening factor, derived from IAU/IAG values
f_{Moon}	Moon flattening factor, derived from IAU/IAG values
FMS	Fictitious Mean Sun

g_{Earth}	Earth standard acceleration of gravity
$g_{Moon\text{-}Mean}$	Mean lunar gravitation at the surface
GM_{Deimos}	Gravitational parameter of Deimos
GM_{Earth}	Gravitational parameter of Earth
GM_{Mars}	Gravitational parameter of Mars
GM_{Moon}	Gravitational parameter of Moon
GM_{Phobos}	Gravitational parameter of Phobos
GPS	Global Positioning System
GRACE	Gravity Recovery and Climate Experiment
GSFC	Goddard Space Flight Center
GTDS	Goddard Trajectory Determination System
HP	Horizontal Parallax
IAU	International Astronomical Union
IAG	International Association of Geodesy
ICRF	International Celestial Reference Frame
IERS	International Earth Rotation and Reference Systems Service
ILE	Improved Lunar Ephemeris
ISO	International Organization for Standards
ITRF	International Terrestrial Reference Frame
JPL	Jet Propulsion Laboratory
$J_{3\ Mars}$	Mars 3rd Degree Zonal, Un-normalized
$\hat{J}_{3\ Mars}$	Mars 3rd Degree Zonal, Normalized
$J_{2\ Earth}$	Earth 2nd degree zonal, Un-normalized
$\hat{J}_{2\ Earth}$	Earth 2nd degree zonal, Normalized
$J_{2\ Mars}$	Mars 2nd Degree Zonal, Un-normalized
$\hat{J}_{2\ Mars}$	Mars 2nd Degree Zonal, Normalized
$J_{2\ Moon\text{-}Tide}$	Zonal value adjusted for permanent tide - Rigid J_2
J2000	Reference epoch of J2000 in Julian days; Calendar date of J2000 ref. epoch

k_{20}	Moon Love Number for 2nd degree zonal, J_2
k_{22}	Moon Love Number for 2nd degree sectorial, C_{22}
LEO	Low Earth Orbit
LIDAR	Light Detection and Ranging
LLR	Lunar Laser Ranging
LM	Lunar Module Descent Stage
LM-AS	Lunar Module-Ascent Stage
LM-DS	Lunar Module-Descent Stage
LMEBF	Lunar Mean Earth Body-Fixed
LMST	Lunar Mean Solar Time
LPAE	Lunar Principal Axis of Epoch
LPABF	Lunar Principal Axis Body-Fixed
LPI	Lunar and Planetary Institute
LRRR	Lunar laser Ranging RetroReflector
LRV	Lunar Roving Vehicle
LTST	Local True Solar Time
mas	milliarcsecond
MER	Mars Exploration Rover
MET	Modularized Equipment Transporter
MGS	Mars Global Surveyor
MOLA	Mars Orbiter Laser Altimiter
mrad	Milliradians
MS	Mass Spectrometer
MSL	Mars Science Laboratory
MUSES	Mu Space Engineering Satellite
NAIF	Navigation Ancillary Information Facility
NEDD	Natural Environment Definition for Design
NGS	National Geographic Society
NIST	National Institute of Standards and Technology
nrad	Nanoradians
NSSDC	National Space Science Data Center

ODP/DPTRAJ	Orbit Determination Program/Double Precision Trajectory Program
OLST	Orbit Local Solar Time
OPR	Office of Primary Responsibility
P&FS or PFS	Particles and Fields Subsatellite
PDS	Planetary Data System
PSEP	Passive Seismic Experiment Package
R.A.	Right Ascension
$R_{Deimos\text{-}equatx}$	Subplanet equatorial radius of Deimos (IAU/IAG)
$R_{Deimos\text{-}equaty}$	Along orbit equatorial radius of Deimos (IAU/IAG)
$R_{Deimos\text{-}mean}$	Mean radius of Deimos from IAU/IAG
$R_{Deimos\text{-}polar}$	Polar radius of Deimos from IAU/IAG
$R_{Earth\text{-}Equator}$	Radius of Earth equator from IAU/IAG
$R_{Earth\text{-}Pole}$	Radius of Earth pole from IAU/IAG
$R_{Earth\text{-}Ref}$	Dynamical reference radius
$R_{Mars\text{-}Equator}$	Mean radius of Mars Equator
$R_{Mars\text{-}Pole}$	Mean radius of Mars Poles
$R_{Moon\text{-}Equator}$	Radius of Moon equator from IAU/IAG
$R_{Moon\text{-}Pole}$	Radius of Moon pole from IAU/IAG
$R_{Moon\text{-}Ref}$	Mean dynamical radius of Moon
$R_{Phobos\text{-}equatx}$	Subplanet equatorial radius of Phobos from IAU/IAG
$R_{Phobos\text{-}equaty}$	Along orbit equatorial radius of Phobos from IAU/IAG
$R_{Phobos\text{-}mean}$	Mean radius of Phobos from IAU/IAG
$R_{Phobos\text{-}polar}$	Polar radius of Phobos from IAU/IAG
R_{ref}	Reference radius
$R_{Atmos\text{-}Interface}$	Radius at atmospheric entry interface
SI	International System of Units
SIG	Systems Integration Group
SIM	Scientific Instrument Module
S-IVB	Saturn IV-B (third stage of Saturn V rocket)

SLR	Satellite Laser Ranging
SLST	Surface Local Solar Time
SM	Service Module
SOI	Sphere of Influence
SPK	SPICE kernel
T	Julian centuries past epoch of J2000
TAI	Temps Atomique International (or International Atomic Time)
TCB	Barycentric Coordinate Time
TDB	Barycentric Dynamical Time
TDT	Terrestrial Dynamical Time
T_{eph}	Solar system barycentric based time scale
TT	Terrestrial Time
ULCN	Unified Lunar Control Network
USGS	United States Geological Survey
USNO	U.S. Naval Observatory
UT	Universal Time
UTC	Coordinated Universal Time
VLBI	Very Long Baseline Interferometry
$\dot{W}_{Earth}$	Rotational rate of Earth
$W_{Earth\text{-}IAU}$	Prime meridian with respect to Earth IAU-Node vector
W_{Mars}	Prime meridian with respect to Mars IAU Vector
W_{Moon}	Prime meridian, mean Earth direction
$\dot{W}_{Mars}$	Rotational rate of Mars
α_{Mars}	Right ascension of Mars Pole in EME2000
$\alpha_{Moon\text{-}IAU}$	Right ascension of Moon rotation pole
$\alpha_{Earth\text{-}IAU}$	Right ascension of Earth pole in EME2000
δ_{Mars}	Declination of Mars Pole in EME2000
$\delta_{Moon\text{-}IAU}$	Declination of Moon rotation pole
$\delta_{Earth\text{-}IAU}$	Declination of Earth pole in EME2000

A2.0 GLOSSARY OF TERMS

Term	Description
Constellation Reference Time	A time reference scale without leap seconds. Constellation Reference Time provides an alternative to UTC for expressing continuous elapsed time from epoch. This alternative is necessary for computing applications that cannot tolerate discontinuities or leap seconds

APPENDIX B
OPEN WORK

B1.0 TO BE DETERMINED

Table B1-1 lists the specific To Be Determined (TBD) items in the document that are not yet known. The TBD is inserted as a placeholder wherever the required data is needed and is formatted in bold type within brackets. The TBD item is numbered based on the section where the first occurrence of the item is located as the first digit and a consecutive number as the second digit (i.e., **<TBD 4-1>** is the first undetermined item assigned in Section 4 of the document). As each TBD is solved, the updated text is inserted in each place that the TBD appears in the document and the item is removed from this table. As new TBD items are assigned, they will be added to this list in accordance with the above described numbering scheme. Original TBDs will not be renumbered.

TABLE B1-1 TO BE DETERMINED ITEMS

TBD	Section	Description
None		

B2.0 TO BE RESOLVED

Table B2-1 lists the specific To Be Resolved (TBR) issues in the document that are not yet known. The TBR is inserted as a placeholder wherever the required data is needed and is formatted in bold type within brackets. The TBR issue is numbered based on the section where the first occurrence of the issue is located as the first digit and a consecutive number as the second digit (i.e., **<TBR 4-1>** is the first unresolved issue assigned in Section 4 of the document). As each TBR is resolved, the updated text is inserted in each place that the TBR appears in the document and the issue is removed from this table. As new TBR issues are assigned, they will be added to this list in accordance with the above described numbering scheme. Original TBRs will not be renumbered.

TABLE B2-1 TO BE RESOLVED ISSUES

TBR	Section	Description
TBR 3-1	3.5	Add a section to Section 3.0 describing ground tracking station networks, including a table of locations for selected stations, which can be used for initial coverage analysis.
TBR 6-1		Add a subsection to 6.2 to describe GPS time.
TBR 9-1	9.0	Add a section to describe mean orbit elements.
TBR C1-1	C1.1	Find a location to archived lunar maps and add URL to C1.1 for that location.
TBR C1-2	C1.2	Find a location to archived lunar maps and add URL to C1.2 for that location.
TBR C1-3	C1.3	Find a location to archived lunar maps and add URL to C1.3 for that location.

APPENDIX C
LUNAR MAPS

C1.0 GLOBAL LUNAR MAPS

Many different types of global lunar maps have been produced over the past 30–40 years. The following represent just a few of the useful types.

C1.1 LUNAR NEAR SIDE

Miscellaneous Investigations Series, Map I-2276, Scale 1:5M, published in 1992 by the United States Geological Survey (USGS)

- Sheet 1: Shaded Relief and Surface Markings Map of the Lunar Near Side
- Sheet 2: Shaded Relief Map of the Lunar Near Side (Mercator map projections)

Copies of these maps were provided by the Lunar and Planetary Institute (LPI) in Houston, Texas. The maps are located at:

<TBR C1-1>

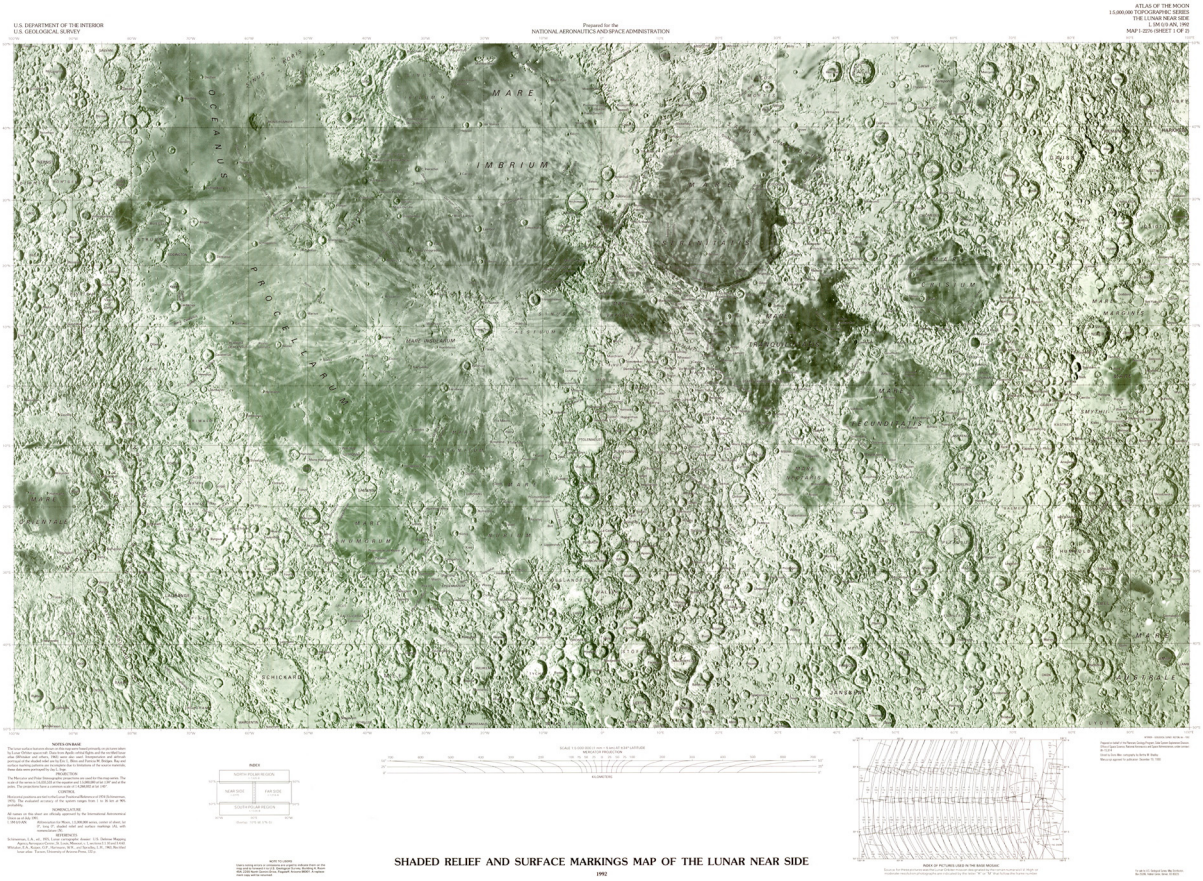

FIGURE C1.1-1 SHADED RELIEF MAP OF THE LUNAR NEAR SIDE

C1.2 LUNAR FAR SIDE

Miscellaneous Investigations Series, Map I-1218, Scale 1:5M, published in 1980 by the USGS

- I-1218A: Shaded Relief and Surface Markings Map of the Lunar Far Side
- I-1218B: Shaded Relief Map of the Lunar Far Side (Mercator map projections)

The LPI provided copies of these maps. The maps are located at:

<TBR C1-2>

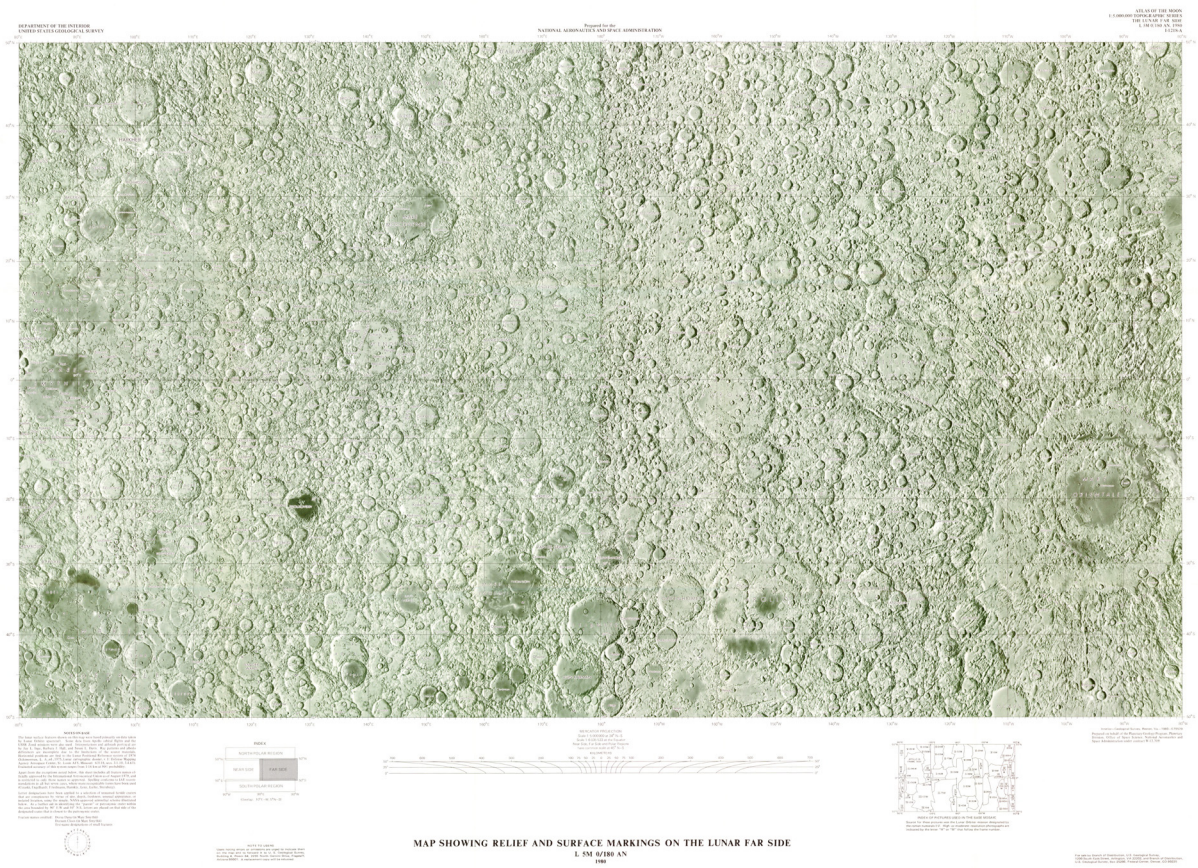

FIGURE C1.2-1 SHADED RELIEF MAP OF THE LUNAR FAR SIDE

C1.3 LUNAR POLAR REGIONS

Miscellaneous Investigations Series, Map I-1326, Scale 1:5M, published in 1981 by USGS

- I-1326A: Shaded Relief Map of the Lunar Polar Regions
- I-1326B: Shaded Relief and Surface Markings Map of the Lunar Polar Regions
  (Polar Stereographic map projections)

The LPI provided copies of these maps. The maps are located at:

<TBR C1-3>

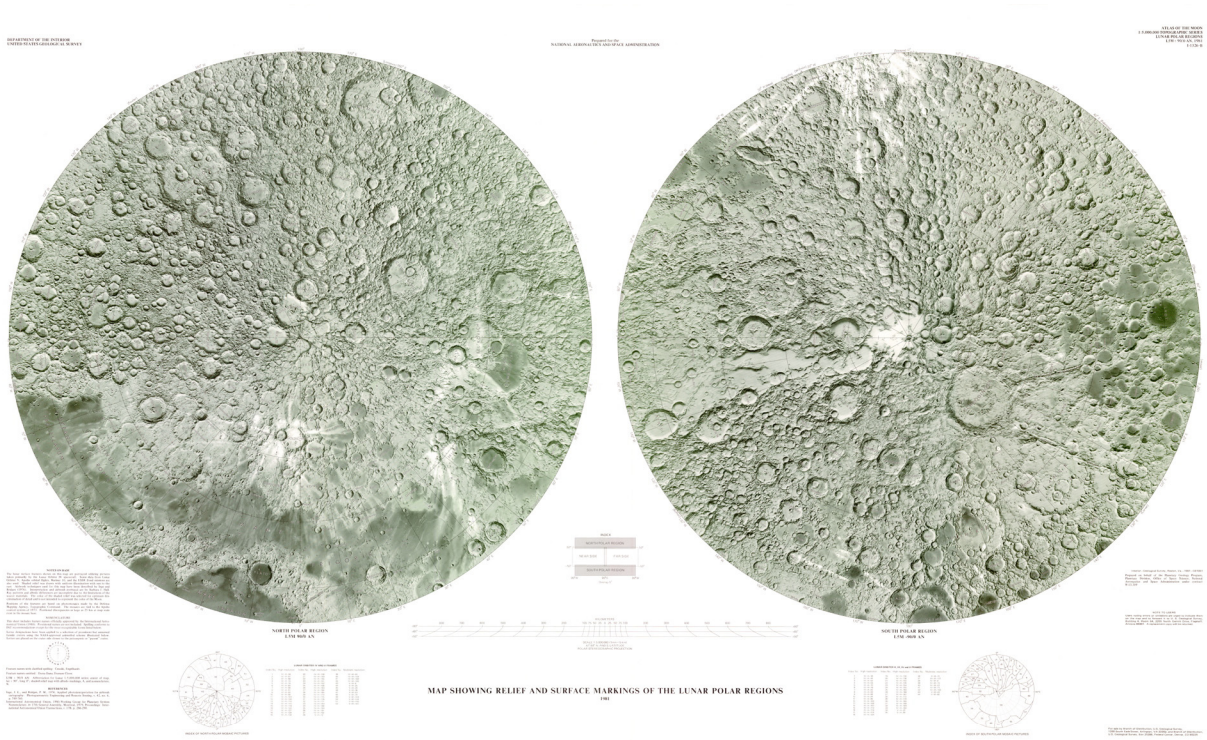

FIGURE C1.3-1 SHADED RELIEF MAP OF THE LUNAR POLAR REGIONS

C1.4 COLOR-CODED TOPOGRAPHY AND SHADED RELIEF MAPS OF THE LUNAR HEMISPHERES

Geologic Investigations Series I-2769, Scale 1:10M, published by the USGS in 2002

- Sheet 1: Lunar Near Side and Far Side Hemispheres – (see Figures 4.6.1-1 and 4.6.1-2)
- Sheet 2: Lunar East and West Hemispheres
- Sheet 3: Lunar North and South Hemispheres (Lambert-Azimuthal Equal Area map projections)

The maps can be found at the following website: http://geopubs.wr.usgs.gov/i-map/i2769/

C1.5 ONLINE LUNAR MAP WALL POSTER

Many commercial companies have marketed the sale of lunar maps in the form of wall posters. While not endorsing the purchase of any particular map, one lunar map wall poster, produced by the National Geographic Society (NGS), is worth mentioning since the map is essentially available online. The NGS map is protected by copyright, but a "browse-able" version of the map can be found via the following NGS website: *http://shop.nationalgeographic.com/product/307/47/173.html.* With "zoom" and "scroll" capability, the entire map can be viewed at a high resolution. The map is a shaded relief map with surface markings and is depicted using a Lambert-Azimuthal Equal Area projection. The map also indicates landing site locations of many lunar missions. Below are example screen shots from the NGS website.

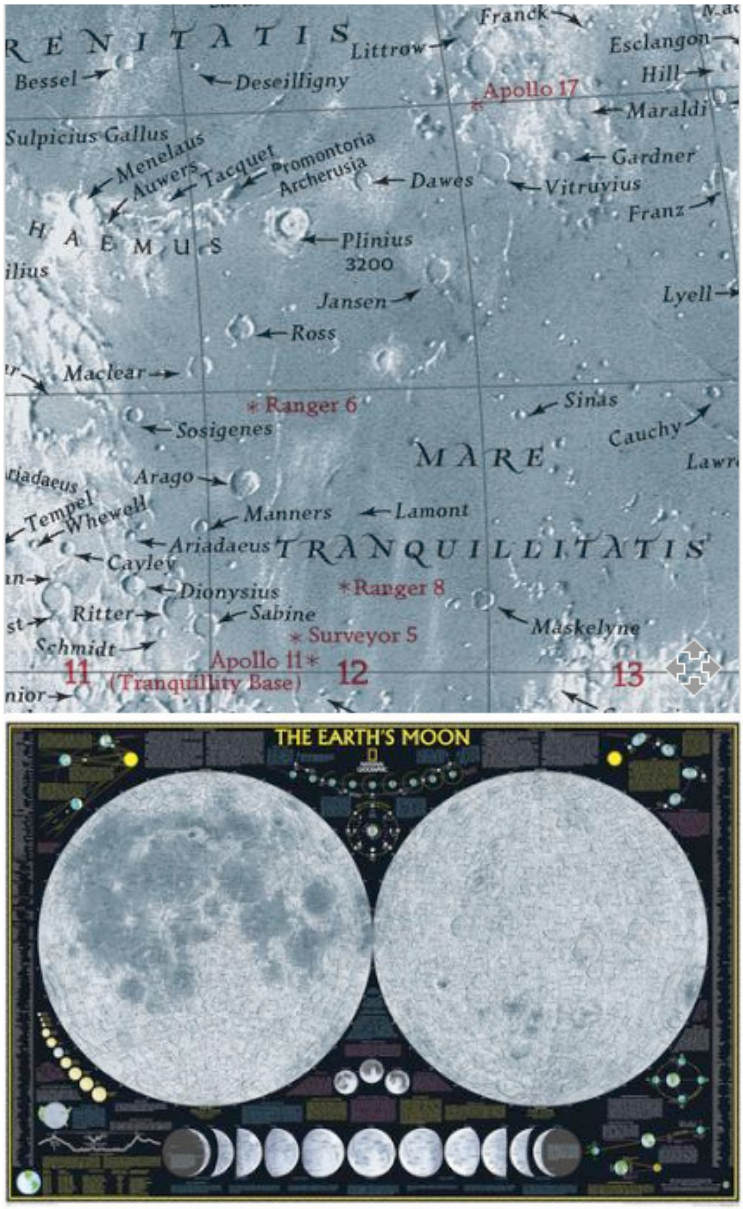

FIGURE C1.5-1 SAMPLE FROM THE NATIONAL GEOGRAPHIC SOCIETY WEBSITE

APPENDIX D
LUNAR EXPLORATION

D1.0 LUNAR EXPLORATION MISSION SUMMARY (FOR MISSIONS THAT HAVE REACHED THE LUNAR SURFACE)

The majority of the data presented in this section was extracted from the Lunar Exploration Timeline compiled by the NASA National Space Science Data Center (NSSDC). (See Appendix F, reference 27). The list of missions summarized in Appendix B of reference 27 only includes those missions that are known to have (or possibly have) deposited terrestrial material (whether intended or not) onto the surface of the Moon. This list of missions includes lunar orbiters whose orbit lifetimes have (or are believed to have) expired (i.e., the orbiters crashed into the surface of the Moon). Some of the data and descriptive text presented in this section were augmented by data and text from Appendix F, references 28 and 29.

D1.1 SOVIET LUNA PROBES

The Luna series of unmanned probes included the first probe to fly by the Moon and photograph the far side of the Moon, the first probe to impact the Moon, the first probe to soft land and return photographs, the first robotic sample return (which occurred after the manned Apollo 11 and Apollo 12 had already returned their lunar samples), and the first probe to deploy a remotely-controlled rover.

Mission	Mission Type	Launch Date	Remarks
Luna 2	Impact	12 Sep 1959	First spacecraft to reach another celestial body.
Luna 5	Lander	9 May 1965	First soft landing attempt. Lost attitude 40 km from the Moon.
Luna 7	Lander	4 Oct 1965	Lost attitude prior to retro-rocket ignition – ignition aborted.
Luna 8	Lander	3 Dec 1965	Entered uncontrolled spin – retro-rocket burn prematurely terminated.
Luna 9	Lander	31 Jan 1966	First successful soft landing.
Luna 10	Orbiter	31 Mar 1966	First orbiter. Initial period 178.05 min, Inclination 21.9 deg, Eccentricity 0.14, Operated for 460 orbits.
Luna 11	Orbiter	24 Aug 1966	Initial period 178 min, Inclination 27 deg, Eccentricity 0.22, Operated for 277 orbits.
Luna 12	Orbiter	22 Oct 1966	Initial period 205 min, Inclination 4 deg, Eccentricity 0.31, Operated for 602 orbits.
Luna 13	Lander	21 Dec 1966	Transmitted panoramic views of lunar landscape.
Luna 14	Orbiter	7 Apr 1968	Initial period 160 min, Inclination 42 deg, Eccentricity 0.16.
Luna 15	Sample Return	13 Jul 1969	First sample return attempt. Completed 52 orbits. Lost signal upon impact after descent burn – while Apollo 11 Lunar Module (Eagle) was on the surface.

Luna 16	Sample Return	12 Sep 1970	First successful robotic lunar sample return. Landed in darkness. 101 g returned to Earth on 24 Sep 1970.
Luna 17	Rover	10 Nov 1970	Lunokhod 1 rover traveled 10.5 km and survived 11 months.
Luna 18	Lander	2 Sep 1971	Completed 54 orbits. Lost signal upon impact after descent burn.
Luna 19	Orbiter	28 Sep 1971	Initial period 121.13 min, Inclination 40.6 deg, Eccentricity 0.18.
Luna 20	Sample Return	14 Feb 1972	Landed approximately 120 km from where Luna 16 landed. 30 g of lunar material returned to Earth on 25 Feb 1972.
Luna 21	Rover	8 Jan 1973	Lunokhod 2 rover traveled 37 km and survived about 4 months.
Luna 22	Orbiter	29 May 1974	Period 192 min, Inclination 21 deg, Eccentricity 0.279 (final orbit).
Luna 23	Sample Return	28 Oct 1974	Spacecraft damaged during landing. Survived 3 days. No samples returned.
Luna 24	Sample Return	9 Aug 1976	Landed a few hundred meters from Luna 23. 170 g of lunar material returned to Earth on 22 Aug 1976.

D1.2 U.S. RANGER PROBES

The Ranger series included both probes which impacted the Moon at high velocity, returning images with increasing resolution up to the moment of impact, and "hard landers" which fired a braking motor at the last moment, dropping an instrument package protected by a balsa wood spherical shock absorber. The early Ranger missions were plagued by problems – the first successful mission was Ranger 7 in 1964. None of the hard landers succeeded. The three successful missions were all imaging impact probes. Ranger 8 flew a direct-in trajectory toward *Mare Tranquillitatis*, the Sea of Tranquility, providing the first close-up views which indicated the surface was smooth enough for the Apollo Lunar Module to land there.

Mission	Mission Type	Launch Date	Remarks
Ranger 4	Impact	23 Apr 1962	Computer failure, no telemetry received. Impacted far side of Moon.
Ranger 6	Impact/Photo	30 Jan 1964	Camera system failure. No images returned.
Ranger 7	Impact/Photo	28 Jul 1964	Transmitted 4,308 photographs over the final 17 minutes of flight.
Ranger 8	Impact/Photo	17 Feb 1965	Transmitted 7,137 photographs over the final 23 minutes of flight.
Ranger 9	Impact/Photo	21 Mar 1965	Transmitted 5,814 photographs over the final 19 minutes of flight.

D1.3 U.S. SURVEYOR LANDERS

The Surveyor soft landers proved the lunar surface was sufficiently flat and strong to allow the Apollo Lunar Module to land. (Prior to the soft landings by Luna 9 and Surveyor 1 in 1966, some believed that the Moon was covered by a deep sea of dust which would be unable to support the weight of a lander – i.e., any landed vehicle would sink beneath the surface.) The Surveyor probes were equipped with steerable cameras which provided panoramic views of their landing sites. Later Surveyors carried a robotic scoop which could excavate soil, move rocks, and deposit soil into instruments for analysis, which provided the first in situ data about the composition of the lunar regolith.

Mission	Mission Type	Launch Date	Remarks
Surveyor 1	Lander	30 May 1966	Operated until 7 Jul 1966. No operation during lunar night.
Surveyor 2	Lander	20 Sep 1966	One of three vernier engines failed to ignite during a mid-course maneuver. Impacted the Moon.
Surveyor 3	Lander	17 Apr 1967	Vernier engines continued to fire during landing — spacecraft lifted off the surface twice before engines finally shut down.
Surveyor 4	Lander	14 Jul 1967	Lost contact approximately 2.5 minutes before touchdown. Landing might have been successful.
Surveyor 5	Lander	8 Sep 1967	First in situ chemical soil analysis. Operated until 17 Dec 1967. No operation during lunar night.
Surveyor 6	Lander	7 Nov 1967	Spacecraft engines were restarted after landing, lifting the vehicle about 4 m off the ground and coming down about 2.4 m from the original landing site.
Surveyor 7	Lander	7 Jan 1968	Operated 80 hours past sunset on first lunar day. Operated until 21 Feb 1968.

D1.4 U.S. LUNAR ORBITERS

The Lunar Orbiter program consisted of five Lunar Orbiters which returned photography over 99% of the lunar surface (near and far side) with a resolution, in some images, down to 1 meter. Altogether the Orbiters returned 2180 high-resolution and 882 medium-resolution frames. The micrometeoroid experiments recorded 22 impacts showing the average micrometeoroid flux near the Moon was about two orders of magnitude greater than in interplanetary space but slightly less than the near-Earth environment. The radiation experiments confirmed that the design of Apollo hardware would protect the astronauts from average and greater-than-average short-term exposure to solar particle events. The Lunar Orbiters were all eventually commanded to crash on the Moon before their attitude control gas ran out so they would not present navigational or communications hazards to later Apollo flights.

Mission	Mission Type	Launch Date	Remarks
Lunar Orb 1	Orbiter	10 Aug 1966	Initial period 208.1 min, Inclination 12 deg, Eccentricity 0.33.
Lunar Orb 2	Orbiter	6 Nov 1966	Initial period 208.07 min, Inclination 11.9 deg, Eccentricity 0.35.
Lunar Orb 3	Orbiter	5 Feb 1967	Initial period 208.1 min, Inclination 20.9 deg, Eccentricity 0.33.
Lunar Orb 4	Orbiter	4 May 1967	Initial period 721 min, Inclination 85.5 deg, Eccentricity 0.28.
Lunar Orb 5	Orbiter	1 Aug 1967	Initial period 510.08 min, Inclination 85 deg, Eccentricity 0.26.

D1.5 U.S. APOLLO MANNED LUNAR LANDINGS

The Apollo manned lunar landings returned more than 380 kilograms of samples from a variety of lunar terrain types and emplaced instrument packages which performed measurements long after the astronauts had left. Seismometers allowed study of the lunar interior, both from response to natural moonquakes and impacts from spent Saturn IV-B stages (that boosted the Apollo spacecraft to the Moon) and Lunar Module ascent stages (jettisoned in lunar orbit) that were deliberately crashed into the Moon. Laser retro-reflectors left by Apollo missions remain in use today, providing data for research in topics ranging from dynamics of the Earth-Moon system to tests of general relativity.

Mission	Mission Type	Launch Date	Remarks
Apollo 11	Manned/Lander	16 Jul 1969	First humans to step foot onto another celestial body. EVA 2.53 hrs. Traverse distance 250 m. Sample return 21.7 kg.
Apollo 12	Manned/Lander	14 Nov 1969	Apollo 12 landed within walking distance of Surveyor 3. The Ascent Stage of the Lunar Module was intentionally crashed into the Moon creating the first recorded artificial moonquake. EVA 7.75 hrs. Traverse distance 1.35 km. Sample return 34.4 kg.
Apollo 14	Manned/Lander	31 Jan 1971	EVA 9.38 hrs. Traverse distance 3.45 km. Sample return 42.9 kg.
Apollo 15	Manned/Lander	26 Jul 1971	The Lunar Roving Vehicle (LRV) explored regions within 5 km of the landing site. A scientific sub-satellite was deployed from the Service Module in lunar orbit. EVA 19.13 hrs. Traverse distance 27.9 km. Sample return 76.8 kg.
Apollo 16	Manned/Lander	16 Apr 1972	The LRV explored regions within 4.5 km of the landing site. A scientific sub-satellite was deployed from the Service Module into an elliptical orbit with an estimated lifetime of one month. EVA 20.23 hrs. Traverse distance 27 km. Sample return 94.7 kg.
Apollo 17	Manned/Lander	7 Dec 1972	Last mission to carry humans to the Moon. The LRV explored regions within 7.5 km of the landing site. EVA 22.07 hrs. Traverse distance 35 km. Sample return 110.5 kg.

D1.6 OTHER LUNAR ORBITING MISSIONS

Mission	Mission Type	Launch Date	Remarks
Explorer 35	Orbiter	19 July 1967	U.S. spacecraft also known as IMP-6 for the sixth spacecraft in the Interplanetary Monitoring Platform series.
Explorer 49	Orbiter	4 July 1968	U.S. spacecraft also known as RAE-2 (or RAE-B) for the second spacecraft in the Radio Astronomy Explorer series.
Hiten	Orbiter	24 Jan 1990	Japanese Earth orbiting satellite, Mu Space Engineering Satellite (MUSES), originally called MUSES-A designed primarily to test and verify technologies for future lunar and planetary missions. Included 10 lunar flybys before going into lunar orbit.
Hagoromo	Orbiter		Sub-satellite deployed from Hiten on 18 March 1990.
Lunar Prospector	Orbiter	7 Jan 1998	U.S. spacecraft to study the Moon – the third mission in NASA's Discovery program.

Note: The Clementine mission, which orbited the Moon for seven months in 1994, is not included because it left the Earth-Moon system without leaving any material on the surface of the Moon.

D2.0 TERRESTRIAL OBJECTS ON THE MOON

Table D2-1 indicates the impact and landing sites of all of the missions that are known to have deposited terrestrial material onto the surface the Moon. The list includes staged or jettisoned spacecraft hardware (referred to as "mission elements"). Table D2-2 provides the locations of the major Apollo mission elements on the surface of the Moon including those deployed by the Apollo astronauts. Table D2-3 indicates the locations of the Apollo mission elements that were directed to impact the Moon from either a trans-lunar trajectory or from lunar orbit. This list includes those mission elements left in lunar orbit, but whose orbits are believed to have decayed to the point of impact with the lunar surface. Finally, Table D2-4 provides a listing of those missions (and mission elements) known to have been in orbit about the Moon when contact was lost with the spacecraft. The orbits of most (but perhaps not all) of these spacecraft have decayed to the point of impact with the surface of the Moon.

Finding the definitive source for the impact/landing site locations for all of these missions (and mission elements) is extremely difficult to impossible. An attempt has been made in each of the tables in this section to indicate the source of the site location information. The majority of data were extracted from Appendix F, references 27 and 29–32. Additional sources were also consulted for comparison and corroboration, but the tables here list only those sources that were used. Unless another source was deemed superior, the default source for the data in this section was the NSSDC website. (See Appendix F, reference 27.)

TABLE D2-1 IMPACT/LANDING SITES FOR LUNAR MISSIONS (AND MISSION ELEMENTS)

Mission Msn Element	Impact / Landing Date (UTC)	Latitude (deg)	East Long. (deg)	Impact / Landing Site Location	Source (Ref. No.)
Luna 2	13 Sep 1959	29.1 [1]	0.0 [1]	Palus Putredinis – Near Autolycus crater	27
Launch vehicle 3rd stage – impact 30 min after Luna 2				Assume same location as Luna 2	27
Ranger 4	26 Apr 1962	-15.5	229.3	Far side of the Moon – Near Ioffe crater	27
Ranger 6	2 Feb 1964	9.33	21.52	Mare Tranquillitatis (Sea of Tranquility)	27
Ranger 7	31 Jul 1964	-10.70	339.33	Near Mare Cognitum (the sea that has become known)	27
Ranger 8	20 Feb 1965	2.71	24.81	Mare Tranquillitatis (Sea of Tranquility)	27
Ranger 9	24 Mar 1965	-12.91	357.62	Alphonsus crater	27
Luna 5	12 May 1965	-31 [2]	352 [2]	Mare Nubium (Sea of Clouds)	29
Luna 7	7 Oct 1965	9	311	Oceanus Procellarum (Ocean of Storms)	29
Two auxiliary modules jettisoned before retro-rocket ignition				Assume same location as Luna 7	29
Luna 8	6 Dec 1965	9.13	296.7	Oceanus Procellarum (Ocean of Storms)	29
Two auxiliary modules jettisoned before retro-rocket ignition				Assume same location as Luna 8	29
Luna 9	3 Feb 1966	7.13	295.63	Oceanus Procellarum (Ocean of Storms)	29
Two auxiliary modules jettisoned before retro-rocket ignition				Assume same location as Luna 9	29
Retro-rocket				Assume same location as Luna 9	29
Surveyor 1	02 Jun 1966	-2.44	316.66	Oceanus Procellarum (Ocean of Storms)	32
Retro-rocket				Assume same location as Surveyor 1	29
Surveyor 2	23 Sep 1966	5.5	348	Southeast of Copernicus crater	29
Lunar Orb 1	29 Oct 1966	6.7	162	Far side of the Moon – Mandel'shtam crater	29
Luna 13	24 Dec 1966	18.87	297.95	Oceanus Procellarum (Ocean of Storms)	27
Two auxiliary modules jettisoned before retro-rocket ignition				Assume same location as Luna 13	29
Retro-rocket				Assume same location as Luna 13	29
Surveyor 3	20 Apr 1967	-3.0159 [3]	336.5822 [3]	Near Oceanus Procellarum (Ocean of Storms)	33
Retro-rocket				Assume same location as Surveyor 3	29
Surveyor 4	17 Jul 1967	0.4	358.67	Sinus Medii (Bay of the Center or Central Bay)	29
Surveyor 5	11 Sep 1967	1.49	23.20	Mare Tranquillitatus (Sea of Tranquility)	32
Retro-rocket				Assume same location as Surveyor 5	29
Lunar Orb 3	9 Oct 1967	14.6 [4]	268.3 [4]	Far side of the Moon – Near Einstein crater	29
Lunar Orb 2	11 Oct 1967	-4 [5]	98 [5]	Far side of the Moon – South of Wyld crater	29
Lunar Orb 4	~31 Oct 1967	-	330 - 338	Natural Orbit Decay – Impact Site Unknown	27
Surveyor 6	10 Nov 1967	0.42	358.62	Sinus Medii (Bay of the Center or Central Bay)	32
Retro-rocket				Assume same location as Surveyor 6	29
Surveyor 7	10 Jan 1968	-41.01	348.59	Outer rim of Tycho crater	32
Retro-rocket				Assume same location as Surveyor 7	29
Lunar Orb 5	31 Jan 1968	-2.79	277	West of Oceanus Procellarum	27
Apollo 10				Natural Orbit Decay – Impact Site Unknown §	29
Apollo 11	20 Jul 1969	0.67	23.47	Mare Tranquillitatus (Sea of Tranquility) §	30

TABLE D2-1 IMPACT/LANDING SITES FOR LUNAR MISSIONS (AND MISSION ELEMENTS) - CONCLUDED

Mission Msn Element	Impact / Landing Date (UTC)	Latitude (deg)	East Long. (deg)	Impact / Landing Site Location	Source (Ref. No.)
Luna 15	21 Jul 1969	17	60	Mare Crisium (Sea of Crises)	29
Apollo 12	19 Nov 1969	-3.01	336.58	Near Oceanus Procellarum (Ocean of Storms) §	30
Luna 16	20 Sep 1970	-0.68	56.30	Mare Fecunditatis (Sea of Fertility) – West of Webb crater	29
Luna 17	17 Nov 1970	38.213 [6]	324.803 [6]	Mare Imbrium (Sea of Showers or Sea of Rains)	34,35
Lunokhod 1 Rover		38.287 [6]	324.810 [6]	See footnote below	34,35
Apollo 14	5 Feb 1971	-3.65	342.53	Near Fra Mauro crater §	30
Apollo 15	30 Jul 1971	26.13	3.63	Palus Putredinis (Marsh of Decay) – Hadley Rille §	30
Luna 18	11 Sep 1971	3.57	56.50	Near Mare Fecunditatis (Sea of Fertility)	27
Luna 20	21 Feb 1972	3.53	56.55	Near Mare Fecunditatis (Sea of Fertility)	29
Apollo 16	21 Apr 1972	-8.97	15.50	Descartes highland region §	30
Apollo 17	11 Dec 1972	20.19	30.77	Near Mare Serenitatis (Sea of Serenity) – Taurus Littrow §	30
Luna 21	15 Jan 1973	25.85	30.45	Near Mare Serenitatis (Sea of Serenity)	27
Lunokhod 2 Rover		25.83	30.92	See also Table D2-2	30
Luna 23	06 Nov 1974	13	62	Mare Crisium (Sea of Crises)	29
Luna 24	18 Aug 1976	12.75	62.20	Mare Crisium (Sea of Crises)	29
Hiten	10 Apr 1993	-34.3 [7]	55.6 [7]	Near Stevinus crater	27
Lunar Prospector	31 Jul 1999	-87.7	42.0	Crater near South Pole	29
SMART 1	3 Sep 2006	-34.4	313.8	on the edge of Lacus Excellentiae (Lake of Excellence)	45

Notes:

- In all cases where retro-rockets and additional mission elements (e.g., auxiliary modules) were jettisoned prior to landing, the impact site location of those elements is assumed to be the same as the landing site of the primary mission element (e.g., the lander). This assumption, of course, is not correct, but at the moment no better information is available. For example, the impact site of the Surveyor 3 retro-rocket was not seen by the Apollo 12 astronauts when they visited the Surveyor 3 landing site, yet the impact site of the retro-rocket is indicated in Table D2-1 as having the same landing site coordinates as the Surveyor 3 lander.

[1] The impact site of Luna 2 is often quoted within the range 29º–31º in latitude and 359ºE-1ºE in longitude.

[2] A few references place the impact site of Luna 5 in Mare Cognitum (the sea that has become known) – near Lansberg crater at –2º, 335ºE.

[3] Reference 33 indicates that the Surveyor 3 lander is located 155 m (Az 133º) from the Apollo 12 LM. The location of Surveyor 3 was computed using the Apollo 12 LM coordinates listed in Table D2-2.

[4] Some references place the impact site of Lunar Orbiter 3 at 14.3º, 262.3ºE.

[5] Some references place the impact site of Lunar Orbiter 2 at 3º, 119.1ºE.

[6] The landing site coordinates usually quoted for Luna 17 are 38.28º, 325ºE. (See Appendix F, reference 27.) Appendix F, reference 34, however, proposes alternate (but unconfirmed) coordinates for Luna 17 and Lunokhod 1 based upon Apollo 15 and Lunokhod 1 images. Appendix F, reference 35 includes an estimate of the traverse path of the Lunokhod 1 rover relative to the Luna 17 lander. The combination of data in Appendix F, references 34 and 35 produced the locations indicated above.

[7] Some references place the impact site of the Hiten orbiter at -34.0º, 55.3ºE.

§ See also Tables D2-2 and D2-3 for the locations of other Apollo mission elements.

TABLE D2-2 SITE COORDINATES OF APOLLO SURFACE MISSION ELEMENTS AND LUNOKHOD 2 ROVER

Mission	Latitude	East Longitude	Radius		Source
Mission Element	**(deg)**	**(deg)**	**(km)**	**Comments**	**(Ref. No.)**
Apollo 11					
LRRR	0.67337	23.47293	1735.472		30
PSEP	0.67322	23.47299		Deployed ~5 m SSE of LRRR	27
LM (Eagle)	0.67408	23.47297			30
Apollo 12					
ALSEP	-3.00942	336.57542	1736.014		30
LM (Intrepid)	-3.01239	336.57843			30
Apollo 14					
LRRR	-3.64421	342.52120	1736.335		30
ALSEP	-3.64398	342.52252	1736.343		30
LM (Antares)	-3.64530	342.52864			30
MET	-3.64530	342.52864		Assume same location as LM – photos	
Apollo 15					
LRRR	26.13333	3.62837	1735.476		30
ALSEP	26.13407	3.62981	1735.477		30
LM (Falcon	26.13222	3.63386			30
LRV	26.13110	3.63972		163 m (102º Az) from LM	37
Apollo 16					
ALSEP	-8.97537	15.49812	1737.453		30
LM (Orion)	-8.97301	15.50019			30
LRV	-8.97292	15.50279		78 m (88º Az) from LM	37
Apollo 17					
ALSEP	20.19209	30.76492	1734.814		30
LM (Challenger)	20.19080	30.77168			30
LRV	20.19043	30.77726		159 m (94º Az) from LM	37

TABLE D2-2 SITE COORDINATES OF APOLLO SURFACE MISSION ELEMENTS AND LUNOKHOD 2 ROVER - CONCLUDED

Mission Element	Latitude (deg)	East Longitude (deg)	Radius (km)	Comments	Source (Ref. No.)
Luna 21 – Lunokhod 2 Rover					
LRRR	25.83223	30.92201	1734.638		30

Notes:

- In this table the list of Apollo artifacts left on the surface of the Moon only includes the major surface mission elements and does not include things like American flags, seismic mortars, discarded items, and personal artifacts (e.g., pictures, plaques, Alan Shepard's golf balls, etc.).
- Site coordinates are expressed in the IAU/IAG mean Earth/rotation system. See Section 4.2.
- Acronyms

  LRRR: Lunar laser Ranging RetroReflector, PSEP: Passive Seismic Experiment Package

NOTE: The combination of the Apollo 11 LRRR and PSEP were referred to as the EASEP – Early Apollo Scientific Experiment Package.

LM: Lunar Module (Descent Stage), ALSEP: Apollo Lunar Surface Experiment Package

MET: Modularized Equipment Transporter, LRV: Lunar Roving Vehicle

- The ALSEP locations in this table really just indicate the location of the antenna on the ALSEP central station. The layout or configuration of ALSEP components on the surface of the Moon differed substantially for each Apollo mission (as did many of the components themselves). For example, the Radioisotope Thermoelectric Generators (RTGs) that powered the ALSEP investigations were generally located only about 3 m from the central station, but the placement of some of the seismic sensors (geophones), for a few of the Apollo missions, extended out to a range of approximately 90 m from the ALSEP central station. For more information on the deployment configuration of the Apollo ALSEP investigations. (See Appendix F, reference 36.)
- Appendix F, reference 37 indicates the results of an analysis performed by E. M. Jones using photographs taken by the Apollo 15, 16, and 17 astronauts of the LMs from the LRVs in their final, parked positions and photographs of the parked LRVs taken from the LMs to estimate the final positions of the LRVs relative to the LMs.

TABLE D2-3 IMPACT SITE COORDINATES OF APOLLO ORBITAL MISSION ELEMENTS

Mission Element	Impact Date (UTC)	Latitude (deg)	East Long. (deg)	Impact Site Location
Apollo 10 LM-DS	*Natural Orbit Decay*			*Impact Site Unknown*
Apollo 11 LM-AS	*Natural Orbit Decay*			*Impact Site Unknown*
Apollo 12 LM-AS	20 Nov 1969	-3.94	338.80	73 km (112º Az) from Apollo 12 ALSEP
Apollo 13 S-IVB	15 Apr 1970	-2.75	332.14	135 km (274º Az) from Apollo 12 ALSEP
Apollo 14 S-IVB	4 Feb 1971	-8.09	333.98	172 km (207º Az) from Apollo 12 ALSEP
Apollo 14 LM-AS	7 Feb 1971	-3.42	340.33	67 km (276º Az) from Apollo 14 ALSEP
Apollo 15 S-IVB	29 Jul 1971	-1.51	348.19	184 km (69º Az) from Apollo 14 ALSEP
Apollo 15 LM-AS	3 Aug 1971	26.36	0.25	93 km (276º Az) from Apollo 15 ALSEP
Apollo 15 Sub-Satellite	*Natural Orbit Decay*			*Impact Site Unknown*
Apollo 16 S-IVB	19 Apr 1972	1.3	336.2	132 km (355º Az) from Apollo 12 ALSEP
Apollo 16 LM-AS	*Natural Orbit Decay*			*Impact Site Unknown*
Apollo 16 MS	*Natural Orbit Decay*			*Impact Site Unknown*
Apollo 16 Sub-Satellite	29 May 1972	10.16	111.94	Far side of the Moon, near Lobachevskij crater
Apollo 17 S-IVB	10 Dec 1972	-4.21	347.69	157 km (96º Az) from Apollo 14 ALSEP
Apollo 17 LM-AS	15 Dec 1972	19.96	30.50	770 km (98º Az) from Apollo 15 ALSEP

NOTES:

- The impact site location data for all mission elements except the Apollo 16 sub-satellite were taken from Appendix F, reference 31. The impact location of the Apollo 16 sub-satellite was taken from Appendix F, reference 29.
- Site coordinates from Appendix F, reference 31 are “derived from the manned space flight network Apollo tracking data”. These coordinates are believed to be consistent with the IAU/IAG mean Earth/rotation system. See Section 4.2.
- Acronyms

  LM-DS: Lunar Module-Descent Stage

  LM-AS: Lunar Module-Ascent Stage

  ALSEP: Apollo Lunar Surface Experiment Package

  S-IVB: Saturn IV-B (third stage of Saturn V rocket)

  Sub-Satellite: Also known as the Particles and Fields Subsatellite (P&FS or PFS)

  MS: Mass Spectrometer

Apollo 10

- The S-IVB was injected into a heliocentric orbit.
- The LM-DS was jettisoned in lunar orbit approximately 15 km above the lunar surface over the southwest corner of Mare Tranquillitatus (Sea of Tranquility).
- The LM-AS was injected into a heliocentric orbit.

Apollo 11

- The S-IVB was injected into a heliocentric orbit.
- The LM-AS was jettisoned into lunar orbit.

Apollo 12

- The S-IVB was supposed to have been injected into a heliocentric orbit, but observations of a near-Earth object in late 2002 and early 2003 seem to indicate that the Apollo 12 S-IVB was probably injected into a distant Earth orbit, escaped the Earth-Moon system in 1971, was temporarily captured in early 2002, and escaped again in early 2003.

Apollo 13

- The LM re-entered the Earth’s atmosphere on 17 April 1970.

Apollo 15

- The sub-satellite was deployed into lunar orbit.

NOTES (from Table D2-3 continued):

Apollo 16

- A malfunction resulted in the premature loss of tracking data for the Apollo 16 S-IVB. Location estimates are based on interpretation of seismic data. Uncertainty in the impact location is approximately 0.7º in latitude and 0.3º in longitude. The impact location estimated is based on tracking prior to signal loss is 2.24º, 335.51ºE. (See Appendix F, reference 31.)
- A malfunction prevented executing an LM-AS de-orbit maneuver. The estimated orbital lifetime of the LM-AS was approximately one year.
- A malfunction prevented the retraction of a 7.3 m long MS boom deployed from the Scientific Instrument Module (SIM) bay while in lunar orbit. As a result, the MS boom was jettisoned from the Service Module (SM) in lunar orbit prior to the trans-Earth injection burn.
- Due to the fact that an orbital shaping maneuver was cancelled prior to ejection, the sub-satellite was deployed into an elliptical lunar orbit with a limited lifetime — estimated to be approximately one month.

D3.0 SPACECRAFT ORBITING THE MOON WHEN CONTACT WAS LOST (INCLUDING MISSION ELEMENTS JETTISONED INTO LUNAR ORBIT)

TABLE D3-1 SPACECRAFT/MISSION ELEMENTS THAT PROBABLY HAVE IMPACTED THE MOON

(due to Natural Orbit Decay)

Mission Msn Element	Orbit Insertion Date (UTC)	Last Contact Date	Comments	Source (Ref. No.)
Luna 10	3 Apr 1966	30 May 1966		27
Retro-rocket			Retro-rocket and cruise stage were jettisoned together	29
Luna 11	28 Aug 1966	1 Oct 1966		27
Luna 12	25 Oct 1966	19 Jan 1967		27
Explorer 35 †	21 Jul 1967	24 Jun 1973		29
Retro-rocket				29
Luna 14	10 Apr 1968	April 1968		27
Luna 15-Tanks	17 Jul 1969		Two auxiliary “pods” (4 tanks) jettisoned prior to descent	29
Luna 16-Tanks	17 Sep 1970		Two auxiliary pods (4 tanks) jettisoned prior to descent	29
Luna 17-Tanks	15 Nov 1970		Two auxiliary pods” (4 tanks) jettisoned prior to descent	29
Luna 18-Tanks	7 Sep 1971		Two auxiliary pods (4 tanks) jettisoned prior to descent	29
Luna 19	3 Oct 1971	Oct 1972		29
Luna 20-Tanks	18 Feb 1972		Two auxiliary pods (4 tanks) jettisoned prior to descent	29
Luna 21-Tanks	12 Jan 1973		Two auxiliary pods (4 tanks) jettisoned prior to descent	29
Explorer 49 ‡	15 Jun 1973	Aug 1977		29
Retro-rocket				29
Luna 22	2 Jun 1974	Nov 1974		27
Luna 23-Tanks	2 Nov 1974		Two auxiliary pods (4 tanks) jettisoned prior to descent	29
Luna 24-Tanks	13 Aug 1976		Two auxiliary pods (4 tanks) jettisoned prior to descent	29
Hagoromo	18 Mar 1990	18 Mar 1990	Ignition of retro-rocket confirmed by Earth observations	27

NOTES:

† Also known as IMP-6 for the sixth spacecraft in the Interplanetary Monitoring Platform series.

‡ Also known as RAE-2 (or RAE-B) for the second spacecraft in the Radio Astronomy Explorer series.

APPENDIX E
GRAVITY FIELD INFORMATION

E1.0 LP150Q LUNAR GRAVITY FIELD

E1.1 FILE LOCATIONS

The normalized gravity field coefficients for the LP150Q field are available in the sha directory at:

http://pds-geosciences.wustl.edu/missions/lunarp/shadr.html ,

which has the direct URL: *http://pds-geosciences.wustl.edu/geodata/lp-l-rss-5-gravity-v1/lp_1001/sha/*.

NOTE: The PDS website also includes a number of previously developed (now outdated) lunar gravity fields.

E1.2 8X8 SUBSET OF LP150Q GRAVITY FIELD

(Including Zonals up to Degree 50, Normalized, No Permanent Tide)

GM = 4902.801076 km^3/s^2 R_{Ref} = 1738.0 km

J(1) = 0.000000000000D+00,
J(2) = 0.909010949481D-04,
J(3) = 0.320307167959D-05,
J(4) = -0.321409545028D-05,
J(5) = 0.221009876393D-06,
J(6) = -0.376479064475D-05,
J(7) = -0.561330656403D-05,
J(8) = -0.231953905520D-05,
J(9) = 0.354241582136D-05,
J(10) = 0.933036285877D-06,
J(11) = 0.960353139804D-06,
J(12) = 0.188692162540D-05,
J(13) = -0.258650494877D-06,
J(14) = -0.326300330782D-06,
J(15) = 0.972530852999D-07,
J(16) = -0.318446040132D-06,
J(17) = 0.103822696054D-05,
J(18) = 0.372937482506D-06,
J(19) = -0.555446218485D-07,
J(20) = -0.647952861685D-06,
J(21) = 0.971099122315D-07,
J(22) = 0.122392450387D-06,
J(23) = 0.196589333948D-06,
J(24) = 0.277798576353D-06,
J(25) = 0.162944553469D-06,
J(26) = -0.924403243020D-08,
J(27) = 0.776646019845D-06,
J(28) = -0.928771487846D-06,
J(29) = 0.627814558687D-06,
J(30) = -0.169625724228D-06,
J(31) = -0.615811103571D-06,
J(32) = 0.324113765082D-06,
J(33) = -0.995925930600D-07,
J(34) = -0.797167560251D-07,
J(35) = -0.177393818401D-06,
J(36) = -0.612788905278D-08,
J(37) = -0.225693717039D-06,
J(38) = -0.449830332452D-08,
J(39) = 0.311259412103D-06,
J(40) = -0.652544567689D-07,
J(41) = -0.173282860391D-06,
J(42) = -0.215218698890D-06,
J(43) = 0.945325046231D-07,
J(44) = 0.849348275934D-07,
J(45) = -0.185440783353D-06,
J(46) = 0.213600262245D-06,
J(47) = -0.174907671686D-06,
J(48) = 0.840684422498D-07,
J(49) = -0.401931394977D-07,
J(50) = -0.168369827480D-07,

E.1.2 8X8 SUBSET OF LP150Q GRAVITY FIELD (CONTINUED)

(Including Zonals up to Degree 50, Normalized, No Permanent Tide)

C(1, 1) = 0.000000000000D+00, S(1, 1) = 0.000000000000D+00,
C(2, 1) = -0.186273608184D-08, S(2, 1) = -0.142453894610D-08,
C(2, 2) = 0.346376274208D-04, S(2, 2) = 0.144063503540D-07,
C(3, 1) = 0.263418358622D-04, S(3, 1) = 0.546307860882D-05,
C(3, 2) = 0.141853316786D-04, S(3, 2) = 0.488913911795D-05,
C(3, 3) = 0.122862645044D-04, S(3, 3) = -0.178246270720D-05,
C(4, 1) = -0.600061939740D-05, S(4, 1) = 0.165955644727D-05,
C(4, 2) = -0.709370101544D-05, S(4, 2) = -0.678562735558D-05,
C(4, 3) = -0.135880466594D-05, S(4, 3) = -0.134332571737D-04,
C(4, 4) = -0.602939150193D-05, S(4, 4) = 0.393525694440D-05,
C(5, 1) = -0.103560812630D-05, S(5, 1) = -0.411585726681D-05,
C(5, 2) = 0.438127609376D-05, S(5, 2) = 0.109502526551D-05,
C(5, 3) = 0.454694228437D-06, S(5, 3) = 0.870152146591D-05,
C(5, 4) = 0.277279104390D-05, S(5, 4) = 0.307793712297D-07,
C(5, 5) = 0.312687726844D-05, S(5, 5) = -0.275386200669D-05,
C(6, 1) = 0.153429993945D-05, S(6, 1) = -0.257237276906D-05,
C(6, 2) = -0.434494761436D-05, S(6, 2) = -0.217950819643D-05,
C(6, 3) = -0.328182654012D-05, S(6, 3) = -0.349862907452D-05,
C(6, 4) = 0.371921281230D-06, S(6, 4) = -0.405761602001D-05,
C(6, 5) = 0.142835081872D-05, S(6, 5) = -0.102833744711D-04,
C(6, 6) = -0.471022454058D-05, S(6, 6) = 0.722662556338D-05,
C(7, 1) = 0.753347997634D-05, S(7, 1) = -0.131539563288D-06,
C(7, 2) = -0.660779046120D-06, S(7, 2) = 0.237864383691D-05,
C(7, 3) = 0.574652315024D-06, S(7, 3) = 0.236446570289D-05,
C(7, 4) = -0.899605382165D-06, S(7, 4) = 0.843758330286D-06,
C(7, 5) = -0.279193000638D-06, S(7, 5) = 0.108913355675D-05,
C(7, 6) = -0.103476355233D-05, S(7, 6) = 0.103172986529D-05,
C(7, 7) = -0.178499996340D-05, S(7, 7) = -0.160311972598D-05,
C(8, 1) = -0.398659493146D-07, S(8, 1) = 0.111757157884D-05,
C(8, 2) = 0.301238176996D-05, S(8, 2) = 0.194296603146D-05,
C(8, 3) = -0.188460320268D-05, S(8, 3) = 0.953692588674D-06,
C(8, 4) = 0.338733082124D-05, S(8, 4) = -0.502575576501D-06,
C(8, 5) = -0.117868237022D-05, S(8, 5) = 0.284167245453D-05,
C(8, 6) = -0.153768837893D-05, S(8, 6) = -0.217660584641D-05,
C(8, 7) = -0.153454236110D-05, S(8, 7) = 0.332054075243D-05,
C(8, 8) = -0.252624025278D-05, S(8, 8) = 0.212716792161D-05,

E2.0 GGM02C EARTH GRAVITY FIELD

E2.1 FILE LOCATIONS

The normalized gravity field coefficients for the GGM02C field are available at: *http://www.csr.utexas.edu/grace/gravity/.*

E2.2 8X8 SUBSET OF GGM02C GRAVITY FIELD

(Normalized, No Permanent Tide,
Epoch = J2000, Normalized Rates / Year:

$$\dot{\bar{J}}_2 = -1.162755\text{x}10^{-11}$$
$$\dot{\bar{C}}_{21} = -0.337\text{x}10^{-11}$$
$$\dot{\bar{S}}_{21} = +1.606\text{x}10^{-11})$$

NOTE: The Earth GM value indicated below has been scaled from its value in the geocentric reference frame to its value in the solar system barycentric reference frame (see the NOTE in Section 3.1). If the gravity field is downloaded from the external website, the Earth GM value will not have been scaled to the solar system barycentric value. In addition, the C20 (-J2) value of -4.8416938905481D-04 from the external website includes the effects of permanent tides, so that it derives from the C20 (-J2) value in this table by subtracting 4.173D-09.

GM = 398600.4356 km^3/s^2 R_{Ref} = 6378.1363 km

J(1) = 0.0000000000000D+00,	J(5) = -6.8715981001179D-08,
J(2) = 4.8416521605481D-04,	J(6) = 1.4994011973125D-07,
J(3) = -9.5718508415439D-07,	J(7) = -9.0504630229132D-08,
J(4) = -5.3999143526074D-07,	J(8) = -4.9481334104780D-08,

C(1, 1) = 0.0000000000000D+00,	S(1, 1) = 0.0000000000000D+00
C(2, 1) = -2.0458338184745D-10,	S(2, 1) = 1.3968195379551D-09
C(2, 2) = 2.4393233001191D-06,	S(2, 2) = -1.4002662003867D-06
C(3, 1) = 2.0304752656064D-06,	S(3, 1) = 2.4817416903031D-07
C(3, 2) = 9.0480066975068D-07,	S(3, 2) = -6.1900441427103D-07
C(3, 3) = 7.2128924247650D-07,	S(3, 3) = 1.4143556434052D-06
C(4, 1) = -5.3617583789434D-07,	S(4, 1) = -4.7356802287476D-07
C(4, 2) = 3.5051159931087D-07,	S(4, 2) = 6.6243944849186D-07
C(4, 3) = 9.9085503541734D-07,	S(4, 3) = -2.0097529442342D-07
C(4, 4) = -1.8846750474516D-07,	S(4, 4) = 3.0882228278756D-07
C(5, 1) = -6.2904051380481D-08,	S(5, 1) = -9.4373263356928D-08
C(5, 2) = 6.5210393080303D-07,	S(5, 2) = -3.2334838450788D-07
C(5, 3) = -4.5187965449909D-07,	S(5, 3) = -2.1500140801223D-07
C(5, 4) = -2.9533633996919D-07,	S(5, 4) = 4.9817834613976D-08

E2.3 8X8 SUBSET OF GGM02C GRAVITY FIELD (CONTINUED)

(Normalized, No Permanent Tide,
Epoch = J2000, Normalized Rates/Year: $\dot{\bar{J}}_2 = -1.162755\text{x}10^{-11}$
$\dot{\bar{C}}_{21} = -0.337\text{x}10^{-11}$
$\dot{\bar{S}}_{21} = +1.606\text{x}10^{-11}$)

C(5, 5) = 1.7479367861529D-07,	S(5, 5) = -6.6937444851133D-07
C(6, 1) = -7.5903534713091D-08,	S(6, 1) = 2.6516969820404D-08
C(6, 2) = 4.8671477410889D-08,	S(6, 2) = -3.7379063632786D-07
C(6, 3) = 5.7235251140830D-08,	S(6, 3) = 8.9355908317172D-09
C(6, 4) = -8.6024306020762D-08,	S(6, 4) = -4.7142492778928D-07
C(6, 5) = -2.6717044535375D-07,	S(6, 5) = -5.3648870593762D-07
C(6, 6) = 9.4667858117668D-09,	S(6, 6) = -2.3740563878695D-07
C(7, 1) = 2.8088898145081D-07,	S(7, 1) = 9.5119644062781D-08
C(7, 2) = 3.3041560746535D-07,	S(7, 2) = 9.2985239787248D-08
C(7, 3) = 2.5045166263142D-07,	S(7, 3) = -2.1714748211003D-07
C(7, 4) = -2.7498938059553D-07,	S(7, 4) = -1.2406704411494D-07
C(7, 5) = 1.6601317328580D-09,	S(7, 5) = 1.7933888039325D-08
C(7, 6) = -3.5880775879961D-07,	S(7, 6) = 1.5179454735699D-07
C(7, 7) = 1.5062884219099D-09,	S(7, 7) = 2.4116259277940D-08
C(8, 1) = 2.3159979727734D-08,	S(8, 1) = 5.8896665124862D-08
C(8, 2) = 8.0015152191272D-08,	S(8, 2) = 6.5278835020898D-08
C(8, 3) = -1.9378833774969D-08,	S(8, 3) = -8.5977473175173D-08
C(8, 4) = -2.4436744168468D-07,	S(8, 4) = 6.9808169573661D-08
C(8, 5) = -2.5695381020603D-08,	S(8, 5) = 8.9195503483206D-08
C(8, 6) = -6.5962471839471D-08,	S(8, 6) = 3.0894479673499D-07
C(8, 7) = 6.7261439849585D-08,	S(8, 7) = 7.4875670873080D-08
C(8, 8) = -1.2403873503204D-07,	S(8, 8) = 1.2055330686769D-07

E3.0 MGS95J MARS GRAVITY FIELD

E3.1 FILE LOCATIONS

The normalized gravity field coefficients for the MGS95J field are available in the sha directory in the mors_1033 volume at:

http://pds-geosciences.wustl.edu/missions/mgs/rsdata.html.

E3.2 8 BY 8 SUBSET OF MGS95J (NORMALIZED):

GM = 42828.375214 km^3/s^2, R_{ref} = 3396.0 km,

J(1) = 0.000000000000D+00,	J(5) = 0.172668396687D-05,
J(2) = 0.875021446929D-03,	J(6) = -0.134656551267D-05,
J(3) = 0.118964606688D-04,	J(7) = -0.105972947422D-05,
J(4) = -0.512858494511D-05,	J(8) = -0.144331627687D-06,

C(1, 1) = 0.000000000000D+00,	S(1, 1) = 0.000000000000D+00,
C(2, 1) = 0.240451042309D-09,	S(2, 1) = 0.228413102704D-09,
C(2, 2) = -0.846358311289D-04,	S(2, 2) = 0.489345125134D-04,
C(3, 1) = 0.380357442952D-05,	S(3, 1) = 0.251773635684D-04,
C(3, 2) = -0.159478874998D-04,	S(3, 2) = 0.836138008473D-05,
C(3, 3) = 0.350540798135D-04,	S(3, 3) = 0.255743497063D-04,
C(4, 1) = 0.421638746590D-05,	S(4, 1) = 0.376328546232D-05,
C(4, 2) = -0.952535652905D-06,	S(4, 2) = -0.898086689309D-05,
C(4, 3) = 0.645681353157D-05,	S(4, 3) = -0.193214277044D-06,
C(4, 4) = 0.309733337931D-06,	S(4, 4) = -0.128730202815D-04,
C(5, 1) = 0.483677232262D-06,	S(5, 1) = 0.212295197817D-05,
C(5, 2) = -0.429813347661D-05,	S(5, 2) = -0.116591979700D-05,
C(5, 3) = 0.331265830999D-05,	S(5, 3) = 0.271690379049D-06,
C(5, 4) = -0.464038529224D-05,	S(5, 4) = -0.338210309185D-05,
C(5, 5) = -0.444981755945D-05,	S(5, 5) = 0.377981318403D-05,
C(6, 1) = 0.180242741110D-05,	S(6, 1) = -0.151852420686D-05,
C(6, 2) = 0.861644908198D-06,	S(6, 2) = 0.146917475088D-05,
C(6, 3) = 0.955674962032D-06,	S(6, 3) = 0.332998653921D-06,
C(6, 4) = 0.100842697274D-05,	S(6, 4) = 0.263879196537D-05,
C(6, 5) = 0.165766056879D-05,	S(6, 5) = 0.162292625814D-05,
C(6, 6) = 0.276207213764D-05,	S(6, 6) = 0.821842251075D-06,
C(7, 1) = 0.137497808076D-05,	S(7, 1) = -0.227356012264D-06,
C(7, 2) = 0.281403478456D-05,	S(7, 2) = -0.629497609199D-06,
C(7, 3) = 0.880520186494D-06,	S(7, 3) = -0.396898124404D-06,
C(7, 4) = 0.246901994220D-05,	S(7, 4) = -0.422173626432D-06,
C(7, 5) = -0.191466010090D-06,	S(7, 5) = -0.135855064596D-05,

C(7, 6) = -0.559263665369D-06,	S(7, 6) = -0.190146569930D-05,
C(7, 7) = 0.440747185248D-06,	S(7, 7) = -0.177559653014D-05,
C(8, 1) = -0.132579467190D-06,	S(8, 1) = 0.750586368668D-06,
C(8, 2) = 0.181036248667D-05,	S(8, 2) = 0.507112948195D-06,
C(8, 3) = -0.120694579356D-05,	S(8, 3) = -0.134140289966D-05,
C(8, 4) = 0.158829680202D-05,	S(8, 4) = 0.148292283973D-06,
C(8, 5) = -0.279151404438D-05,	S(8, 5) = -0.163014206155D-05,
C(8, 6) = -0.914075437553D-06,	S(8, 6) = -0.179005819793D-05,
C(8, 7) = -0.473993767619D-06,	S(8, 7) = 0.164458014917D-05,
C(8, 8) = -0.310595232396D-06,	S(8, 8) = -0.250343527157D-06,

E4.0 CONVERSION FROM NORMALIZED TO UN-NORMALIZED GRAVITY FIELD COEFFICIENTS

$$S_{nm} = \frac{\bar{S}_{nm}}{\Pi_{nm}} \qquad C_{nm} = \frac{\bar{C}_{nm}}{\Pi_{nm}} \qquad J_n = \frac{\bar{J}_n}{\Pi_{n0}}$$

where $\bar{S}, \bar{C}, \bar{J}$ are the normalized gravity field coefficients and S, C, J are the un-normalized coefficients. The conversion factor Π is given by the formula:

$$\Pi_{nm} = \sqrt{\frac{(n+m)!}{(n-m)!\ k\ (2n+1)}}$$

$k = 1$ if $m = 0$

$k = 2$ if $m \neq 0$

APPENDIX F
BIBLIOGRAPHY

1. "Recent Gravity Models as a Result of the Lunar Prospector Mission," A. S. Konopliv, S. W. Asmar, E. Carranza, W. L. Sjogren, and D. N. Yuan, Academic Press, *Icarus* 150, 1–18 (2001).

   [Note: The latest lunar gravity field, LP150Q, is considered the best available lunar gravity field by A. S. Konopliv. It represents an improvement over the gravity fields presented in reference 1. A published reference for LP150Q is not yet available.]

2. "A Global Solution for the Gravity Field, Rotation, Landmarks, and Ephemeris of Eros," A. S. Konopliv, J. K. Miller, W. M. Owen, D. K. Yeomans, and J. D. Giorgini, Academic Press, *Icarus* 160, 289–299 (2002).

3. "International Earth Rotation and Reference Systems Service (IERS) Conventions (2003), IERS Technical Note No. 32," edited by D. D. McCarthy and G. Petit, Verlag des Bundesamts für Kartographie und Geodäsie, Frankfurt am Main 2004, *http://www.iers.org/iers/products/conv/*.

4. "A High Resolution Lunar Gravity Field and Predicted Orbit Behavior," A. S. Konopliv, W. L. Sjogren, R. N. Wimberly, R. A. Cook, and A. Vijayaraghavan, Paper AAS 93–622, AAS/AIAA Astrodynamics Specialist Conference, Victoria, British Columbia, Canada, August 16–19, 1993.

5. "Lunar Laser Ranging Science: Gravitational Physics and Lunar Interior and Geodesy," J. G. Williams, S. G. Turyshev, D. H. Boggs, and J. T. Ratcliff, 35th COSPAR Scientific Assembly, Paris, France, July 18–24, 2004, *Advances in Space Research*, in press 2005, *http://arxiv.org/abs/gr-qc/?412049.*

6. "Report of the IAU/IAG Working Group on Cartographic Coordinates and Rotational Elements of the Planets and Satellites: 2000," P.K. Seidelmann, V. K. Abalakin, M. Bursa, M. E. Davies, C. DeBergh, J. H. Lieske, J. Oberst, J. L. Simon, E. M. Standish, P. Stooke, and P. C. Thomas, *Celestial Mechanics and Dynamical Astronomy* 82, Pages 83–110, 2002. *[JPL'ers should have access to the following website http://springerlink.metapress.com. Follow the links from "Browse by Online Libraries (subject areas)", then "Physics and Astronomy", then "Celestial Mechanics and Dynamical Astronomy", then "Volume 82 – Number 1 / January 2002", then follow the links to download the paper].*

7. "Topography of the Moon from the Clementine Lidar," D. E. Smith, M. T. Zuber, G. A. Neumann, and F. G. Lemoine, *Journal of Geophysical Research,* Vol. 102, No. E1, Pages 1591–1611, January 25, 1997, *http://adsabs.harvard.edu/cgi-bin/nph-bib_query?bibcode=1997JGR...102.1591S&db_key=AST&data_type=HTML&format=&high=42f69184bd08762*.

8. "Lunar Geophysics, Geodesy, and Dynamics," J. G. Williams and J. O. Dickey, 13th International Workshop on Laser Ranging: Proceedings from the Science Session, Washington, D.C., October 7–11, 2002, edited by R. Noomen, S. Klosko, C. Noll, and M. Pearlman, NASA/CP-2003-212248, Pages 75–86, 2003, *http://cddis.gsfc.nasa.gov/lw13/lw_proceedings.html.*

9. *Explanatory Supplement to the Astronomical Almanac*, Edited by P. K. Seidelmann, Published by University Science Books, Mill Valley, California, 1992.

10. *Orbital Motion* Second Edition, A. E. Roy, Published by Adam Hilger Ltd., Bristol, England, 1982.

11. *Theory of Orbits*, V. Szebehely, Published by Academic Press, New York, New York, 1967.

12. *Introductory Astronomy and Astrophysics*, E. P. Smith and K. C. Jacobs, Published by W. B. Saunders Company, Philadelphia, Pennsylvania, 1973.

13. Personal communication, J. G. Williams to R. B. Roncoli, October 20, 2004.

14. "Color-coded Topography and Shaded Relief Maps of the Lunar Hemispheres," M. R. Rosiek, R. Kirk, and E. Howington-Kraus, 33rd Annual Lunar and Planetary Science Conference, March 11–15, 2002, Houston, Texas, abstract no. 1792, (Geologic Investigations Series I-2769, USGS 2002), *http://astrogeology.usgs.gov/Teams/Geomatics/photogrammetry/topography_lunar.html.*

15. "The unified lunar control network: 1994 version," M. E. Davies, T. R. Colvin, D. L. Meyer, and S. Nelson, *Journal of Geophysical Research,* Vol. 99, No. E11, Pages 23,211–23,214, November 25, 1994, *http://adsabs.harvard.edu/cgi-bin/nph-bib_query?bibcode=1994JGR....9923211D&db_key=AST&data_type=HTML&format=&high=42f69184bd05345.*

16. "Unified Lunar Control Network 2005 and Topographic Model," B. A. Archinal, M. R. Rosiek, and B. L. Redding, Poster Session II: Lunar Potpourri for the Lunar and Planetary Science XXXVI (2005), March 2005, *http://www.lpi.usra.edu/meetings/lpsc2005/pdf/2106.pdf.*

17. *Lunar Sourcebook – A User's Guide to the Moon*, G. H. Heiken, D. T. Vaniman, and B. M. French, Cambridge University Press, Lunar and Planetary Institute, Houston, Texas, 1991.

18. The Artemis Project, Graph of Planetary Surface Temperatures, *http://www.asi.org/adb/02/05/01/surface-temp-chart.html.*

19. The Artemis Project, Rotating Moon Globe, *http://www.asi.org/adb/m/moonglobe.html.*

20. "GGM02 - An improved Earth gravity field model from GRACE," B. Tapley, J. Ries, S. Bettadpur, D. Chambers, M. Cheng, F. Condi, B. Gunter, Z. Kang, P. Nagel, R. Pastor, T. Pekker, S. Poole, F. Wang, *Journal of Geodesy* (2005), doi 10.1007/s00190-005-0480-z, *http://www.csr.utexas.edu/grace/gravity/*.

21. "CODATA Recommended Values of the Fundamental Physical Constants: 1998," Peter J. Mohr and Barry N. Taylor, National Institute of Standards and Technology, Gaithersburg, MD 20899-8401. *[See also the following website http://physics.nist.gov/cgi-bin/cuu/Category?view=html&Adopted+values.x=91&Adopted+values.y=15].*

22. *Formulation for Observed and Computed Values of Deep Space Network Data Types for Navigation*, T. D. Moyer, JPL Publication 00-7, Monograph 2, Issued by the Deep Space Communications and Navigation Systems Center of Excellence, Jet Propulsion Laboratory, October 2000.

23. "Time scales in the JPL and CfA ephemerides," E. M. Standish, *Astronomy and Astrophysics* 336, 381–384, 1998.

24. "Planetary Ephemeris DE421 for Phoenix Navigation," W. M. Folkner, J. G. Williams, and D. W. Boggs, JPL IOM 343R-08-002, 13 February 2008, available at *http://ssd.jpl.nasa.gov/iau-comm4/de421iom/* or *http://ssd.jpl.nasa.gov/pub/eph/planets/ioms/*.

25. "Status of ISO Draft International Standard for Determining Solar Irradiances (DIS 21348)," W. K. Tobiska and A. A. Nusinov, 35th COSPAR Scientific Assembly, Paris, France, July 18–25, 2004, *http://www.spacewx.com/ISOconfirm.html.*

    [Note: The Draft International Standard (DIS) 21348 of the International Organization for Standards (ISO) solar irradiance standard is protected by copyright by ISO and thus is not referenced directly].

26. "The adoption of ICRS on 1 January 1998: meaning and consequences," *Letter to the Editor*, M. Feissel and F. Mignard, *Astronomy and Astrophysics,* 331, L33-L36, 1998, *http://adsabs.harvard.edu/cgi-bin/nph-bib_query?bibcode=1998A%26A...331L..33F&db_key=AST&data_type=HTML&format=.*

27. National Space Science Data Center (NSSDC) at NASA GSFC, Lunar Exploration.

28. Summary of lunar landing site data. Data are compiled and adapted from reference 27, *http://www.fourmilab.ch/earthview/lunarform/landing.html.*

29. *Lunar Exploration: Human Pioneers and Robotic Surveyors*, P. Ulivi with D. M. Harland, Published by Praxis Publishing Ltd., Chichester, United Kingdom, 2004.

30. "Lunar coordinates in the regions of the Apollo landers," M. E. Davies and T. R. Colvin, *Journal of Geophysical Research,* Vol. 105, No. E8, Pages 20,277–20,280, August 25, 2000.

31. "Structure of the Moon," M. N. Toksöz, A. M. Dainty, S. C. Solomon, and K. R. Anderson, *Reviews of Geophysics and Space Physics*, Vol. 12, No. 4, Pages 539–567, November 1974.

32. *Surveyor Program Results*, NASA Special Publication 184 (NASA SP-184), published by the U.S. Government Printing Office, Washington, D.C., 1969.

33. *Analysis of Surveyor 3 material and photographs returned by Apollo 12*, NASA Special Publication 284 (NASA SP-284), published by the U.S. Government Printing Office, Washington, D.C., 1972, *http://www.hq.nasa.gov/office/pao/History/alsj/a12/AnalysSurvIIIMtrial.html.*

34. "Lunar Laser Ranging and the Location of the Lunokhod 1," P. J. Stooke, Print-Only Presentation for the Lunar and Planetary Science XXXVI (2005), March 2005, *http://www.lpi.usra.edu/meetings/lpsc2005/pdf/1194.pdf.*

35. *Lunokhod-1, a mobile laboratory on the moon. Volume 2*, V. L. Barsukov, Moscow, Izdatel'stvo Nauka, (book is in Russian), 1978.

36. *ALSEP Termination Report*, J. R. Bates, W. W. Lauderdale, H. Kernaghan, NASA Reference Publication 1036, April 1979, *http://ntrs.nasa.gov/archive/nasa/casi.ntrs.nasa.gov/19790014808_1979014808.pdf.*

37. Apollo Lunar Surface Journal, edited by E. M. Jones, *http://www.hq.nasa.gov/alsj/alsj-LRVFinalParking.html.*

38. "The International System of Units (SI) - Conversion Factors for General Use," NIST Special Publication 1038, available at http://www.nist.gov/metric.

39. Federal Standard 376B: Preferred Metric Units for General Use by the Federal Government, January 27, 1993, available at http://ts.nist.gov/WeightsAndMeasures/Metric/fs376b.cfm.

40. "Update to Mars Coordinate Frame Definitions," Robert A. Mase, internal JPL memorandum IOM 312.B/015-99, July 15, 1999.

41. "Expressions for the Precession Quantities Based upon the IAU (1976) System of Astronomical Constants," J. H. Lieske, T. Lederle, W. Fricke, and B. Morando, *Astronomy and Astrophysics,* vol. 58, no. 1–2, Pages 1–16, June 1977.

42. "Precession Matrix Based upon IAU (1976) System of Astronomical Constants," J. H. Lieske, *Astronomy and Astrophysics,* vol. 73, no. 3, Pages 282–284, March 1979.

43. "1980 IAU Theory of Nutation: The Final Report of the IAU Working Group on Nutation," P. K. Seidelmann *et al.*, *Celestial Mechanics,* vol. 27, no. 1, Pages 79–106, May 1982.

44. ESA web sites, http://sci.esa.int/science-e/www/object/index.cfm?fobjectid=39961 and http://sci.esa.int/science-e/www/area/index.cfm?fareaid=98.

45. "Interior Structure and Seasonal Mass Redistribution of Mars from Radio Tracking of Mars Pathfinder," W. M. Folkner et al., *Science*, Vol. 278, No. 5344, Pages 1749–1752, December 5, 1997.

46. "Mars Exploration Rover Project Planetary Constants and Models - Version 2," Ralph Roncoli, Bill Strauss, and Dolan Highsmith, internal JPL memorandum IOM 312.F-02-003, November 27, 2002.

47. "A Post-Pathfinder Evaluation of Areocentric Solar Coordinates with Improved Timing Recipes for Mars Seasonal/Diurnal Climate Studies," M. Allison and M. McEwen, Planetary and Space Science, Vol. 48 (2000), Pages 215–235, September 28, 1999.

48. "DE421 Lunar Orbit, Physical Librations, and Surface Coordinates," J. G. Williams, D. H. Boggs and W. M. Folkner, JPL IOM 335-JW,DB,WF-20080314-001, March 14, 2008, available at *http://ssd.jpl.nasa.gov/iau-comm4/de421iom/* or *http://ssd.jpl.nasa.gov/pub/eph/planets/ioms/* or ftp://naif.jpl.nasa.gov/pub/naif/generic_kernels/spk/planets/de421_lunar_ephemeris_and_orientation.pdf.

49. “Guide for the Use of the International System of Units (SI),” NIST Special Publication 811, 1995 edition, available at *http://www.nist.gov/metric*.

50. “Lunar Constants and Models Document,” R. Roncoli, JPL D-32296, available at http://ssd.jpl.nasa.gov/?lunar_doc.

51. “Mars Science Laboratory Planetary Constants and Models Document,” J. Kangas, JPL D-27212.

52. "Mars Pathfinder Planetary Constants and Models", Robin Vaughan, JPL D-12947, Dec. 1995.